2021

ALPHA-SYNUCLEIN MULTIMERIZATION IS DEPENDENT ON STRUCTURAL CHARACTERISTICS OF REPEATED KTKEGV REGIONS

Benjamin Ira Rosen
Saint John's University, Jamaica New York

ALPHA-SYNUCLEIN MULTIMERIZATION IS DEPENDENT ON STRUCTURAL CHARACTERISTICS OF REPEATED KTKEGV REGIONS

A dissertation submitted in partial fulfillment
of the requirements for the degree of

DOCTOR OF PHILOSOPHY

to the faculty of the

DEPARTMENT OF BIOLOGICAL SCIENCES

of

ST. JOHN'S COLLEGE OF LIBERAL ARTS AND SCIENCES

at

ST. JOHN'S UNIVERSITY
New York
by
Benjamin Ira Rosen

Date Submitted _____ Date Approved _____

_____ _____

Benjamin Ira Rosen **Simon Geir Møller**

ABSTRACT

ALPHA-SYNUCLEIN MULTIMERIZATION IS DEPENDENT ON STRUCTURAL CHARACTERISTICS OF REPEATED KTKEGV REGIONS

Benjamin Ira Rosen

Parkinson's disease (PD) is the most common movement disorder and is characterized by neuronal loss and the presence of Lewy bodies in dopaminergic neurons of the substantia nigra pars compacta. PD is a chronic, progressive, and irreversible neurodegenerative disorder associated with the selective loss of dopaminergic neurons. Initially described in an Ayurvedic medical treatise and Galen's writings, and later by James Parkinson in 1817, the most common symptoms of PD are resting tremors, abnormal posture and gait, and muscle rigidity.

Approximately 1 million people are living with PD in the United States and worldwide estimates are between 7 and 10 million. Approximately 5-10% of PD cases are genetic, while the vast majority are sporadic and idiopathic. Mutations in genes such as *SNCA, GBA, PRKN, PINK1, DJ-1* and *LRRK2* along with environmental factors such as pesticides, gut-bacteria and metal toxicity have been associated with PD. The vast array of possible causes paired with the variance of appearance and rate of progression make the disease difficult to diagnose and study both at a clinical and molecular level.

Perhaps the most studied protein in the field of PD is alpha-synuclein (a-syn). Indeed, the interest in the protein was sparked in 1997 by the finding that an alanine to threonine substitution (A53T) in a-syn co-segregated with PD subjects [1]. Both genetic lesions in a-syn and the intrinsic accumulation of the protein in neurons are associated with

early- and late-onset PD [1, 2]. A neuropathological hallmark of PD is the presence of insoluble intra-neuronal protein aggregates called Lewy Bodies (LB) which are highly enriched in a-syn [3]. A-syn is an intrinsically disordered and natively unfolded protein with a theoretical size of 14 kDa, which has the propensity to form higher order multimers. Although the genetics of *SNCA*/a-syn are well known, the physiological function of a-syn is largely unknown as is its ability to influence neurodegeneration and cell death in PD.

It has been suggested that a-syn may represent a prime target for future diagnostic and therapeutic intervention strategies. However, to further this notion, it will be important to understand the aggregation dynamics of a-syn and how intermediate a-syn multimers may indeed positively and/or negatively impact the death of neurons in PD.

TABLE OF CONTENTS

LIST OF TABLES

LIST OF FIGURES

1 Introduction

1.1 Parkinson's Disease

Parkinson's disease (PD), initially described in an Ayurvedic medical treatise and Galen's writings, and later by James Parkinson in 1817 as "shaking Palsy", is the most common movement disorder and the second-most common neurodegenerative disease [4]. Parkinson identified resting tremor, irregular posture and gait, and muscular weakness as motor symptoms of the disease (Parkinson 1817). In 1861, Jean-Martin Charcot coined the term "Parkinson's Disease" and described slowness of movement, or bradykinesia, as a distinct cardinal symptom [5]. PD is a chronic, progressive, and irreversible neurodegenerative disorder associated with the selective loss of dopaminergic neurons of the substantia nigra pars compacta and the presence of neuronal inclusions called Lewy Bodies (LBs). It is this loss and dysfunction of dopaminergic neurons that leads to both motor and non-motor symptoms associated with PD. While the motor symptoms are more widely known, non-motor symptoms such as loss-of-smell, depression, cognitive decline, and sleep disorders are prevalent in patients [6]. In addition to its wide range of symptoms, PD is one of many neurodegenerative diseases, including Alzheimer's Disease (AD), Huntington's Disease (HD), Amyotrophic Lateral Sclerosis (ALS) and prion diseases, that has a complex set of intersecting risk factors: genetic, environmental, protein dysfunction, and aging [7].

The pathological hallmark of PD is the LB. In 1912, Fritz Jakob Heinrich Lewy discovered the neuronal inclusion [8]. LBs are aggregates of mostly protein which are highly enriched in a-syn. LB composition and the presence of genetic PD-risk factors

within a-syn's encoding gene, *SNCA*, have led to a-syn being the most studied PD-associated protein. Indeed, a-syn may represent a valuable target for future therapeutic intervention strategies by either preventing its aggregation or promoting its destruction as it transitions through multimeric intermediates prior to aggregation formation. In addition, the ability to detect and define different a-syn states in PD may provide a possible diagnostic and prognostic roadmap improving disease management scenarios. To unlock this potential a more detailed understanding of a-syn is required, particularly the relationship between different a-syn structures and its aggregation potential.

1.2 Epidemiology

Inconsistencies in diagnostic practices and procedures has created difficulty in estimating the exact prevalence of PD, however, it is thought that over 6 million individuals in the world are living with PD [9]. Indeed, PD affects between 0.1-0.2% of the general population but the prevalence increases with age affecting approximately 1% of the population above 60 years of age and approximately 4% in individuals over 80 [10]. Interestingly, this number is thought to be on the rise due to the increasing lifespan of the global population and from1990 to 2015, the prevalence of PD more than doubled [9]. Using the Global Burden of Disease's study of standard life expectancy, PD prevalence is conservatively projected to reach almost 13 million by 2040 [11].

1.3 Symptoms

PD is characterized by the loss of dopaminergic neurons, however there may also be neuronal loss in other neurons and the causes of neuronal loss vary broadly. Such broad pathology results in PD being quite heterogenous, making diagnosis based on symptoms

difficult. The four cardinal motor symptoms of PD are tremors, rigidity, bradykinesia, and postural instability which represent the primary basis for diagnosing patients [12]. However, many non-motor symptoms are also involved.

Bradykinesia is generally defined as slow initiation of voluntary movement as well as progressive lessening of speed and amplitude of repeated actions [13, 14]. It can lead to the loss of facial expression and minute hand-writing [14]. Bradykinesia is present in all PD cases, and it is an essential requirement of the initial step of diagnosis [15]. Bradykinesia may be caused by muscle weakness, rigidity, tremor, movement variability, and slowness of thought [16].

Tremor is the most well-known symptom of PD, most likely due to its unavoidable outward manifestation at rest. Indeed, James Parkinson's famous essay highlighted the "shaking" it caused. Tremors are often asymmetric and usually persist at a frequency of 4-6 Hz and are most common in the hands and legs [14, 15]. Resting tremor is used as a positive diagnostic for PD, however action tremors are present in 92% of cases [17]. The outward manifestation of tremors often makes its psychosocial impact devastating to patients [18].

Rigidity of muscles is present in approximately 89% of PD patients [19]. It is defined by stiffness and increased resistance of muscles, making movement difficult and painful. Patients can experience axial or limb rigidity, but it is most common in the extremities. It often begins in the limbs of one side before spreading to trunk and subsequently the limbs of the other side of the body. A combination of rigidity and tremor may create a cogwheel phenomenon, where a joint is resistant to movement, but it moves with small jerks due to tremors.

Postural instability is the loss of control over maintaining an upright posture and the tendency to lose balance and fall. Patients find it difficult to turn or make sudden movements, probably due to the loss of the reflexes needed to maintain balance and reactivity [12]. Postural instability is especially dangerous combined with the advanced age of PD patients since falls might lead to more serious injury. Postural instability and rigidity often lead to Parkinsonian gait, characterized by short shuffling steps, flexed posture, lack of arm swinging, and festination [20].

As PD progresses, non-motor symptoms typically emerge. Absence of any non-motor symptoms after 5 years of PD is considered a red flag in diagnosing patients [15]. Common non-motor symptoms include sleep dysfunction, autonomic dysfunction, hyposmia or anosmia, and psychiatric dysfunction [15]. Loss of smell develops in 90% of patients and is one of the earliest signs of PD, a fact that supports the Braak hypothesis [21]. Autonomic, sleep, and psychiatric dysfunctions worsen with disease progression and may be affected by fluctuating dopamine levels resulting from treatments [22].

1.4 Treatment

There is no treatment for PD, however, there are many medications that treat symptoms. The most common and most potent medication is Levodopa, a dopamine precursor that acts as dopamine replacement therapy. Chronic Levodopa treatment can result in dyskinesias and therapeutic response fluctuations, probably due to inconsistent plasma concentrations and the brain's loss of capacity to store the drug [23]. It is commonly used in conjunction with Carbidopa, which prevents the conversion of Levodopa into dopamine until after it crosses the blood brain barrier [24]. Additionally, catechol-o-methyl transferase (COMT) inhibitors (such as tolcapone and entacapone) and monoamine oxidase

B (MAO-B) inhibitors (such as selegiline and rasagiline) can have a similar effect of preventing degradation of Levodopa, enabling higher concentrations to cross the blood brain barrier [25]. Dopamine agonists such as pramipexole and ropinirole are sometimes administered to delay Levodopa therapy, but side effects such as sleepiness and impulse-control disorders have resulted in less common use of these drugs [26].

1.5 Cellular proteostasis in Parkinson's Disease

There are many risk factors associated with developing and exacerbating PD and approximately 80% of PD cases are idiopathic, meaning the cause is unknown [27]. It is most likely that PD results from a combination of risk factors and in studying these risk factors, it is important keep in mind their effect on protein homeostasis (proteostasis), a-syn, and the formation of pathological LBs. For instance, PD is an age-related disease, and its incidence rate dramatically increases in individuals over the age of 60 [28]. When considered through the lens of proteostasis, age-related weakening of neuronal repair systems might increase the risk that neurons are unable to recover from cellular perturbations to protein folding, post-translational modifications, endoplasmic reticulum, autophagy, and reactive oxygen species (ROS) clearance [28].

Protein misfolding and aggregation is a common theme amongst many neurodegenerative diseases, therefore maintaining intracellular proteostasis by balancing protein folding and misfolding is vital in protecting the functionality of neurons [29]. Misfolded proteins are generally inactive, but their accumulation can cause stress responses in cells and in organelles. The endoplasmic reticulum (ER) is key in maintaining proteostasis as ER stress via protein accumulation triggers the unfolded protein response (UPR). The UPR diminishes ER protein level and promotes correct protein folding by

proteosomal degradation, translation mitigation and autophagy [30]. Further, autophagy plays a crucial role in maintaining proteostasis because it degrades protein aggregates that cannot be processed by the proteasome [31]. In fact, the autophagosome can degrade and recycle whole organelles to promote cell survival. Protein degradation by autophagy and the proteasome recruit target proteins through ubiquitination [32]. Ubiquitination along with other covalently bound groups, such as phosphorylation, SUMOylation, and oxidation regulate the proteome. Furthermore, Post-Translational Modifications (PTMs) of proteins have been shown to promote aggregation in many neurodegenerative diseases [33].

A hallmark of neurodegenerative diseases is the accumulation and proteotoxicity of pathogenic proteins. Protein accumulation can lead to aggregation and inclusions, which may be either toxic or protective [34]. Proteotoxicity is especially problematic in post-mitotic neurons, drawing a clear relationship between neurodegeneration and age. Similarly, mitochondrial proteostasis is also critical for cell survival. Its dysfunction can lead to the accumulation of ROS. ROS can hamper cellular processes by damaging macromolecules such as DNA, RNA, lipids, and proteins. The disturbance of mitochondrial proteostasis may lead to the irreversible induction of apoptosis. Apoptosis, or programmed cell death, is initiated in stressed cells to avoid the damaging of surrounding cells. While advantageous to organisms in most cases, apoptosis is detrimental to the nervous system because differentiated neurons cannot be reproduced. Although neuronal loss cannot be fully attributed to apoptosis, it is a common culprit in neurodegenerative diseases such as PD, AD, HD and ALS.

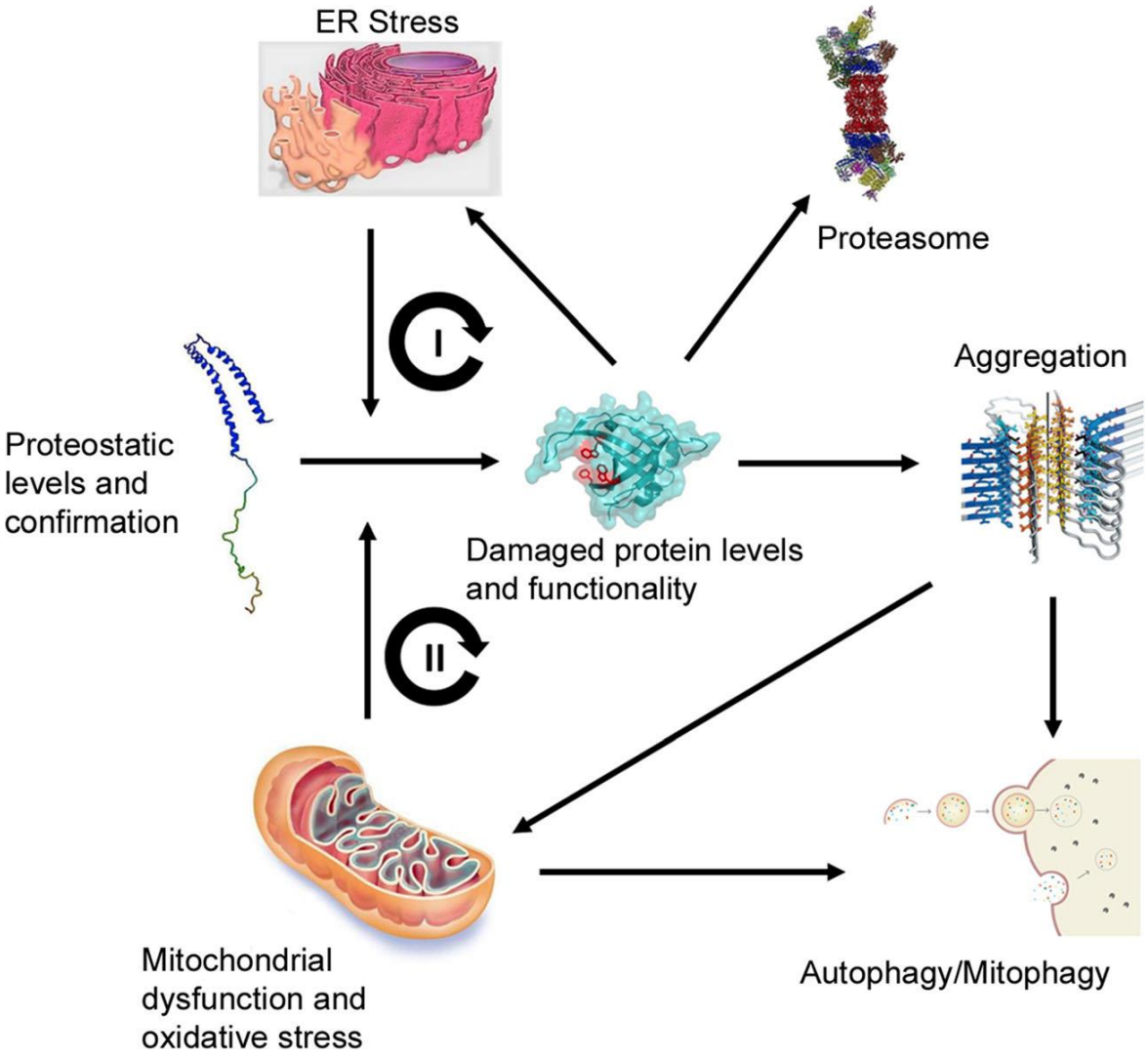

Figure 1. **Altered proteostatic levels and protein conformations lead to hallmark pathological neurodegenerative pathways.** Damaged and excessive protein directly causes ER stress and aggregation as well as mitochondrial dysfunction and oxidative stress indirectly. Additionally, feedback loops (I, II) highlight the destructive nature of damaged proteins propagating ER stress and mitochondrial dysfunction leading to loss of functionality further altering proteostasis. The cellular defense response to these pathways includes proteosome degradation, autophagy/mitophagy, and apoptosis.

1.5.1 A-syn aggregation

The aggregation of a-syn primarily contributes to PD being a proteopathy (Figure 1). It is largely unknown whether a-syn aggregates are toxic or protective. It has been hypothesized that the collection of misfolded protein into aggregates is a defense mechanism to combat their toxicity and maintain proteostasis [35]. These inclusions, however, have themselves been considered toxic by the loss-of-function of aggregating proteins unable to carry out their physiological function and/or by the gain-of-function of a new mechanism which contributes to cell death [36].

LBs contain aggregated a-syn in the form of beta-sheet rich insoluble structures called amyloid fibrils [37]. While it is known that protein misfolding leads to aggregation, the initiation and formation of amyloid fibrils is not well understood. Studying the formation of a-syn amyloid fibrils, their gain-of-function, loss-of-function and neuroprotectivity are critical to the advancement of understanding PD.

Aggregation of a-syn correlates with dysregulation of its post-translational modifications, its accumulation, and its folding. In addition to a-syn, LBs contain but are not limited to PD-associated proteins (DJ-1, LRRK2, parkin, PINK-1, GBA and synphilin-1), a-syn binding proteins, and components of the ubiquitin-proteosome pathway. This complex mixture implies that LBs acquire cytotoxicity by attracting various proteins and thus disturbing proteostasis. PD progression has also been attributed to the extracellular transmission of a-syn fibrils or non-fibrillar multimers, like prion disease, which can presumably accelerate the seeding step of LB formation [38, 39].

Although a-syn neurotoxicity has been attributed to LB formation and the formation of large, protein-magnet-like inclusion inside neurons another hypothesis is that soluble,

non-fibrillar, multimeric species of a-syn contribute even more to PD pathogenesis [40, 41]. Evidence suggests that a-syn multimers interact with and damage cell membranes, which can inhibit axonal transport machinery [42]. If the aggregation of a-syn multimers hinders this toxic effect, LB formation can be described as neuroprotective rather than neurotoxic.

As a-syn aggregates, its inability to perform its physiological role might cause a form of loss-of-function toxicity. A-syn has been implicated in many biological functions based on its localization and molecular interactions, however the physiological effects of those findings are not well understood [43]. A-syn interactions with lipids and phospholipases D1/2 suggest roles in the transport of fatty acids between the cytosol and membrane compartments [44], the inducement of membrane curvature [45], the cleavage of membrane lipids [46], and the packing of lipids [47]. The cleavage of membrane lipids and the packing of lipids in response to lipid-packing defects suggests that a-syn may be able to remodel membranes [43]. Additionally, a-syn has been shown to have a chaperoning function in the assembly of synaptic SNARE complexes in mice [48]. This function may be in addition to other chaperone activity, a hypothesis brought about by a-syn's homology with the 14-3-3 family of molecular chaperone proteins and suppression of the aggregation of thermally denatured proteins [49, 50]. A-syn has been shown to inhibit ER-Golgi trafficking, an effect that is amplified by clinical mutations in *SNCA* [51, 52]. Most relevant to PD, a-syn reduces the phosphorylation of tyrosine hydroxylase and stabilizes its inactive state, thereby inhibiting dopamine synthesis [53]. Additionally, a-syn affects the vesicular transporter of dopamine, altering its homeostasis *in vitro* [54]. Proposed functions of a-syn also include regulation of glucose, suppression of apoptosis,

modulation of calmodulin activity, antioxidation, neuronal differentiation, and transcriptional regulation [55].

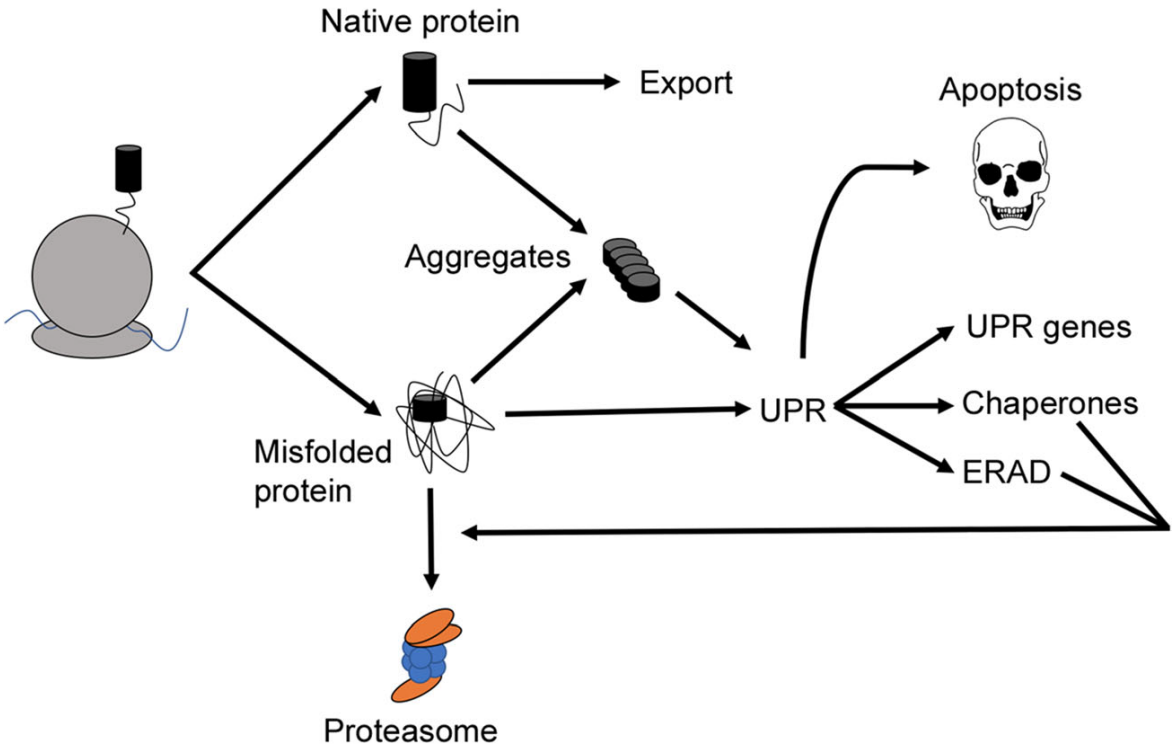

Figure 2. Pathway of protein throughout the ER. Protein is synthesized in the rough ER by ribosomes. Native protein is predominantly exported, while some can aggregate. Misfolded protein aggregates are sent to proteasome for degradation. Misfolded protein and aggregates promote the UPR, which includes UPR associated gene regulation, ERAD pathway, chaperone response, and apoptosis to mitigate the effects of toxic aggregates.

1.5.2 Post-translational modifications

Post-translational modifications (PTMs) play a key role in protein structure and function. They increase the diversity and complexity of protein function by shifting tertiary structures. PTMs involved in PD include, but are not limited to, **ubiquitination**, the attachment of ubiquitin that signals the proteasomal degradation pathway to target the tagged protein; **phosphorylation**, attaching a phosphate group that may alter the activity or structure of a protein; **acetylation**, the attachment of an acetyl group affects protein stability and localization; **glycosylation**, the attachment of a carbohydrate that affects protein folding and stability; **NEDDylation**, the attachment of the ubiquitin-like protein NEDD8 that inactivates proteins and tags them for degradation; and **SUMOylation** the attachment of small ubiquitin-like modifier proteins that affects protein stability, activity, and localization. They play a crucial role in many cellular functions and need to be tightly regulated. Any disruption in PTMs can lead to a cascade of pathological events that can disrupt cellular proteostasis [56].

A-syn's primary structure contains five phosphorylation sites, Ser87, Ser129, Tyr125, Tyr133, and Tyr 136, that can be phosphorylated by different protein kinases [57]. Phosphorylation of Ser129 occurs at a frequency of approximately 4% in normal physiological conditions, but several studies have shown that the Ser129 phosphorylated form of a-syn in LBs reaches approximately 90% [58]. This evidence has propelled the hypothesis that the hyper-phosphorylation of Ser129 has a strong connection with the aggregation of a-syn. Phosphorylation of the other residues also increases in PD patients with the exception of Tyr125, which shows lower phosphorylation in PD patients as compared to the healthy control individuals [59]. The phosphorylation of Ser129 has also

been shown to play a cytotoxic role by facilitating trafficking between the cytosol and the nucleus [60]. In the nucleus the Ser129-a-syn interacts with histones and interferes with histone deacetylase activity [60]. Increased histone acetylation has been associated with PD, however, there have been conflicting claims that indicate HDAC inhibitors are neuroprotective [61].

Targeted protein degradation is necessary for maintaining cellular proteostasis. Ubiquitination is an enzymatically catalyzed PTM that targets and tags proteins for degradation [62]. Ubiquitination consists of three enzyme classes: Ub activating enzyme (E1), Ub conjugating enzyme (E2), and Ub ligase (E3) [63]. Proteins tagged for degradation can be mono-ubiquitinated or poly-ubiquitinated where the latter targets proteins to the 26S proteasome for degradation. Parkin, a protein associated with PD, is an E3 ubiquitin ligase that tags misfolded proteins. Further, PINK1 (PTEN induced putative kinase 1) is a mitochondrial Ser/Thr kinase that activates and recruits Parkin by phosphorylation. Studies have shown that PINK1 phosphorylates Parkin at serine 65 and recruits Parkin to the mitochondria so that it can ubiquitinate misfolded proteins [64, 65]. Parkin and PINK1 mutations or dysfunction occur in cases of early-onset familial PD, as well as in sporadic PD. This dysfunction can cause the accumulation of ROS in the mitochondria and hinder cellular proteostasis. Phosphorylation of Parkin at Tyr143 inactivates its E3 function and has been reported in postmortem PD brain samples [66]. Parkin ubiquitinates p62, which regulates protein quality control by transporting polyubiquitinated proteins for proteasomal degradation and is a marker for aggregation [31, 67]. Dysfunction Parkin activity can result in unchecked ubiquitination of p62 and the accumulation of aggregated proteins.

Phosphorylation, nitration, and SUMOylation of a-syn are altered in PD and are potential biomarkers for the disease [68]. Tyrosine-125 phosphorylation and Y39 nitration have been shown to be significantly increased in PD patients compared to healthy individuals, whereas SUMO-1 was significantly down in PD patients [68]. Interestingly, SUMOylation reduces a-syn aggregation *in vitro* and *in vivo* [69]. This study presents an interesting application of PTMs as both biomarkers for PD.

1.5.3 ER Stress

PD pathology induces ER stress and inhibits its response mechanism, exacerbating the effect. Misfolded a-syn accumulates in various cell compartments including the ER lumen [70] and a-syn has been shown to inhibit the UPR and ERAD, resulting in apoptosis (Figure 2) [71]. The ERAD exports targeted proteins to the ubiquitin proteosome system (UPS) in the cytosol and the ERAD E3-ligase, HRD1, is elevated in Parkinsonian brain tissue [72]. A-syn inhibits the ERAD pathway, promoting pathogenesis, in a similar and parallel manner as the PD protein, Parkin, inhibits the UPS. Cultured cells treated with Rotenone, an agent used to model PD conditions *in vitro* and *in vivo*, show increased phosphorylation of ER stress markers as well as upregulated UPR components and ER chaperones [73].

1.5.4 Autophagy and mitophagy

Autophagy involves the efficient and selective degradation of misfolded or aggregated proteins as well as damaged organelles [74]. Autophagy is a lysosomal-mediated degradation pathway that is activated under stress (Figure 3) [75]. This process begins with the formation of the double-membrane autophagosome, which engulfs and degrades damaged material [76]. The process is driven by a group of autophagy-related proteins

(ATGs) that are responsible for autophagosome formation, vesicle expansion, infusion with the lysosome, and cargo recruitment [77]. Defects in autophagy are associated with the pathogenesis of many neurodegenerative diseases [78]. It is evident that quality control of the autophagic pathway is vital to the maintenance of proteostasis since the alteration of various regulatory steps in autophagy may lead to global dysfunction in cells [79]. In neurodegenerative disorders, dysfunction in the autophagy pathway leads to accumulation of pathogenic proteins and damaged organelles (Figure 3).

In PD, autophagy can be inhibited by A53T and A30P mutants of a-syn, which block the uptake of damaged material by the lysosome [80]. This inhibition is a key aspect in the pathogenesis and progression of PD. Similarly, mitophagy can be caused by elevated ROS levels and decreased lysosomal-autophagic degradation resulting from mutations in DJ-1, a PD-related protein involved protecting against oxidative stress [81]. Many PD related proteins such as Parkin, PINK1, and Htra2 (Park13) have been shown to be associated with mitochondrial dysfunction, which is exacerbated when the enlarged, damaged mitochondria cannot be removed by mitophagy [82] [64]. Recent therapeutic strategies have been focused on key autophagy-lysosomal pathways (ALP) as it has been suggested that defects in autophagy or mitophagy can be sufficient to cause PD [83].

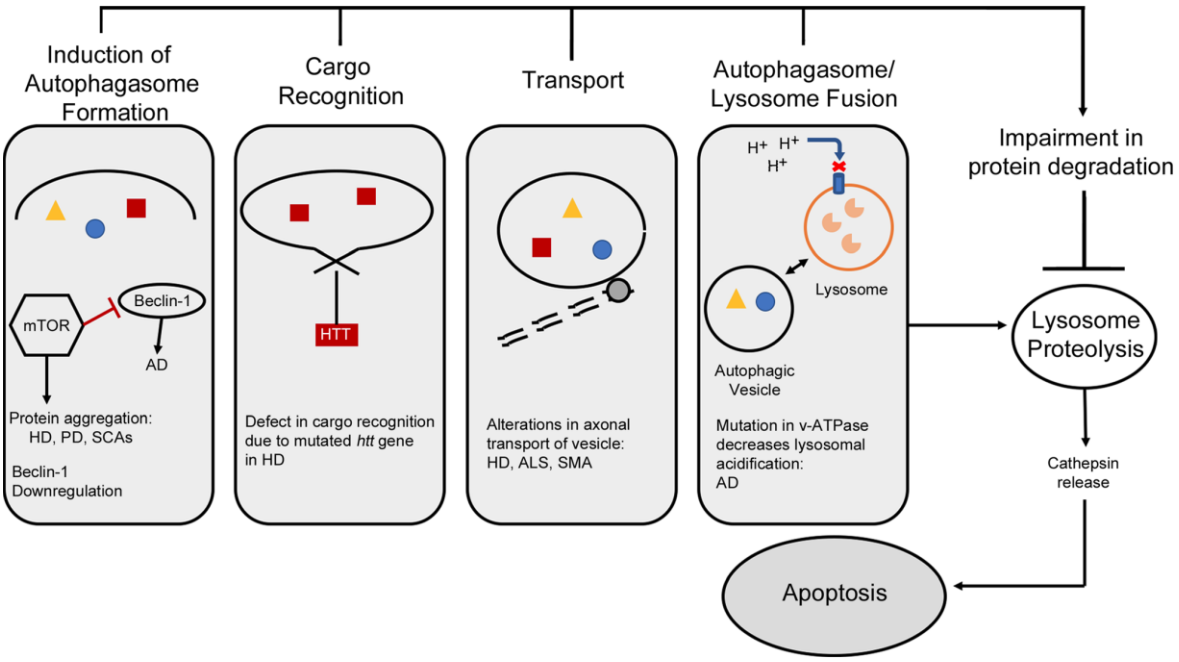

Figure 3 Neurodegenerative disorders alter specific steps in the autophagic pathway, which ultimately leads to neuronal cell death. The altered steps include reduced induction levels due to protein aggregation and defective mTOR inhibition; Defects in cargo recognition resulting in accumulation of toxic proteins; Mutation in VCP leads to inhibited transport of autophagic vesicle in ALS; Defects in lysosome/autophagosome fusion and acidification. All defective steps, leading to impairment of protein degradation by lysosomal degradation, ultimately leads to the release of cathepsin's and apoptosis. Huntington's Disease (HD); Alzheimer's Disease (AD); Parkinson's Disease (PD); Spinocerebellar ataxia (SCA); Spinal muscular atrophy (SMA); Dementia with Lewy Bodies (DLB); Amyotrophic lateral sclerosis (ALS); Valosin-containing protein (VCP)

1.5.5 Mitochondrial dysfunction and oxidative stress

Mitochondrial proteostasis is critical to the proper functioning of the cells' "powerhouses". In highly metabolic post-mitotic neurons, mitochondrial function is key due to ATP demand and the organelle's role in regulating apoptosis. The major source of mitochondrial dysfunction is oxidative stress via ROS, which are produced in the mitochondria, but are tightly regulated through antioxidant pathways. Dysfunctioning mitochondria either produce more ROS or are unable to sustain proper regulation. ROS, extremely reactive molecules containing one or more free or unpaired electrons, can damage lipids, DNA, and proteins. ROS toxicity provides a link between mitochondrial proteostasis, which regulates oxidative stress, to cellular proteostasis, which can be damaged and disrupted by ROS.

The consequences of oxidative stress are overarching and devastating to the cell. Due to its deleterious effects, oxidative stress is a key element in elucidating the link between neurodegenerative diseases and age [84]. In relation to neurodegenerative diseases and proteostasis, oxidative stress can alter the transcription and translation of pathogenic proteins by reacting with transcription factors or altering enzymes and their activities. ROS are also known to affect components of autophagy and proteosome degradation. A feedback loop is therefore obvious where these effects propagate the aggregation of disease proteins, which in turn have been shown to cause mitochondrial dysfunction, leading to oxidative stress and disease progression (Figure 1).

The PD associated proteins PINK1, PARK13, Parkin, DJ-1 and a-syn have been shown to regulate mitochondrial function. PINK1, along with its targets Parkin and Miro, regulate mitophagy in response to mitochondrial dysfunction. PARK13, also activated by PINK1, is a protease, which removes damaged mitochondrial proteins. PARK13mutations

have been associated with oxidative stress and PD phenotypes, while overexpression and knockout mouse models have shown both neuroprotection and PD phenotypes [85, 86]. DJ-1, a cytosolic antioxidant protein, can be recruited to damaged mitochondria and induce mitophagy [87]. The accumulation of a-syn on the outer and inner membranes of mitochondria in dopaminergic neurons decreased mitochondrial Complex I activity and induced oxidative stress by increased ROS [88]. Interestingly, under oxidative stress, a-syn upregulates PGC1-alpha, the "master" mitochondrial biogenesis regulator, which may represent a therapeutic target for neurodegenerative diseases [89].

1.6 Genetics

Genetic lesions account for between 5% and 10% of PD cases [90]. Mutations in genes such as *SNCA, LRRK2, PARK2, PINK1,* and *GBA,* among others, are associated with both early- and late-onset PD [91]. However, monozygotic and dizygotic twin studies have estimated the heritability of PD to be approximately 30% [91]. This, combined with most cases being idiopathic, suggests that even in familial PD, genetics is just one of many risk factors.

1.6.1 SNCA

SNCA is one of the leading topics within the field PD since 1997, when the A53T mutation was identified as PD-related and a-syn was discovered as a major component of LBs (28,41). Interestingly, *SNCA* mutations can be divided into a hierarchy of age-related disease onset. The *SNCA* point mutations A53T, G51D and *SNCA* triplication events, are associated with the early-onset PD [2, 92]. *SNCA* gene duplication is associated with both early- and late-onset PD [2, 92]. The A30P, E46K, and H50Q point mutations are

associated with late-onset PD [2, 92]. Combined, these findings suggest that age-dependent disease onset and neuronal loss, is linked to a-syn levels within neurons and/or mutations that may alter a-syn characteristics.

Although a-syn is the most widely studied PD-related protein, it is still unclear how *SNCA* perturbations affect PD pathology. Do *SNCA* mutations create neurotoxic forms of a-syn? What are those species? Does increased concentration of a-syn affect the cell by the same pathways as a-syn containing clinical mutations? By what means do neurons combat a-syn toxicity and how might that ability diminish over time? These are just some of the fundamental questions whose answers may lead to major breakthroughs in understanding, diagnosing, and treating PD.

1.6.2 LRRK2

LRRK2 encodes for leucine rich repeat kinase 2, a multi-functional cytosolic protein associated with endosomes, lysosomes, autophagosomes, mitochondria, Golgi, transport vesicles, and the plasma membrane [93]. Autosomal dominant missense mutations in *LRRK2* have been shown to be involved in sporadic PD, while seven-point mutations have been shown in familial PD [94, 95]. Although the normal biological function of *LRRK2* is not fully understood, its mutations impair chaperone-mediated autophagy, which results in the accumulation of its substrates, one of which is a-syn [96]. Additionally, the most common point mutation of *LRRK2*, G2019S, is observed in both sporadic and familial PD patients and increases LRRK2 catalytic activity which leads to neuronal toxicity and loss of dopaminergic neurons [97].

1.6.3 PINK1

PINK1 encodes for PTEN-induced putative kinase, a serine-threonine kinase. Mutations in *PINK1* are the second most common cause of early-onset PD, with over 50 PD-related mutations reported [98, 99]. Mutations in *PINK1* have been shown to result in mitochondrial dysfunction, a key PD hallmark [83, 100]. PINK1 phosphorylates and thereby increases the activity of Parkin, Miro and PARK13 which play important roles in protecting against mitochondrial dysfunction [101, 102]. In fact, several mutations in the neuroprotective *PARK13* have been associated with familial PD [103]. The phosphorylation of Parkin and Miro by PINK1 causes the arrest of mitochondrial motion, thereby facilitating mitophagy [104]. The removal of the damaged mitochondria is extremely important for neurons and preventing PD pathogenesis [83].

1.6.4 PARK2

PARK2 encodes for Parkin, a cytosolic E3 ubiquitin ligase which targets mitochondrial proteins for proteosomal degradation and with over 170 mutations reported, it is the most common cause of early-onset familial PD [105]. Parkin induces AT5-dependent mitophagy by recruiting ubiquitin and p62 to the mitochondrial membrane, resulting in damaged mitochondria being taken up by the autophagosome [83, 100]. Mutations in *PARK2* result in a failure of this mechanism to induce mitophagy. While the effects of the numerous mutations must vary, they may include enhanced aggregation, misfolding, dysfunctional activation, or ineffective binding to E2 co-enzymes, ubiquitin, or substrates [106].

1.6.5 GBA

GBA encodes for glucocerebrosidase, a 497-residue lysosomal hydrolase that catalyzes the metabolism of the glycolipid glucosylceramide to ceramide and glucose [107]. The autosomal recessive mutations found in the *GBA* gene were first linked to the lysosomal storage disorder Gaucher's Disease (GD) [108]. The improper functioning of this enzyme may be linked to lysosomal dysfunction and its mutations have been shown to cause a-syn accumulation through autophagic inhibition [109]. Interestingly, PD-related genes *SNCA* and *LRRK2* are also involved in the endolysosomal trafficking system and their mutations have been linked to the aggregation of a-syn and familial PD [110]. Similar to PD, Gaucher's disease is highly variable and the spectrum of disease partially correlating with residual enzyme activity [111]. More than 200 *GBA* mutations, most resulting in a single amino acid change, have been reported in GD patients with N370S and L444P being the more common [108, 112]. Many clinical studies have found a trend of GD patients developing PD in later stages of prognosis. Furthermore, healthy relatives displayed an increase in frequency of Parkinsonism [113]. *GBA* can numerically be the most important genetic factor for the development of PD, evident from the fact that about 5%-10% of PD patients have *GBA* mutations [114]. However, the role of these mutations in PD pathogenesis is not fully understood. Protein aggregates, like those found in Lewy bodies, have been discovered in GD patients. Combined these findings lead to the hypothesis that mutations in *GBA* might constitute a genetic risk factor when it comes to developing PD.

1.7 Specific Aims

The primary objective of this research was to study the relationship between primary structural variations of a-syn and its subcellular multimerization *in vivo*, its secondary and tertiary structures *in silico*, and its associated neurotoxicity.

Additional collaborative projects included: (1) Elucidating the effect of clinical *SNCA* mutations on a-syn subcellular species distribution *in vivo*, (2) Discovering genetic targets of PD-associated miRNAs, and (3) Elucidating the possible effects of SARS-CoV2 on PD-associated molecular and cellular mechanisms and ultimately the effect of the COVID-19 pandemic on PD patients.

2 Materials and Methods

2.1 Buffers

Universal buffers and their composition used in various protocols are listed below. Specific buffers are mentioned together with the specific protocols.

2.1.1 Lysis buffer

RIPA buffer (Radio Immuno Precipitation Assay buffer)

150mM NaCl, 1% NP-40, 50mM Tris at pH 8.0, 0.5% Sodium deoxycholate, and 0.1% Sodium dodecyl sulfate (SDS).

2.1.2 Western blot analysis buffers

The recipes for buffers used for western blot analysis including buffers required for pouring polyacrylamide gels are listed here.

SDS Polyacrylamide gel

Component	**Stacking gel 4%**	**Resolving gel 12%**
Deionized water (DIW)	6.15ml	3.4ml
30% Acrylamide solution	1.25ml	4ml
1.5M Tris buffer pH 8.8	-	2.5ml
0.5M Tris buffer 6.8	2.5ml	-
10% SDS	100µl	100µl
10% APS (Ammonium persulfate)	50µl	50µl
TEMED	10µl	5µl

30% Acrylamide solution is 29.2% acrylamide and 0.8% N',N'-bis-methylene-acrylamide.

Tris Buffer (1.5M at pH 8.8, 0.5M at pH 6.8)

Tris base 54.46g and 18.15g was dissolved in DIW; pH was adjusted with 6N HCl to 8.8 and 6.8 respectively to make up the volume to 300ml with DIW.

Running Buffer (10X) and Transfer Buffer (10X)

Stock solutions (10X) for running and transfer buffers were prepared with 3.84M Glycine and 0.5M tris base. For running buffer 2% was added.

Tris Buffer Saline (TBS) (10X)

TBS stock solution (10X) was prepared by dissolving 160.1g NaCl and 48.45g tris-HCl; pH was adjusted to 7.6 with HCl to make 2L stock buffer.

For **TBS-T**: 100ml of TBS (10X) + 900ml ultra-pure water + 1ml Tween-20

Laemmli Loading buffer

50mM Tris buffer at pH 6.8, 2% SDS, 10% Glycerol, 0.2% Bromophenol Blue, and 5% ß-mercaptoethanol (BME).

2.2 Bacteriological techniques

2.2.1 Bacterial strains

***E. coli* DH5a;** (F^-/*endA1 hsdR17*($r_k^-m_k^+$), supE44, thi1, rec*A1*, *gyrA*(Nal^r), *gyrA96*(Nal^r), *relA1*, Δ(*lacZYA=argF*) U169, *deoR* (Φ80*dlac* Δ(*lacZ*) *M15*)) was used for propagation and preparation of plasmid DNA.

2.2.2 List of vectors

pJET 1.2/blunt (Appendix) (Thermo Fisher Scientific) was used for routine subcloning and DNA manipulations.

pcDNA3^{TM} (Appendix) (Thermo Fisher Scientific) was used for heterologous protein expression and stable cell line generation in mammalian cells.

2.2.3 Growth media and growth conditions

Bacteria were grown using Lysogeny broth (LB – 1% Tryptone, 0.5% Yeast extract, and 1% NaCl) in liquid cultures or LB-agar (1.5% agar added to LB) as colonies. Super optimal broth with catabolite repression (SOC – 2% Tryptone, 0.5% Yeast extract, 0.02% KCl, 0.25% $MgSO_4$, 0.06% NaCl, and 0.36% Glucose; pH 7.0) was used during transformation for recovery of transformants. Liquid cultures for DH5a were grown in a shaking incubator at 270 rpm at 37°C. Colonies were grown on LB-agar plates incubated overnight in an incubator at 37°C. Colonies were picked using sterile pipette tips and added to culture tubes for growing liquid cultures with Ampicillin (100μg/ml) selection.

2.3 Cloning

2.3.1 Primers

Primers used for various cloning experiments are listed below. Restriction endonuclease (RE) sites are underlined and in italics.

Name of the primer (*RE site*)	**Sequence with *RE site***
pcDNA3 forward	CGCAAATGGGCGGTAGGCGTGTACG
pcDNA3 reverse	TGGCACCTTCCAGGGTCAAGGAAGG
pJET1.2 forward	CGACTCACTATAGGGAGAGCGGC
pJET1.2 reverse	AAGAACATCGATTTTCCATGGCAG
SNCA forward (*KpnI*)	AT*GGTACC*ATGGATGTATTCATGAAAGG
SNCA reverse (*XhoI*)	AT*CTCGAG*TTAGGCTTCAGGTTCGTAGTCTTG

2.3.2 Polymerase Chain Reaction (PCR)

PCR was performed to screen for colonies of positive transformants by colony PCR. *Taq* PCR Master mix kit (Qiagen, Inc.) was used to perform colony PCR for screening positive transformants. Colonies grown on LB-agar were picked using sterile pipette tips and added to culture tubes with LB media with Ampicillin (100µg/ml). Cultures were grown overnight at 37°C in an incubator. 1µl of liquid culture was used as a template in each PCR. Specific primer pairs were used to confirm the presence and/or orientation of the gene product. The reactions were set up as follows:

Component	**per reaction (µl)**
PCR Master Mix (2X)	10
Forward primer	1
Reverse primer	1
Template	1
DDW	7

Reactions were set up with the program on the following page

Step	Temperature (°C)	Time
1	95	2 min.
2	94	1 min.
3	58	1 min.
4	72	1 min.
5	Go to step 2, 34 times	
6	72	5 min.
7	4	Until removed

2.3.3 Nucleic acid isolations

All DNA isolations were performed using commercial kits following the manufacturer's protocol. GeneJET plasmid miniprep kit (Thermo Fisher Scientific) was used for isolation of plasmid DNA to be used for mammalian cell transfection. GeneJET Gel Extraction kit (Thermo Fisher Scientific) was used to isolate purified DNA from restriction endonuclease digestions for ligation into pcDNA3 vector.

2.3.4 Nucleic acid measurement

Plasmid DNA and digested DNA concentrations were determined by using a NanoDrop 2000 Fluorospectrometer (Thermo Fisher Scientific) for pcDNA3 ligation and mammalian transfection.

2.3.5 Nucleic acid manipulation

2.3.5.1 pJET cloning

GeneArt Strings DNA Fragments (Thermo Fisher Scientific) were cloned by blunt end cloning into pJET 1.2 vector using the CloneJET PCR cloning kit (Thermo Fisher Scientific) according to the manufacturer's instructions. Ligated products were transformed into *E. coli* DH5a cells. Colonies were grown under Ampicillin (100µg/ml) selection and screened for positive transformants.

2.3.5.2 Restriction endonuclease digestions

Restriction endonuclease digests of isolated (2.3.3) DNA were performed as follows:

Component	**µl per reaction**
Water (Nuclease-free)	3
10X CutSmart Buffer (New England Biolabs)	1
DNA	5
KpnI-HF (New England Biolabs)	0.5
XhoI (New England Biolabs)	0.5

Digestions were carried out for 30 minutes to confirm positive transformants or up to 2 hours for purification and ligation into pcDNA3.

2.3.5.3 Ligations

Ligation reactions were setup as follows:

Component	**µl per reaction**
Digested insert	8
Digested pcDNA3 vector (10-50ng)	0.5
T4 DNA ligase (New England Biolabs)	0.5
T4 DNA ligase buffer (10X) (New England Biolabs)	1

Ligations were carried out for 1 hour at room temperature and used for transformation.

2.3.6 Bacterial transformations

DH5α cells were thawed on ice and 5µl of ligation reaction was added to the cells. The transformation mix was incubated on ice for 30 minutes. The cells were then heat shocked at 42°C for 45 seconds immediately followed by 2 minutes on ice. 900µl SOC media was then added to the cells, which were then incubated at 37°C for 1 hour with shaking. Cells were spread onto LB-agar plates with Ampicillin (100µg/ml) and incubated at 37°C for 16-20 hours. Colonies were first screened by colony PCR (2.3.2). 1-3 positive clones were used for DNA isolation (2.3.3) followed by restriction endonuclease digestion (2.3.5.2). Digestions were analyzed by agarose gel electrophoresis to verify the expected DNA fragment size. Confirmed transformants were verified by DNA sequencing at the Yale DNA analysis facility.

2.3.7 Agarose gel electrophoresis

DNA was analyzed by 1% agarose gel electrophoresis. The DNA was mixed with loading buffer (6X loading buffer: 30% glycerol, 0.25% bromophenol blue) and ethidium bromide to visualize the DNA fragments on a UV transilluminator. Tris-acetate-EDTA buffer (TAE: 40mM Tris-base, 20mM glacial acetic acid, 1mM EDTA at pH 8.0) was used to make the gels and as the running buffer. The gels were prepared by melting the agarose into 1X TAE buffer by microwave oven. Ethidium bromide was then added, and the gel solidified in a gel cassette. HiLo DNA marker (Minnesota Molecular) was used as a size reference (Appendix B-1).

2.3.8 List of constructs generated

Wild-type (WT) *SNCA* was cloned into pcDNA3 by previous laboratory members. pcDNA3 was a generous gift from Dr. Laura Schramm, Department of Biological Sciences, St. John's University.

Name of clone (*flanking RE sites*)	**Application**
pJET GTK (*KpnI/XhoI*)	cloning
pJET KLK (*KpnI/XhoI*)	cloning
pJET KGV (*KpnI/XhoI*)	cloning
pJET EGR (*KpnI/XhoI*)	cloning
pcDNA3 GTK (*KpnI/XhoI*)	mammalian cell transfection
pcDNA3 KLK (*KpnI/XhoI*)	mammalian cell transfection
pcDNA3 KGV (*KpnI/XhoI*)	mammalian cell transfection
pcDNA3 EGR (*KpnI/XhoI*)	mammalian cell transfection
pJET 5'-3'NLS *SNCA*	cloning
pJET 5'-3' NLC *SNCA*	cloning
pJET 5' NLS *SNCA*	cloning
pJET 5' NLC *SNCA*	cloning
pJET 3' NLS *SNCA*	cloning
pJET 3' NLC *SNCA*	cloning
pcDNA3 5'-3' NLS *SNCA*	mammalian cell transfection
pcDNA3 5'-3' NLC *SNCA*	mammalian cell transfection
pcDNA3 5' NLS *SNCA*	mammalian cell transfection
pcDNA3 5' NLC *SNCA*	mammalian cell transfection
pcDNA3 3' NLS *SNCA*	mammalian cell transfection
pcDNA3 3' NLC *SNCA*	mammalian cell transfection
pJET His-EK-G51D *SNCA*	Dr. Rashed Abdullah's thesis project
pJET His-EK-H50Q *SNCA*	Dr. Rashed Abdullah's thesis project
pcDNA3 His-EK-G51D *SNCA*	Dr. Rashed Abdullah's thesis project
pcDNA3 His-EK-G51D *SNCA*	Dr. Rashed Abdullah's thesis project

2.4 RNA processing and analysis

All RNA samples were quantified and quality controlled by Nanodrop 2000 (Thermo Fisher Scientific).

2.4.1 RNA isolation

RNA isolations from mammalian cells were performed 24 hours post-transfection or from stable cell lines in triplicate. Total RNA was extracted by following the manufacturer's instructions of GeneJET RNA purification kit.

2.4.2 cDNA synthesis

RNA samples were treated with 1 unit of DNase I/µg of RNA (Thermo Fisher Scientific) for 30 minutes at 37°C followed by 10 minutes at 65°C with 50mM EDTA. cDNA was synthesized by RevertAid First Strand cDNA Synthesis kit and an oligo dT primer (Thermo Fisher Scientific) by following the manufacturer's instructions.

2.4.3 Real-time qPCR

All qRT-PCR were done with PerfeCTa SYBR GREEN Supermix for IQ containing AccuStart Taq DNA Polymerase (Quanta Biosciences) for 45 cycles followed by dissociation steps with MyiQ Single color Real-Time PCR Detection System (Bio-Rad). Reactions were done using 1µM gene-specific primers. GAPDH was used to normalize Cq values in calculating relative expression. The qRT-PCR protocol included initial denaturation at 95°C for 2 minutes followed by 35 denaturation cycles at 95°C for 15 seconds, annealing at 60°C for 45 seconds, extension at 72°C for 40 seconds, and finally dissociation steps of in increments of 0.5°C.

2.5 Tissue culture and processing

2.5.1 Cell culture and stock information

BE(2)-M17 human neuroblastoma cells (ATCC CRL-2267) and SH-SY5Y human neuroblastoma cells (ATCC CRL-2266) were cultured in a base medium (Thermo Fisher Scientific) supplemented with 2mM GlutaMax (Thermo Fisher Scientific), 1 mM sodium pyruvate (Thermo Fisher Scientific), 100 µM Non-essential amino acids solution (Thermo Fisher Scientific), and 10% fetal bovine serum (Gemini Bio-Products) in a 5% CO_2 incubator at 37°C. Cells were sub-cultured every 4-5 days. Cells were cryopreserved in full medium with 5% DMSO.

2.5.2 Transfections

Transfections were performed at 90% confluency one day after seeding cells in six-well plates at $5x10^5$ cells per well or in 10cm plates with $3x10^6$ cells per plate. For each six-well transfection, 1 µg plasmid DNA was mixed with 50µl Opti-MEM (Thermo Fisher Scientific), and, separately, 1.25µl Lipfectamine-2000 (Invitrogen) was mixed with 50µl Opti-MEM. For transfections in 10 cm plates, 4 µg plasmid DNA was used, and all other quantities were increased proportionally. After 5 minutes incubating at RT, both solutions were mixed and incubated for 15 minutes at RT. The transfection mix was diluted with 2ml Opti-MEM and added to cells for transfection. Cells were incubated at 37°C in 5% CO_2 for 4-6 hours before transfection media was replaced with full media. The cells were harvested 48 hours after transfection for further experimentation.

2.5.3 Stable cell line generation

To create stable cell lines, cells were exposed to antibiotic selection beginning one day after transfection. Antibiotic concentration was determined by a kill curve assay and added to complete medium. Cells were passaged after 7 days for 4 weeks and 8 vials per passage were frozen in liquid nitrogen. An aliquot of cells was analyzed at each passage to observe protein expression by western blot.

Cell line	Selection	Passages
pcDNA3 empty vector in M17D cells	G418	4
pcDNA3 WT-*SNCA* in M17D cells	G418	4
pcDNA3 GTK in M17D cells	G418	4
pcDNA3 KLK in M17D cells	G418	4
pcDNA3 KGV in M17D cells	G418	4
pcDNA3 EGR in M17D cells	G418	4
pcDNA3 empty vector in SH-SY5Y cells	G418	4
pcDNA3 WT-*SNCA* in SH-SY5Y cells	G418	4
pcDNA3 GTK in SH-SY5Y cells	G418	4
pcDNA3 KLK in SH-SY5Y cells	G418	4
pcDNA3 KGV in SH-SY5Y cells	G418	4
pcDNA3 EGR in SH-SY5Y cells	G418	4
pcDNA3 His-EK G51D in SH-SY5Y cells	G418	4
pcDNA3 His-EK H50Q in SH-SY5Y cells	G418	4

2.5.4 Crosslinking of cells

Prior to cells being lysed or fractionated for western blot analysis, 80-90% confluent cells were trypsinized, washed in ice-cold PBS and pelleted by centrifugation at 500xg at 4°C. Supernatant was discarded. Cells were resuspended in 8ml ice-cold PBS and placed onto fresh 10 cm tissue culture dish. The cells were exposed to 150 mJ of energy by UV crosslinker (VWR) and removed to be collected by centrifugation.

2.5.5 Whole cell lysate preparation

Whole cell lysates were prepared with RIPA lysis buffer with Halt Protease Inhibitor Cocktail (Thermo Fisher Scientific) and EDTA. Cells were vortexed with lysis buffer (400µl/10-12x10^6 cells) and incubated for 10 minutes on ice. The mixture was centrifuged at 16,000xg at 4°C for 5 minutes and the supernatant was collected.

2.5.6 Subcellular protein fractionation

The following protocol was performed using the Subcellular Protein Fractionation Kit for Cultured Cells (Thermo Fisher Scientific). Buffer volume used varied proportionally to cell pellet volume:

Cell pellet volume (µl)	CEB	MEB	NEB	NEB+$CaCl_2$+MNase	PEB
10	100	100	50	50	50
20	200	200	100	100	100
50	500	500	250	250	250
100	1000	1000	500	500	500

The cell pellet was gently resuspended in ice-cold cytoplasmic extraction buffer (CEB) containing protease inhibitors and incubated at 4°C for 10 minutes. The tube was centrifuged at 500xg at 4°C for 5 minutes and the supernatant (cytoplasmic extract) was collected on ice. The pellet was resuspended in ice-cold membrane extraction buffer (MEB) containing protease inhibitors and incubated at 4°C for 10 minutes. The tube was centrifuged at 3,000xg at 4°C for 5 minutes and the supernatant (membrane extract) was collected on ice. The pellet was resuspended in ice-cold nuclear extraction buffer (NEB) containing protease inhibitors and incubated at 4°C for 30 minutes. The tube was centrifuged at 5,000xg for 5 minutes. The supernatant (nuclear soluble extract) was collected on ice. The pellet was resuspended in RT NEB containing protease inhibitors,

$CaCl_2$ (5µl 100mM per 100µl NEB), and micrococcal nuclease (MNase, 3µl per 100µl NEB) and incubated at RT for 20 minutes with gentle mixing. The tube was centrifuged at 16,000xg for 5 minutes. The supernatant (chromatin bound) was collected on ice. The pellet was resuspended in RT pellet extraction buffer (PEB) containing protease inhibitors and incubated at RT for 10 minutes. The tube was centrifuged at 16,000xg for 5 minutes. The supernatant (cytoskeletal extract) was collected. Fractions were kept on ice for same-day use or stored at -80°C for long-term storage.

2.6 Western blot analysis

Sample preparation: Freshly isolated whole-cell lysate, fractions or thawed samples were mixed with 5X reduced dye and boiled at 95°C for 5 minutes. Samples were chilled on ice for 1 minute and quickly centrifuged.

SDS-PAGE and Blotting: Samples were run on 12% polyacrylamide resolving gels alongside PageRuler Unstained Broad Range Protein Ladder (Bio-Rad) at 100V for 80 minutes using the Mini-Protean Tetra system (Bio-Rad) in running buffer. The proteins were transferred to PVDF membranes (Thermo Fisher Scientific) using the Trans-Blot SD Semi-Dry Transfer Cell (Bio-Rad) at 20V for 42 minutes in transfer buffer. Membranes were then blocked by shaking in 5% non-fat dry milk and TBS-T for 1 hour at RT. After washing with TBS-T, the membranes were incubated at 4°C overnight in 2.5% nonfat dry milk and TBS-T containing the appropriate primary antibody at the appropriate dilution. The membranes were then washed with TBS-T three times for 10 minutes and incubated for 1 hour at RT with the appropriate secondary antibody at the appropriate dilution. The membranes were washed with TBS-T three times for 10 minutes each. The membrane was

developed with Pierce ECL Western Blot Substrate (Thermo Fisher Scientific) and the signal was detected by the Molecular Imager Chemi Doc XRS1 imaging system (Bio-Rad). ImageJ software (NIH) was used to analyze Western blot images.

Primary Antibody (1:10,000)	**Manufacturer**
Rabbit polyclonal anti-*SNCA*	Abcam
Goat polyclonal anti-LDH	Fitzgerald Industries
Rabbit polyclonal anti-EGFR	Cell Signaling
Rabbit monoclonal anti-SP1	Cell Signaling
Rabbit polyclonal anti-Histone H3	Cell Signaling
Goat polyclonal anti-Tim23	Santa Cruz Biotechnology
Rabbit polyclonal anti-GAPDH	Santa Cruz Biotechnology
Secondary Antibody (1:5,000)	**Manufacturer**
Goat anti-Rabbit IgG (H+L)-HRP	Jackson Immunoresearch
Donkey anti-Goat IgG (H+L)-HRP	Jackson Immunoresearch
Precision Protein StrepTactin-HRP	Bio-Rad

2.7 Assays

2.7.1 Cell viability assay

The neutral red uptake assay was used to measure cell viability beginning 48 hours post transfection. Cells were washed with PBS and incubated for 2 hours in 100µl neutral red working solution (40µg/ml). Cells were washed with PBS and neutral red was extracted with 150µl destain solution (50% ethanol, 1% glacial acetic acid, 49% deionized water) by shaking for 10 minutes. Absorbance was measured at 540nm using a microplate reader.

2.7.2 Kill curve assay for antibiotic selection

M17D and SH-SY5Y cells were seeded in 24-well plates with $2.5x10^5$ cells per well. One day after seeding, cells were treated in triplicate with serial diluted concentrations of Geneticin (Invitrogen) (0.13, 0.25, 0.5, 1, 2, 4, 8 mg/ml) or puromycin (Invitrogen) (12.5, 25, 50, 100, 200, 400, 800 μg/ml).

2.7.3 Bradford assay

Protein concentrations of samples to be used for western blots were measured using Protein Assay Kit II and DC Protein Assay Kit (Bio-Rad). Bovine serum albumin was used to prepare standard solutions from 0.05 to 1.0 mg/ml and samples were diluted from 1:10 to 1:100. Assays were measured by Epoch microplate spectrophotometer (BioTeck) on 96-well plates.

2.8 Molecular dynamics simulations

All molecular dynamics simulations were performed by Dr. Francisco Vazquez, Department of Chemistry, St. John's University, on the full WT, KGV, and GTK a-syn proteins. Gaussian accelerated molecular dynamics (GAMD CITE) were used to sample the folding landscape of the protein. The simulations were performed with Amber 16 CITE using the CHARMM 36 force field CITE. The time step for all simulations was 4fs with hydrogen mass repartitioning. Initial protein structures were prepared by the following: (1) collapsing fully extended polypeptide chains *in vacuo* using energy minimization, (2) equilibrating the collapsed chains at 700K *in vacuo*, (3) solvating the chains with a 20 Å layer of TIP3P water and neutralizing the solution with NaCl to 0.15M, and (4) heating the

system from 298K to 600K and equilibrating at high temperature for 300ns.The resulting structure was used to begin the GAMD simulation. Coordinates were recorded every 1ps with the first 500ns of each simulation discarded. Analysis was performed on the trajectories using the Pytraj library. Secondary structure was analyzed using DSSP CITE. Clusters were analyzed using the K-means method within Pytraj CITE. Molecular structures were visualized and rendered using VMD. (http://www.ks.uiuc.edu/Research/vmd/).

3 A-syn Multimerization is Dependent on Structural Characteristics of Repeated KTKEGV Regions

3.1 Introduction

A-syn is an intrinsically disordered neuronal protein (~14 kDa) involved in various neurodegenerative diseases including PD. The monomeric, native form of a-syn can be defined by three domains: (1) The N-terminal region contains a six-time repeated motif of the residues KTKEGV, forming an amphipathic alpha-helix, (2) The Non-Amyloid Component (NAC) region is largely hydrophobic and aggregation prone, and (3) The C-terminal domain is an acidic, unstructured sequence which has been attributed many biological roles including sites of post-translational modifications and protein interactions.

Although a-syn may be involved in vesicle trafficking, chaperone activity, and is essential to the correct functioning of neurons, its biology is still largely unknown [71]. The majority of a-syn´s involvement in the pathogenesis of PD has been linked both to its insoluble aggregation and soluble multimerization [41, 70]. Because it has been conclusively shown that a-syn is at the core of LBs and that certain a-syn conformations can “seed” or allow a site for initiation of LB-like inclusions, much research has been focused on a-syn self-interaction and self-aggregation. Soluble multimers of a-syn have repeatedly been shown to exist across several PD model systems. The characterization of these multimers has indeed become a popular topic within a-syn research programs as their repeatable and distinct molecular sizes suggest a certain level of stability and possibly distinct oligomeric-specific functions. Many extrinsic factors such as post-translational modifications, oxidative stress and metal binding have been shown to affect multimerization [58, 59]. Pertaining to the structure and sequence of a-syn, most forms of

familial cases of PD are associated with a mutation in the gene *SNCA* which encodes a-syn [92]. Mutations in *SNCA* have been shown to affect both the formation of insoluble fibrils and soluble multimers in PD models.

Although there are still many questions outstanding in terms of the functionality of a-syn multimers and aggregates, some recent studies, using both clinical and non-clinical a-syn variants, have demonstrated a clear cause and effect relationship in terms of multimeric shifting, ultimately leading to neurotoxicity. For example, some a-syn clinical missense mutations, including A53T and E46K, have been shown to shift the native 64 kDa tetramers towards monomeric states as a possible mechanism for disease initiation, neurotoxicity, and increased aggregation [115]. Interestingly, the repeated KTKEGV motif has been implicated as critical to neurotoxicity and the presence of multimers or exclusive presence of monomers in neuroblastoma cells [116].Targeting the KTKEGV repeats is an appropriate approach to studying the critical components of a-syn proteostasis simply due to its prevalence throughout the protein. This study aims to both clarify the importance of the repeats sequence to a-syn multimerization and aggregation in neurons as well as within subcellular compartments of neurons.

3.2 Hypothesis

We hypothesized that a-syn multimerization can be studied by utilizing mutations in a repeated motif throughout the N-terminus of the protein. The primary objective of this research is to further understand the importance of the distinct repeated motif, KTKEGV, to the multimerization and function of a-syn in neurons to gain a deeper understanding of one of the earliest events in the pathogenesis of PD.

3.3 Results and Discussion

3.3.1 KTKEGV repeat regions affect a-syn multimerization

In order to change the nature of KTKEGV repeat regions of a-syn we selected four a-syn mutant sequences (Figure 4A), as previously described [116]: 1) GTK replaced a large basic residue with a small, simple glycine, 2) KLK replaces a hydroxyl-containing R-group with a hydrocarbon, 3) KGV replaces an acidic residue with a basic one, and 4) EGR replaces a hydrocarbon with a basic residue. The mutated variants were generated by as GeneArt Strings DNA Fragments (Thermo Fisher Scientific), cloned into pJET1.2 blunt vector, and finally subcloned into the pcDNA3 mammalian expression vector.

M17D human neuroblastoma cells were transfected with the pcDNA3 constructs containing WT *SNCA* and the mutated variants GTK, KLK, KGV, and EGR in independent transfection experiments. Stable cell lines were generated by Geneticin G418 selection and *SNCA* expression amongst the cell lines was confirmed by a SYBR Green-based quantitative reverse-transcriptase polymerase chain reaction (qRT-PCR) assay. The qRT-PCR results confirmed that the overexpression of *SNCA* was not significantly different between the cell lines (Figure 4B). Having established similar expression of *SNCA* in the different transfection experiments, we measured cell viability while monitoring the cells' morphology to assess an overall effect of the mutations. Cellular morphology was monitored by microscope and was indistinguishable amongst cell lines (data not shown). Cell viability of the stable cell lines was then measured by neutral red uptake assay, with the GTK mutant showing significantly less viability than control cells, suggesting a possible neurotoxic effect [117].

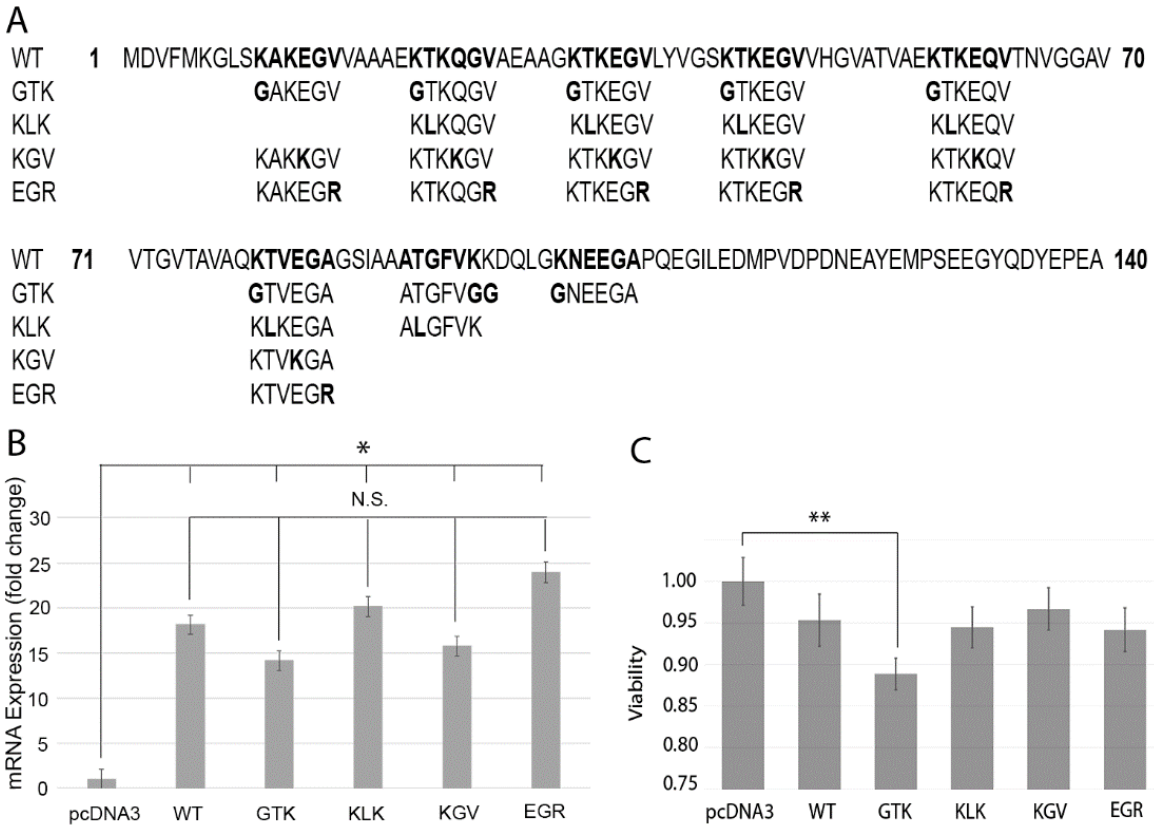

Figure 4 Stable overexpression of WT and KTKEGV-repeat mutant *SNCA* in M17D cells. (A) Amino acid sequences of WT, GTK, KLK, KGV, EGR a-syn. (B) Expression of *SNCA* in M17D cells transfected with pcDNA3 containing *SNCA* variants. (C) Neutral Red Assay of mutant a-syn expressing M17D cells (n=3, *p<0.05, **p<0.01, t-test)

We next aimed to observe the repeat mutant a-syn variants in the cell lines to assess how altering the primary structure of the protein affects its multimerization and how altered multimerization might relate to the decrease in viability of the GTK mutant cells. SDS-polyacrylamide gel electrophoresis (SDS-PAGE) and western blotting was used to observe a-syn multimeric distributions in whole-cell extracts. Prominent bands representing a-syn multimers of sizes 17 kDa, 37 kDa, 50 kDa, 100 kDa and 150 kDa are present in all transfected cell lines (Figure 5A). A 21 kDa species of a-syn is present in the KLK mutant cells, indicating highly modified monomer (Figure 5A). Interestingly, while expression of *SNCA* is not significantly different among these cell lines (Figure 4B), monomeric a-syn is significantly lower in repeat mutant *SNCA* cells compared to WT *SNCA* transfected cells (Figure 5B). We hypothesize that the decreased monomer can be explained in one of two ways: (1) the monomeric a-syn formed higher level species but that did not show significance either due to varied size or through some means of processing and analysis or (2) the repeat mutant monomers or multimers were degraded at an increased rate due to altered structure. Finally, there were no other observable significant differences of the neurotoxic GTK a-syn as compared to WT transfected cells.

3.3.2 KTKEGV mutants are distributed throughout subcellular compartments

Subcellular fractionations of the a-syn repeat mutant cell lines were used to identify where the prevalence of a-syn multimer differ subcellularly with the additional aim to increase the resolution of possible changes in multimers among the a-syn repeat mutants that were not observable in the whole cell lysates (Figure 5). Cells were fractionated using the Subcellular Protein Fraction Kit for Cultured Cells (Thermo Fisher Scientific) by a stepwise lysis and

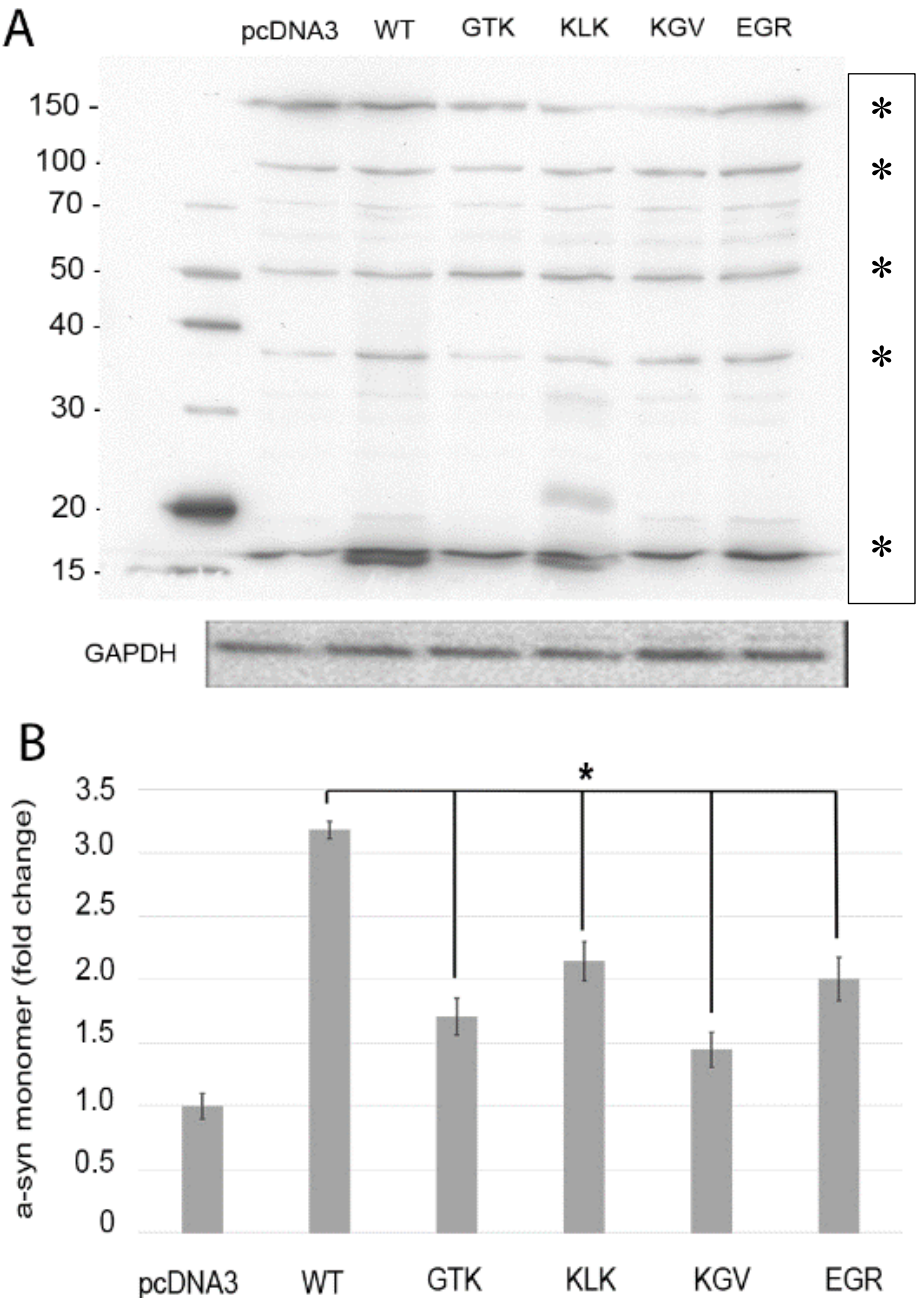

Figure 5 Whole cell a-syn levels vary in transfected M17D cells. (A) Western blot probing whole cell extracts for a-syn. (B) Quantified fold change a-syn monomer (~17 kDa) (n=3, *p<0.05)

centrifugation protocol. A subcellular fractionation into cytosol, membrane bound, nuclear soluble, and chromatin-bound compartments of control, empty pcDNA3 transfected M17D cells is shown by western blot (Figure 6A). The integrity of the fractions was confirmed by probing for fraction-specific markers and showing little to no contamination between fractions (Figure 6B). The distribution of a-syn multimers is not altered by the fractionation protocol as the multimers in each fraction add up to equal the whole cell profile [40]. While the "distinct a-syn profile" of SHSY-5Y neuroblastoma cells has been previously described, we have established with these data that this characteristic is cell-type specific. While not surprising, this emphasizes the importance of the model system and suggests techniques such as dopaminergic differentiation through retinoic acid treatment should be considered in future experiments [118].

Our additional work aiming to knockout *SNCA* to create a system with exclusively exogenous mutant a-syn was motivated by the results reported above. Out of five prevalent a-syn species shown in M17D cells, monomer, 70 kDa and 150 kDa are observed only in the cytosolic and membrane bound fractions, and the 50 kDa multimer is present in all fractions where a-syn is observed (Figure 6A). Interestingly, a shift to lower size and presumably a less modified form of tetrameric a-syn is seen in the nuclear soluble fraction (Figure 6A). The distribution of a-syn throughout the cell suggests that its biological functions vary in different subcellular compartments. Indeed, a-syn, often described as a cytosolic protein, has been implicated as a molecular chaperone, including chaperone activity of the SNARE complex triggered by membrane binding and subsequent multimerization [119, 120]. Additionally, a-syn has been shown to act as a transcriptional

regulator of a master mitochondrial co-activator as well as a modulator of histone modification [89, 121, 122].

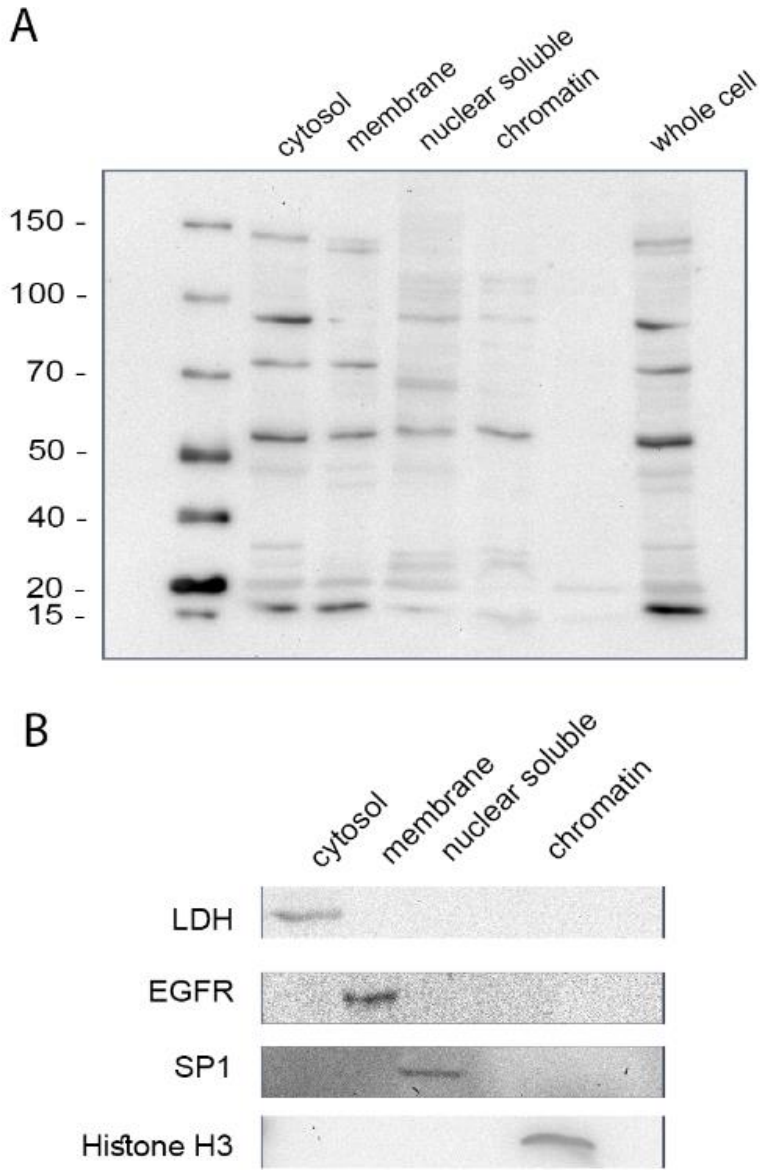

Figure 6. Subcellular a-syn in M17D cells. (A) A-syn multimeric distribution in subcellular compartments of M17D cells transfected with empty pcDNA3 vector. (B) LDH, EGFR, SP1, and Histone H3 were used as quality controls for cytosolic, membrane bound, nuclear soluble, and chromatin bound fractions respectively

A-syn of repeat mutant cells were compared by western blotting of each subcellular compartment and the presence of each multimeric species is mostly consistent (Figure 7), however, the size of monomeric a-syn varies. Doublets, suggesting some form of PTMs, are observed in WT a-syn monomer in every compartment as well as in the membrane and nuclear soluble fractions of KLK cells (Figure 7). A-syn is subject to various PTMs and further experimentation identifying the specific PTMs present throughout the subcellular compartments in WT and KLK cells is a logical next step [123]. All four mutants had less monomer in the cytosolic fractions, mimicking the pattern found in whole cell lysates (Figures 5, 7A, 7D). Significantly less monomer was found in the membrane-bound fractions of GTK and KGV mutant cells when compared to WT (Figure 7B, 7E). Interestingly, KLK expressing cells, only, showed 36 and 21 kDa species in the membrane-bound fraction (Figure 7B). This suggests that future work should focus on the role of the KTKEGV motif on the relationship between multimerization and membrane binding, a relationship that has been previously studied [120].

All the mutant cell lines had significantly less monomer in the nuclear soluble fraction than WT cells, while KGV and EGR showed increased levels of the 50 kDa species (Figure 7C, 7F, 7I). There is significantly less 50 kDa bound to chromatin in GTK, KLK and KGV mutant cells, and interestingly, only GTK cells showed an absence of monomer in the chromatin-bound fraction (Figure 7G-H). These results show that modifying the KTKEGV motif alters the abundance of monomeric a-syn at the cellular and subcellular levels, as well as the abundance of the 50 kDa species subcellularly (Figures 4-7).

Interestingly, the KGV mutant shows a significant difference compared to the WT for every band we analyzed (Figure 7). This result, in addition to the observed neurotoxicity

of the GTK mutant, led us to focus our *in silico* molecular dynamics simulations on WT, GTK, and KGV forms of a-syn.

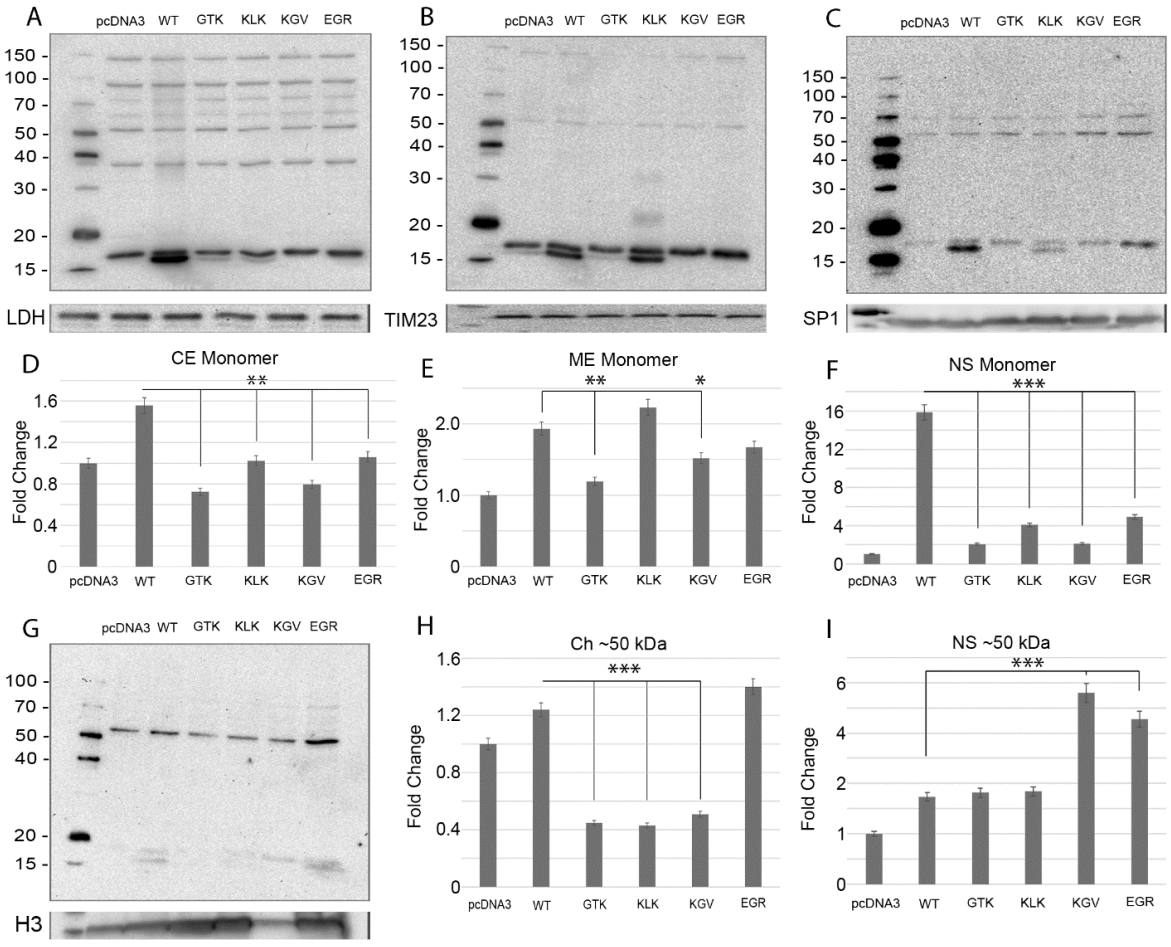

Figure 7. Subcellular fraction comparison of a-syn in M17D cells stably overexpressing repeat mutant *SNCA*. (A, D) Cytosolic (B, E Membrane bound (C, F, I) Nuclear soluble (G, H) Chromatin bound (n=3, *p<0.05, **p<0.01, ***p<0.001)

3.3.3 Molecular Simulations of Repeat Mutants

To understand how the introduction of repeat mutants into the a-syn sequence may lead to aggregation, we used molecular dynamics (MD) simulations to determine how the mutations affect the intermolecular interactions that lead to aggregation. We simulated the GTK and KGV mutants along with the WT variant to quantify how the repeat mutants change the sampling of secondary structure and inter-domain interactions. We used all-atom MD, in which every atom is modeled as a single particle and Newton's classical equations of motion are used to propagate the system forward in time and generate a trajectory of molecular structures [124]. Standard, unbiased molecular dynamics simulations are generally unable to sample many different structures, and this limits their ability to study intrinsically disordered proteins (IDPs) such as a-syn. Because of this, some sort of enhanced sampling method is required to study IDPs to correctly sample the many structures adopted by a disordered protein. Specifically, we used Gaussian accelerated molecular dynamics (GAMD) to enhance the sampling of our simulations [125, 126]. The benefit of this method is that it can correctly reproduce the shape of the potential landscape while still allowing the protein to sample the entire folding landscape. It should be noted that the GAMD does not preserve the exact relative frequency of sampling, but distribution minima and maxima can be determined to understand which structures are most sampled [127, 128].

3.3.4 KGV and GTK change the behavior of the C-terminal Domain

The simulations of the GTK and KGV repeat mutant variants can form significantly different structures than the WT protein *in silico*. Figure 8 shows the representative

structure of the largest structural cluster sampled by each protein variant. The clustering analysis was done by using the K-means method [129].

The structures sampled by the WT do not have much secondary structure and show that the C-domain is interacting with both the N-terminal and the NAC domain (Figure 8A). Specifically, the C-domain is interacting with both the N-terminal and the NAC domains in a way that keeps them from interacting with each other. In this way, the C-terminal may be serving a protective role by mediating the interactions between the N-terminal and NAC domain. It has been shown that removal of the C-terminal domain leads to an increase in aggregation of the monomer [130, 131], and a recent study has shown that the human appendix, even in healthy patients, contains truncated a-syn monomers and various forms of oligomers [132]. This suggests that the C-terminus protects against the aggregation of a-syn monomers. The protective properties of the C-terminal domain may be due to its ability to mediate the interactions between the other domains by forming a correct number of contacts with both the N-terminal and NAC domains.

The GTK mutation seem to perturb the interactions between the C-terminal domain and N-terminal and NAC domains almost completely, leading to a fully extended C-terminal domain in the structure (Figure 8C). The GTK mutant structure is especially interesting because it appears to behave like a C-terminal domain deletion mutant, which are known to form toxic aggregates [130, 131]. Comparison of the radius of gyration, R_g **(**Figure 9A**)**, and the end-to-end distance, R_{ee} (Figure 9B) shows that GTK mutant can sample structures that are much more elongated than either the WT or KGV protein variants. The elongation of the C-terminus may lead to an increase in toxicity that could explain why the GTK mutant cells were less viable than the control cells. An analysis of

the contacts between the N-terminal and C-terminal domains (Figure 10A), the NAC and C-terminal domains (Figure 10B), and the N-terminal and NAC domains (Figure 10C) also shows that the GTK mutation significantly disrupts the number of contacts between the C-terminus and either the N-terminal or NAC domains. Interestingly, in the distribution of contacts between the N-terminal and NAC terminal domains, the GTK and WT distribution curves show similar shapes, except for the regions with very few contacts and the tail with many contacts.

In the case of the KGV mutant, the C-terminal domain still interacts with the other domains, but its ability to reduce the interactions between the N-terminal and NAC domains is diminished. The distributions of R_g and R_{ee} also show that the KGV mutant samples structures that are more compact than the WT protein, due to increases in inter-domain contacts and an increase in the sampling of β-sheet motifs. Compared to the WT, the KGV mutation leads to an increase in the number of contacts between the C-terminal and the N-terminal domains and the number of contacts between the N-terminal and NAC domains. It appears that by mutating the WT protein to the KGV variant, the interaction between the C-terminal domain and the N-terminal domain is changed in a way that disrupts its ability to reduce the interactions between the N-terminal and NAC domains. This disruption also seems to lead to a significant increase in the sampling of β-sheet rich structures for the KGV mutant (Figure 11). The figure shows the distribution of the number of residues that have a β-sheet configuration according to the DSSP method [133]. Mutation of the protein to the KGV variant leads to large enhancement of β-rich structure. Structures with many β-sheet motifs are generally associated with protein aggregation and

increased toxicity and this may explain why fewer KGV monomers were found in the cytosolic region of the cells.

From our simulations, it appears that both the KGV and GTK mutations may lead to aggregation or toxicity prone monomeric behavior, but through two quite different pathways caused by a perturbation to C-terminal domain behavior. Too many or too few contacts between C-terminal and N-terminal domains appear to result in structures that may be prone to aggregation.

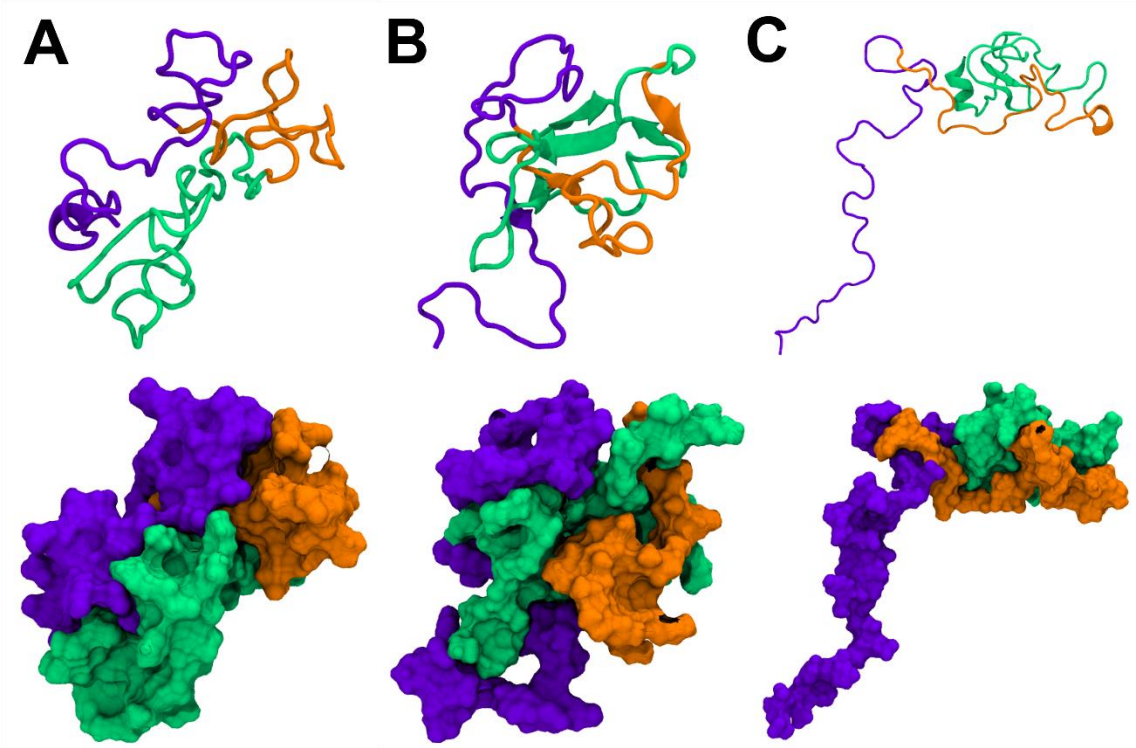

Figure 8. The representative structures determined by clustering analysis for the WT (a), KGV (b), and GTK (b) a-syn variants. The New Cartoon representation is shown on the top and the Solvent Accessible Surface is shown on the bottom for each variant. The N-terminal, NAC, and C-terminal domains are shown in green, orange, and violet, respectively. The structures show how in the WT protein the C-terminal domain interacts with the other two domains in a way the reduces their contacts. The KGV mutant changes leads to more interaction between the N-terminal and NAC domains, along with more beta-sheet rich structures. The GTK mutation disrupts the interacts between the C-terminal domain and other N-terminal and NAC domains.

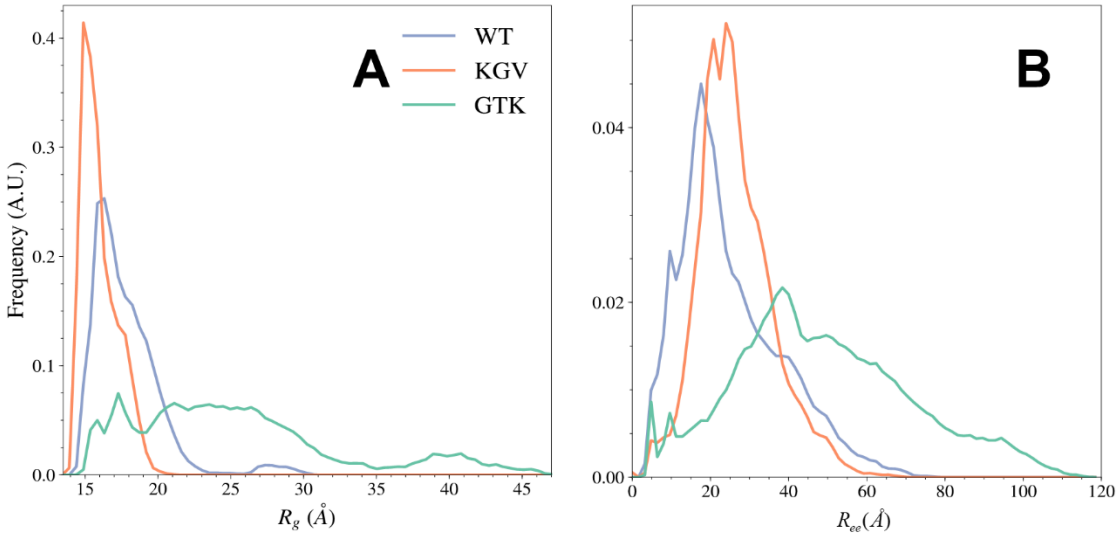

Figure 9. Radius of gyration and end-to-end distance measurements for WT, KGV, and GTK a-syn variants. Comparison of the radius of gyration, R_g (**a**), and the end-to-end distance, R_{ee} (**b**) for the WT, KGV, and GTK protein variants shows that the GTK mutant can sample much more elongated structures than the either the WT or KGV variants, due to the decrease in interactions between the C-domain and the rest of the protein. The KGV mutant, on the other hand, samples structures that are more compact, due to increased contacts between the N-terminal and NAC domain and increased sampling of beta sheet rich structures.

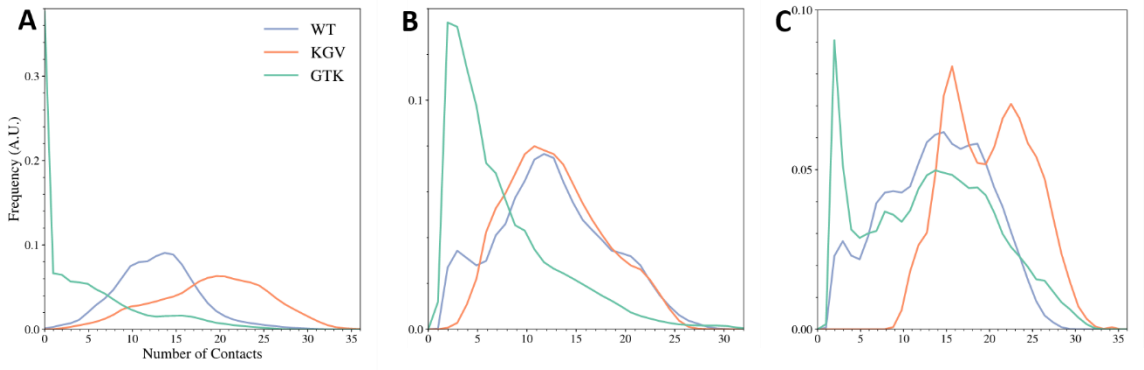

Figure 10. Inter-domain contacts in WT, KGV, and GTK a-syn variants. The distribution of inter-domain contacts between the N-terminal and C-terminal domains **(a)**, the NAC and C-terminal domains **(b)**, and the N-terminal and NAC domains **(c)** shows that the GTK mutations leads to significantly reduced interactions between the C-terminal domain and the other two domains. The contact distributions also show that that the KGV mutations leads to a large increase in the number of contacts between the N-terminal and NAC domains.

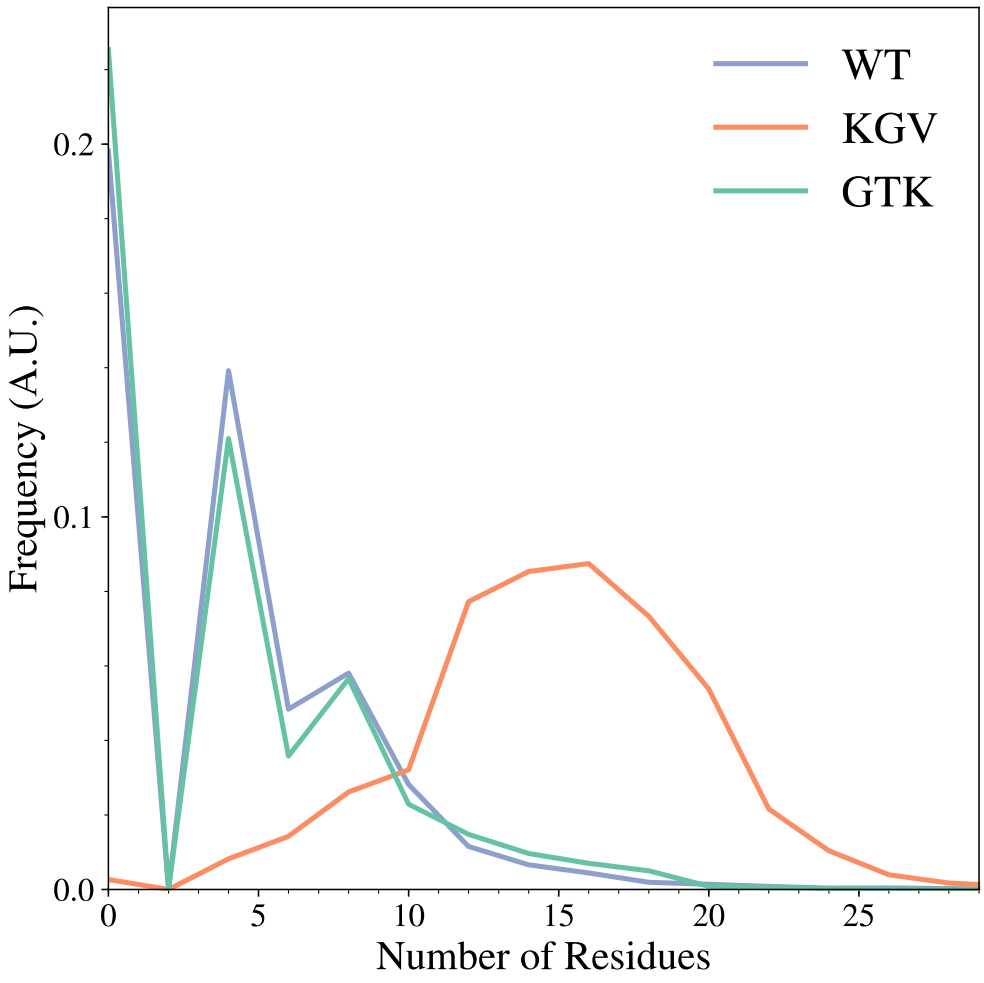

Figure 11. Beta-sheet content of WT, KGV, and GTK a-syn variants. The distribution plots of the number of residues found to have a beta-sheet configuration in each frame of the trajectory shows that the KGV mutant samples much more beta-sheet content than the either the WT or the GTK protein variants.

4 The Intersection of Parkinson's Disease, Viral Infections, and COVID-19

4.1 Introduction

Parkinson's Disease is the most common neurodegenerative movement disorder that primarily affects dopaminergic neurons in the substantia nigra [134]. Although, this disorder mainly pertains to motor complication, PD patients also experience many non-motor symptoms such as neuropsychiatric (depression, dementia, apathy, anxiety) autonomic (constipation, urinary incontinence, excessive sweating) sleep disorders and sensory abnormalities (loss of smell, pain and paresthesia) [134]. The exact causes of sporadic PD are largely unknown, but both environmental and genetic factors play a role. Indeed, the Braak hypothesis suggests that sporadic PD originates from an external pathogen that enters the body through the nasal cavity, which then migrates via the vagus nerve to the gut, causing complications such as changes in the gut microbiome and the advancement of Lewy Body (LB) pathology in the gut and in the nose similar to that of a viral infection [135, 136].

The novel SARS-CoV-2 coronavirus (COVID-19) pandemic was a result of a virus outbreak originating in Wuhan, China which quickly spread throughout the world. Whilst flu-like symptoms such as a fever, cough and difficulty breathing appeared to be the predominant early warning signs of a COVID-19 infection a large number of patients admitted to hospitals experienced a host of neurological symptoms including, dizziness, loss of smell and taste, seizures, difficulty concentrating, decreased alertness and brain inflammation [137]. In addition, complications in the gut microbiomes have also been noted as a result of COVID-19 [138].

Strikingly, a number of the neurological symptoms seen in COVID-19 patients, as well as the alterations in the gut microbiome, are also prevalent in patients with PD. Moreover, several biochemical pathways, including oxidative stress, inflammation, and protein aggregation, show similarities between PD and COVID-19. In this review we describe the many intersections between neurodegeneration in PD and viral infections, with an emphasis on the novel SARS-CoV-2.

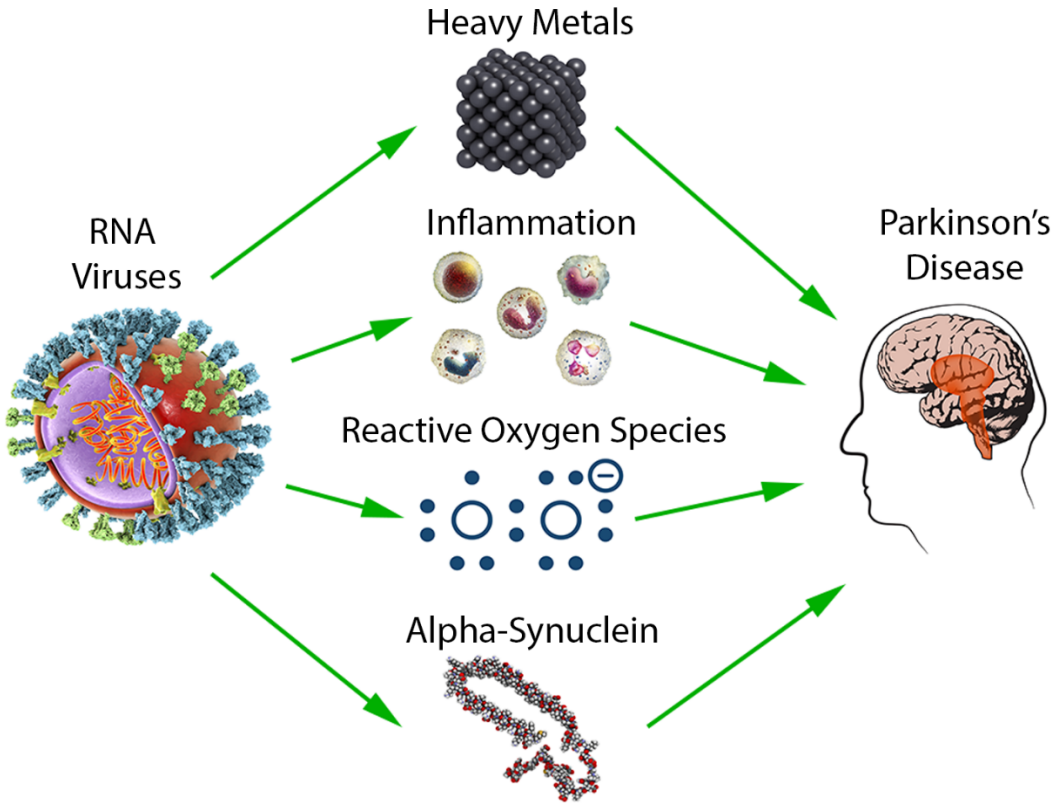

Figure 12. Common factors in Parkinson's Disease and RNA virus infection. PD contributing factors including heavy metals, inflammation, reactive oxygen species, and alpha-synuclein are elevated in response to RNA virus infection illustrating commonalities between neurodegeneration and viral infections.

4.2 PD, a-syn and RNA viruses

The pathological hallmark of PD is the presence of LBs, neuronal inclusions constituted of aggregate protein [32]. The formation of LBs is seeded by the aggregation of its major component, the protein a-syn. A-syn is an intrinsically disordered protein mainly found in neurons at the presynaptic terminals but a-syn is also found in other tissues such as kidney, heart and muscle cells [43]. While the physiological function of a-syn is not fully understood, a-syn has been implicated as a pre-synaptic protein that mediates neurotransmitter release [139, 140]. Duplications, triplications, and mutations of the a-syn encoding gene *SNCA* are linked to familial PD suggesting that an increase in a-syn and or the expression of mutational variants contributes to neurodegeneration (Figure 12) [141]. Many extrinsic factors such as post-translational modifications, oxidative stress and metal binding have also been shown to affect multimerization and aggregation of a-syn and due to its central effect on LB pathology, factors which affect the behavior or prevalence of a-syn are generally thought to be associated with PD [58, 59].

RNA-viruses are linked to PD by their effect on a-syn (Table 1). For example, a-syn expression is up-regulated in response to neurons infected by RNA viruses (Figure 12) [142, 143]. It has been shown that a-syn supports expression of anti-viral interferon-stimulated genes [142]. In fact, a-syn restricts RNA viral replication, protecting the central nervous system (CNS) in infected mice [144]. Interestingly, a-syn expression also increases in enteric neurons of the gastrointestinal tract in response to infections with the single-stranded RNA norovirus followed by an inflammatory immune response [145, 146]. While the prevention of RNA virus progression is of immediate and primary concern to an

individual's health, elevated a-syn levels and prolonged inflammation are both linked to LB pathology and increased risk for PD [143].

The protective function of a-syn against RNA viruses has obvious implications to the novel coronavirus SARS-CoV-2, especially in individuals with PD. Elevated a-syn expression may indeed serve as a protective mechanism against this RNA-virus, however, it is unlikely that aggregated a-syn contained within LBs will be affective in restricting RNA viral replication. In addition to viral replication, a-syn can also inhibit RNA virus transmission from the peripheral nervous system (PNS) to the CNS [147]. When peripherally injected with a non-neuroinvasive RNA virus, the brains of a-syn knockout mice showed a much higher viral load than the brains of heterozygous a-syn expressing mice [144, 147]. Additionally, the same difference was not observed when inoculation was done intracerebrally or done on brain slice cultures [144, 147]. Since COVID-19 can manifest itself in both the CNS and PNS, its replication and its spread may be inhibited by elevated a-syn in individuals living with PD or possibly other synucleinopathies [148].

4.3 Viral infections and neurotransmitters

With regards to viral infections, it has been noted that there is a link between viruses, neurotransmitters, and neurotransmitter protein pathways. The acetylcholine (ACh) and dopaminergic pathways are obstructed during PD, as a result of degeneration of the substantia nigra and motor neurons [149]. However, in the case of viral infections, it has been shown that acetylcholine levels are affected throughout the progression of the virus. In the early stages of infection, acetylcholine levels seem to remain constant. However, ACh levels seem to rise around the peak point of the immune response. In addition, cholinergic lymphocytes, which make direct contact with macrophages in the lungs, appear

as ACh levels increase which may be present because of the SARS-CoV-2 virus [150]. These lymphocytes, however, are also known to regulate pulmonary inflammation, a common symptom of COVID-19 [151]. In addition, it has also been shown that viruses lead to production of ACh via choline acetyltransferase (CHAT) enzyme activation [152]. With regards to recovery, however, the role of ACh is still unknown [151]. In addition to ACh, it has also been shown that viral infections play a role in the dopaminergic pathway. Theiler's virus, a type of encephalomyelitis RNA virus, has been known to destroy the substantia nigra, which is the site of dopamine production [153]. In an additional study involving mice, the presence of viral RNA was observed, and the viral RNA was present in the substantia nigra within three days of infection and spread further throughout the brain within ten days. However, three weeks later, the viral RNA was no longer detected [153]. As a result, it could be argued that these interactions between the substantia nigra and viral pathogens may support the PD Braak hypothesis. Furthermore, the interactions between neurotransmitter pathways and viral infections may lead to further research regarding the intersection of viral infections such as COVID-19 and PD.

4.4 Oxidative stress

Oxidative stress plays an important role PD and reactive oxygen species (ROS) and their extensive production in the brain play an important role in dopaminergic neuronal cell loss death involving dopamine metabolism and high levels of iron and calcium (Figure 12) [154]. ROS are naturally occurring in cells and are a necessary component of cellular homeostasis. Despite the importance of ROS in normal physiology, failure in ROS regulation by antioxidant proteins, such as superoxide dismutase (SOD1) and glutathione (GSH), can lead to oxidative stress which can have detrimental effects on cellular functions

(Table 1) [155]. Mitochondria are key sites of ROS production and targets of ROS-induced damage by inhibition of the mitochondrial election transport chain (ETC) [156]. PINK1 and Parkin are PD-associated proteins important in mitochondrial homeostasis as well as ROS homeostasis [156].

Many viruses, such as Hepatitis C (HCV), are known to cause oxidative stress by changing the antioxidant balance within cells (Figure 12) [157]. HCV belongs to a family of RNA viruses that cause damage and cirrhosis of the liver and patients with chronic hepatitis c have increased ROS levels triggering immune responses and increased inflammation [158]. Another virus, Zika virus (ZIKV), which has been extensively studied due to its link with congenital malformations has revealed that astrocytes are the targets of ZIKV [158]. In a recent study it was shown that ROS imbalance, coupled with mitochondrial defects, trigger DNA damage in Induced Pluripotent Stem Cells (iPSC)-derived astrocytes, causing neuronal loss and motor defects [159]. Interestingly, ZIKV belongs to the *Flaviviridae* family of viruses, as does HCV, and it replicates within the Endoplasmic Reticulum (ER) causing an increase in ROS in both the ER and mitochondria [160, 161]. This increase in ROS causes breaks in DNA, activating the DNA damage response ultimately causing apoptosis [160, 161]. Reactive gliosis is a condition whereby neuroinflammatory conditions caused by bacterial or viral infections cause an inflammatory environment culminating in astrocyte reactivity [162]. These infected astrocytes correlate to an increase in pro-inflammatory chemokines and cytokines, and it has been speculated that surviving children infected by ZIKV might show an increased rate of neurological disorders such as PD or Alzheimer's disease (AD) later in life [160, 161]. Although a definite connection is yet to be made between viral infections, such as ZIKV

and hepatitis C, with respect to increased risk of sporadic PD it is noteworthy that increased ROS and mitochondrial dysfunction are found in both viral infections and in PD (Table 1).

	Alpha-synuclein	Oxidative Stress	Inflammation	Metals	Gut Microbiome	Olfactory Tract
Parkinson's Disease	Aggregation leads to neurotoxic Lewy Bodies [32]	Dysfunctional regulation of ROS by several genes including SOD1 leads to oxidative stress and apoptosis [146]	Protective short term, exacerbates non-motor symptoms long term [163, 164]	Exposure to heavy metals such as Mn is a risk factor for PD [165]	GI problems such as dysbiosis, constipation, and dysphasia [166]	Olfactory dysfunction is one of the earliest signs of PD [135, 136]
RNA Virus Infection	Upregulated in infected cells and restricts RNA virus replication [142-144]	Can create ROS imbalance causing DNA damage and neuroinflammation [153]	Neuro-inflammatory response can be triggered by infection [143, 167]	RNA virus replication depends on and may cause increase in Mn and Fe [165, 168, 169]	Microbiota depletion leads to GI issues causing inflammation and lack of gut flora [170]	Olfactory dysfunction is one of the earliest signs of COVID-19 infection [171, 172]

Table 1. Commonalities between Parkinson's Disease and RNA virus infection

4.5 Inflammation

Brain inflammation has long been implicated as a risk factor (Figure 12) [163, 173], as well as a pathological effect of PD (Table 1) [164, 167, 174, 175]. The primary facilitators of the neuroinflammatory response are microglia. Microglia release immune factors when activated in response to trauma, viral infection, and aggregated proteins such as a-syn [143, 176]. Additionally, astrocytes can contribute to the inflammatory response when activated by RNA viral infection (Figure 12) [177]. Neuroinflammation has been described as a double-edged sword in regard to PD as on one hand it is neuroprotective in the short-term but acts in a neurotoxic manner when chronically sustained [176, 178]. Inflammatory cytokines, reported as increased in PD patients [165], have been shown to exacerbate cognition, depression, anxiety and sleep disturbances [168, 169]. Similarly, COVID-19

patients have shown a wide range of neurological disorders including psychosis/delirium, inflammation of the brain, ischemic stroke, and multisystem inflammatory syndrome (Table 1) [179, 180]. Interestingly, pro-inflammatory cytokines tumor necrosis factor alpha (TNFα), interleukin (IL)-2, and IL-6 are found at higher levels in the brains of PD patients and the cerebrospinal fluid of COVID-19 patients [181, 182]. Additionally, many COVID-19 cases result in a cytokine storm, a massive immune response that upregulates pro-inflammatory cytokines [183]. Increased inflammation, due to COVID-19 in PD patients, may exacerbate non-motor symptoms and it has been suggested that PD patients recovering from COVID-19 show an extended period before reaching baseline. However, it is unclear if the exact mechanisms of inflammation in PD, MSA, and COVID-19 are the same.

4.6 Metals, Viral Infections, and PD

It has been noted that exposure to heavy metals such as manganese and iron have played a role in the progression of PD and other neurological diseases (Figure 12) [184]. The most common form of exposure to these metals is the environment and abnormal accumulations in the body. The presence of these metals result in multiple oxidative stress pathways that can lead to the oxidation of dopamine and production of free radicals [184]. Similarly, it has been noted that heavy metals also play a role regarding some viral infections. Because many viruses use iron to replicate themselves, large iron buildups may form leading to potential neurodegeneration (Figure 12) [185]. Like many RNA viruses including most coronaviruses, the replication of the SARS-CoV-2 virus is dependent on manganese and iron, so it is possible that contracting COVID-19 may lead to the future onset of PD [166]. In addition, it has been found that heavy metals are found at higher concentrations in Hepatitis C infected individuals [186]. Therefore, people that contract RNA viral infections

that are dependent on heavy metals should be aware of the potential risk of developing PD in the future.

4.7 COVID-19 and the Braak hypothesis

The Braak hypothesis states that sporadic PD originates in the gut and the nasal cavity where a pathogen travels along the vagus nerve and olfactory tract towards the brain [187, 188]. The Braak hypothesis is supported by longitudinal clinical data which demonstrate that loss of smell and gastrointestinal dysfunction represent early PD symptoms, often preceding a definite PD diagnosis once motor symptoms present themselves [136, 170, 189-191]. Further, due to evidence of LB formation in the olfactory epithelium [192, 193] and the enteric nervous system [194, 195], a-syn aggregation has been implicated as the pathogen referenced in the Braak Hypothesis. That the staging presented by the Braak hypothesis resembles in many cases that of COVID-19 symptom progression is cause for concern. In essence, the Braak hypothesis describes a mode of pathogen transmission, likely a-syn aggregates, which can bypass the blood-brain-barrier and originate in two areas that are indeed affected by COVID-19.

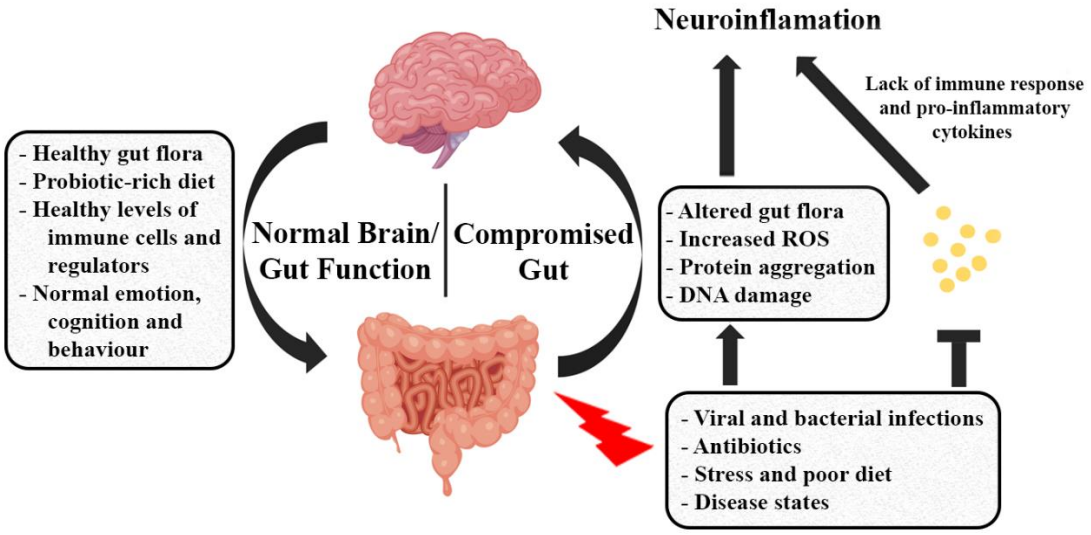

Figure 13. The Brain-Gut microbiota axis: Schematic diagram highlighting the relationship between the brain and gut microbiota. A rich and diverse microflora allows for healthy immune and regulatory mediators, whereby a compromised gut microflora caused by viral infections, stress, antibiotics, and poor diet can cause a lack in immune response contributing to abnormal production of inflammatory cytokines which can lead to neuroinflammation.

4.7.1 Viral infections, the gut and PD

The human body is inhabited by a diverse microflora which plays a role in many physiological and metabolic processes [196]. A healthy commensal microbiota plays a role in the breakdown of dietary substances that are too large to be digested and it has been shown to be essential for protecting the host against a variety of pathogenic infections [197]. Viral infections are among some of the most common invading pathogens that effect the host microbiota. In fact our gut flora regulates viral expression yielding beneficial

outcomes, however it can also be regulated by viruses causing dysbiosis and a multitude of gastrointestinal (GI) issues [198]. The gut microbiota is decreased in older adults due to several factors that include diet, environmental factors, and genetics and the rate and duration of viral infections are much higher in those with a compromised gut flora [199]. Patients with PD display an array of GI complications such as dysbiosis, constipation, and dysphasia (Table 1) [200] and these complications can occur up to ten years before hallmark motor symptoms occur suggesting a possible link between the gut and the progression of PD (Figure 13) [201]. Indeed, individuals with PD are at a higher risk of infection due to a compromised gut microbiota as well as severity of infections and emerging evidence has suggested that a rich and microbiota can play an essential role in modulating host immune response [202]. This occurs by stimulating the production of various pro-inflammatory cytokines during infection (Figure 13).

Commensal microbiota has also been shown to directly suppress viral infections especially in certain sites where viruses can gain entry into the host [198]. Supporting this notion, is the fact that *Enterococcus faecium* can prevent infection by the influenza virus by direct absorption and trapping as well as producing various metabolites to prevent viral infection [203]. Studies have also shown that microbiota depletion, due to antibiotic treatment, can result in significantly higher viral shedding [204]. Similarly, a study found that fecal microbiota transplants in rhesus macaques infected with simian immunodeficiency virus (SIV) induced greater antiviral immunity [205]. The immune gut homeostasis is delicately orchestrated by the fine tuning of the regulatory balance of pro-inflammatory responses, such as Th17, versus inflammatory regulatory T cells (Tregs) (Figure 13) [205]. For example, gut probiotics like *Lactobacillus paracasei* increase pro-

inflammatory cytokines like IL-33, IL-β, IL-12, and INFγ during influenza virus infection [206]. Quite a few studies have also shown that viral infections such as HCV/HBV can cause a profound alteration in gut microbiota causing dysbiosis, and this reduced gut diversity caused an increase in severity of infections [207]. A healthy gut microbiome is therefore essential in maintaining an optimal immune system to fight off pathogenic infections including viral infections.

It has been noted that severe viral infections could possibly increase the risk of developing PD later in life [208]. Clearly viral infections are not the primary cause of PD but may act as vital triggers as eluded to previously in this review [209]. For example, it is known that virions can pass the blood-brain barrier and elicit inflammatory responses in the brain such as observed in encephalitis [209]. It has also been documented that individuals infected with hepatitis C are 30% more likely to develop PD than individuals who never had the virus [210]. Similarly, PD patients show a statistically higher antibody titer against the HSV-1 virus than healthy controls, and this autoimmunity has been further highlighted in mechanisms of a-syn molecular mimicry [211]. Indeed, the immunological cross-reactivity between HSV-1 and a-syn has been shown to cause destruction of dopaminergic neurons of the substantia nigra [172]. In many cases SARS-CoV-2 primarily affects lung function through binding to ACE2 receptors present on the alveolar epithelial cells [171]. However, evidence has suggested that SARS-CoV-2 RNA can be detected in the stool of some patients with COVID-19 [212]. A recent study obtained blood and stool records from 100 patients with confirmed COVID-19, and 27 out of the 100 stool samples were collected 30 days after infection. The study discovered that the gut microbiome was significantly altered in patients with COVID-19 compared to control patients [213],

showing a decrease in *Faecalibacterium prausnitzii*, *Eubacterium rectale* and bifidobacterial. Further, the study showed elevated levels of C reactive protein and lactate dehydrogenase and it was suggested that altered gut microbiota is involved in COVID-19 severity and this dysbiosis is observed after the infection has passed.

This data suggests that there may be a link between the gut microbiota and COVID-19 severity, particularly as the higher COVID-19 mortality rate is seen within the elderly population that have a decreased gut microbiota. Interestingly, PD patients with chronic GI conditions suffer from a decrease in gut flora causing constant bacterial infections [214]. This may suggest an increased chance of COVID-19 mortality for a patient with PD.

4.7.2 The olfactory tract

Loss of smell is one of the earliest symptoms of PD and the olfactory epithelium (OE) is becoming a target tissue to study PD and brain aging in general (Table 1) [21, 135, 136, 215, 216]. Indeed, olfactory dysfunction is as common as the other cardinal motor symptoms in PD and more prevalent than resting tremor [217]. Idiopathic hyposmia has been associated with an increased risk for PD in first-degree relatives of PD individuals [21, 218] and it has been suggested that neurologists should screen high-risk patients with olfactory tests [219].

Like PD, olfactory dysfunction is one of the earliest symptoms of COVID-19 infection and is therefore a key diagnostic criterion (Table 1) [220, 221]. With inhalation of SARS-CoV-2, the primary mode of infection, the nasal cavity and olfactory epithelium represent important targets for the virus. ACE2, critical to SARS-CoV-2 entry into cells, is expressed in sustentacular cells and basal cells of the olfactory epithelium, but is absent in olfactory sensory neurons [222]. Sustentacular cells act as support cells which provide

major physical, metabolic, secretory, and absorptive supports functions for the olfactory sensory neurons (OSN) [223] whilst basal cells of the OE act as stem cells producing OSNs since their lifespan is only a few weeks [223]. There are two mechanisms that could be at play here. First, RNA viral infection has been previously shown to be capable of inducing a-syn seeding in neurons [224]. Due to the prion-like activity of a-syn aggregates, a seeding event in any cell type of the OE can cause the propagation of aggregation throughout the OE towards the brain. Another mechanism of PD pathogenesis could be that the sustentacular cells and basal cells cannot function normally after infection and cause alterations in the OSNs. In fact, glial cells loss-of-function or gain-of-toxic-function has been thought to participate in the pathogenesis of PD [225]. A variety of PD risk factors are associated with altered proteostasis and metabolism in neurons and a single seeding event, be it caused by viral infection or disrupted homeostasis, could contribute to the pathology established in the Braak hypothesis [226].

4.8 PD non-motor symptoms and COVID-19

One of the most common non-motor symptoms of PD is depression and typically, 30%-40% of PD patients experience some form of depression in their lifetime post diagnosis [227]. It has been hypothesized that increased stress and a loss of emotional control is a result of a lack of dopamine-dependent adaptation [227]. In times of crisis, such as during the COVID-19 pandemic, stress induced depression and anxiety may increase because of medical, financial, and social factors. For PD patients who have contracted the SARS-CoV-2 virus, it has been found that there is an increase in non-motor symptoms including trouble sleeping, mood changes, cognitive changes, and autonomic problems which all have ties to depression [228]. However, not only PD patients have experienced an increase in

depression because of the pandemic. Factors including a lack of knowledge of infectious diseases, the effects of quarantine, inadaptability, and the fear for one's health all affect one's mental health whether that person has been infected or not [229].

4.9 COVID-19 and PD guidelines

During the COVID-19 pandemic, numerous guidelines have been published to keep the world's populations safe and healthy. For many patients with PD, these guidelines are of course generally identical including the practice of social distancing and self-isolation if infected in order to prevent any further spread of the virus [230]. However, it has been noted that people with PD should remain active and engage in different forms of physical activity, particularly whilst spending time at home[231].

With regards to contagion, there does not seem to be a correlation between PD and contraction of the SARS-CoV-2 virus. However, if a PD patient does contract COVID-19, several complications may arise. It has been noted that PD patients are at larger risk of developing pneumonia and other respiratory infection so clearly a SARS-CoV-2 infection may in many cases lead to a worsening of PD symptoms [230]. Indeed, urinary tract infections, pneumonia or the flu can temporarily worsen PD symptoms and it is therefore important for patients to have their PD medications readily available

As with any underlying conditions PD patients should consult with their physician to ensure that their PD medications are compatible with medications used to treat symptoms of COVID-19. It should be noted that certain cold and flu medications should not be administered together with, for example MAO-B inhibitors, such as Azilect/rasagiline or Xadago/safinamide, frequently used to treat PD symptoms [230].

In the past few years, it has been noted that the number of PD cases has been on the rise. Although this rise in cases may be in part be attributed to an increasingly aging population it is also believed that external factors such as pesticides, smoking and viral infections may contribute to the increase [232].

4.10 Concluding remarks

The global COVID-19 health crisis has challenged the way of life across the planet, affecting the economy, social interactions and our health and safety. In his review we have highlighted the intersections between PD, viral infections, and COVID-19 with an emphasis on the many similarities between RNA viral pathways and neurodegeneration in PD. Indeed, the onset and progression of PD, as detailed in the Braak hypothesis, as well as the pathogenic nature, molecular mechanisms, and symptom development of the disorder share many similarities with the SARS-CoV-2 virus and COVID-19. As further research is conducted, more evidence of a possible correlation between PD, viral infections and the current SARS-CoV-2 virus will become available.

5 Additional work

5.1 Shuttling a-syn into the nucleus

5.1.1 Introduction

The varied locations a-syn suggest its biological functions also vary, however, its normal functions are debated and not fully understood. It is important to study the regular biological function of a-syn to deduce its loss-of-function or gain-of-function toxicity under various conditions. It has been conclusively shown by subcellular fractionation and chromatin precipitation that a-syn exists in the nucleus of neurons, and many proposed functions of nuclear a-syn involve direct DNA-binding or modulating histone modification [40, 233, 234]. In fact, a-syn has been found to act as a transcriptional regulator of PGC1a, a master mitochondrial transcriptional co-activator, which interestingly has been identified as a potential therapeutic target for early PD intervention [89, 235]. The aim of this body of work was to identify all DNA sites, genome-wide, that can bind a-syn. While a-syn was shown to bind promoters of various genes by ChIP-on-chip analysis, the study was performed using a microarray of probes for promoters [89]. We were interested in conducting a similar study using a more modern technique, ChIP-seq. ChIP-seq allows for the identification of genome-wide a-syn-DNA interactions without predetermined probes, thereby able to identify all possible enrichment sites. ChIP-seq can analyze a lane of samples, providing for the opportunity to analyze a-syn-DNA interactions in samples with mutant a-syn, overexpressed a-syn, and chemical stress. We attempted to flood the nucleus with a-syn by transfecting cells with *SNCA* that was tagged with nuclear localization

signals. Flooding the nucleus in this way creates a different condition than overexpressing WT *SNCA* and is likely to provide more or different potential binding sites for a-syn.

5.1.2 Results and future work

We used primers for *SNCA* containing nuclear localization signals (NLS) and nuclear localization control signals (NLC) in our cloning experiments to generate pcDNA3 vectors containing single and double tagged *SNCA*. We transfected SH-SY5Y cells and analyzed the nuclear to cytosolic ratio of a-syn (Figure 14). While the double tagged a-syn showed the highest nuclear to cytosolic ratio, it did not necessarily result in flooding the nucleus in greater amount than cells transfected with WT *SNCA* (Figure 14). However, it is interesting that we were able to achieve a similar level of nuclear a-syn to the WT transfected cells without also flooding the cytosol (Figure 14B). The double tagged *SNCA* transfected cells represent a promising candidate for analyzing by ChIP-seq, however we did not flood the nucleus to a higher degree than wild type *SNCA* transfected cells. Testing and improving the transfection efficiency and combining with stress known to impact a-syn subcellular localization are a couple improvements and future steps to take in this study.

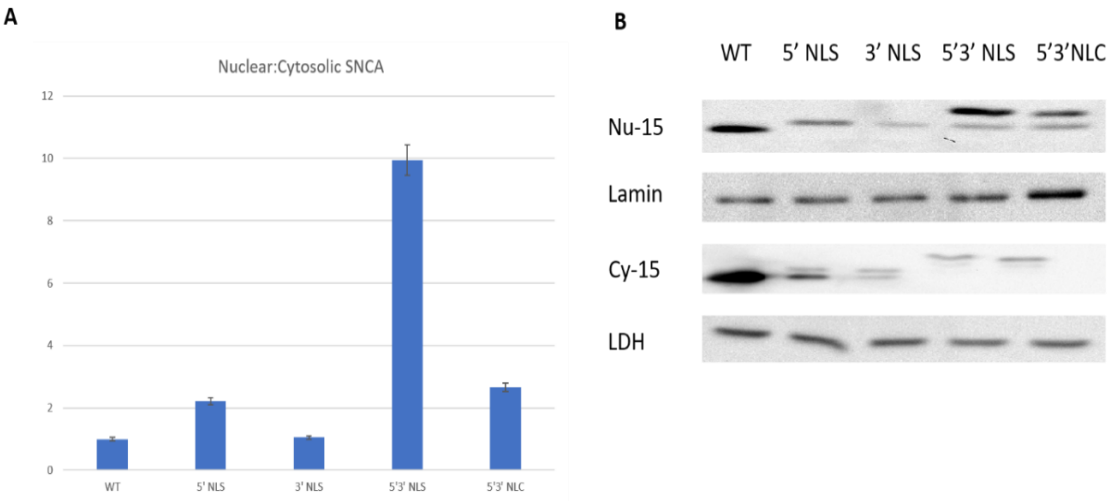

Figure 14. Ratio of localization signal tagged a-syn in the nucleus to cytosol. *SNCA* was tagged with nuclear localization sequence (NLS) or an inactive control sequence (NLC) at 5' and/or 3' ends. (A-B) Abundance of a-syn monomer (15 kDa) was analyzed and quantified by Western blot.

5.2 CRISPR knockdown of *SNCA*

5.2.1 Introduction

The most common tissue culture models used to study PD are SH-SY5Y and M17D human neuroblastoma cell lines. Often, cells are transfected, subjected to stress, and analyzed but may also be differentiated into a more dopaminergic phenotype [40, 236]. Although different models have different strengths and weaknesses, we sought to generate a cell model with no a-syn present. While our a-syn studies often include overexpressing *SNCA* or transfecting mutant forms of *SNCA*, we have no way of knowing how exogenous and endogenous *SNCA* expression are affecting each other. Additionally, and in line with our work of shuttling a-syn into the nucleus, this would present a powerful tool to study a-syn as a transcriptional regulator and would enhance the use of ChIP-seq technology to find binding sites of various forms of a-syn to chromatin without the interference of WT endogenous a-syn.

5.2.2 Results and future work

We attempted to knockout *SNCA* using CRISPR/Cas9 gene editing technology with the aim of creating a model that contained only exogenous *SNCA* expression. We achieved only 20% knockdown by transient transfections, so we attempted to create a stable cell line by co-transfection with HDR plasmid (Figure 15). A selection dosage of puromycin was determined by kill curve assay to be 10 µg/ml for both M17D and SH-SY5Y, however, transfected cells never survived under selection. Literature showing knocked out *SNCA* in cell lines is lacking, however knockout has been achieved in human embryonic stem cells which were then resistant to Lewy Body seeding by a-syn fibrils [237]. This work in human

embryonic stem cells is a similar approach to the goal of this study: knocking out *SNCA* followed by the introduction of exogenous *SNCA* (or in that case, a-syn fibrils). However, our cell lines are consistent with our previous studies, making data more easily comparable. Therefore, it would be advantageous to continue to pursue this study in M17D and SH-SY5Y cells. The human embryonic stem cell study also used puromycin for selection, so *SNCA* expression likely does not interfere with survivability under selection [237]. A possible key difference in our studies is the source of the guide-RNA of the CRISPR/Cas9 system. We purchased our plasmids, which were a mix of three guide-RNAs. The human embryonic stem cell study generated four guide-RNAs of their own [237]. The additional guide-RNA as well as the intentional location in the *SNCA* gene might lead to higher gene editing efficiency.

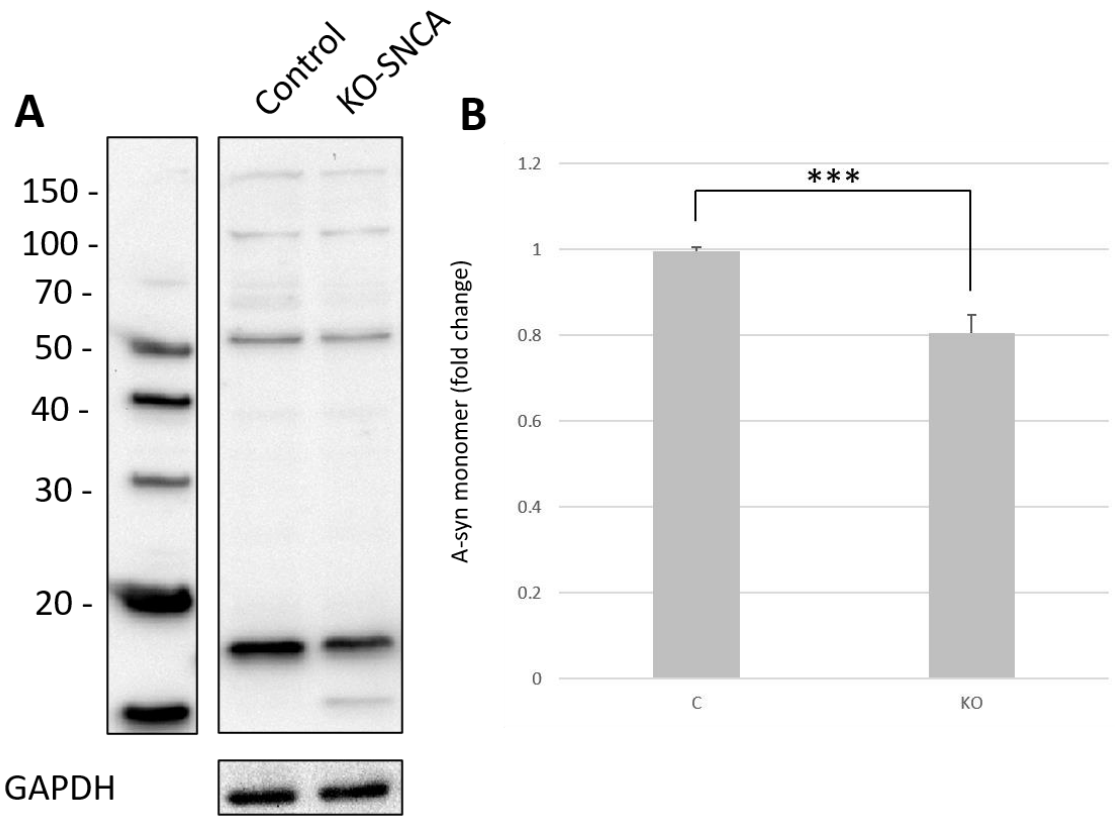

Figure 15. Transient knockdown of *SNCA* in M17D cells. (A) Western blot analysis of M17D cells transfected with CRISPR/Cas9 KO-plasmid (KO-*SNCA*) or control plasmids containing scrambled guide-RNA. (B) Quantification of a-syn monomer (***p<0.001, t-test).

6 Collaborative Projects

6.1 Subcellular Parkinson's Disease-Specific A-syn Species Show Altered Behavior in Neurodegeneration

6.1.1 Introduction

Lewy bodies, with protein aggregates enriched with *SNCA*, is pathology of PD and other synucleinopathies [238]. *SNCA*, otherwise ubiquitously expressed protein, becomes neurotoxic with increasing evidence suggesting that *SNCA* oligomerization and post translational modifications have central roles in PD pathogenesis [239, 240]. It is suggested that the monomeric form of *SNCA* is probably the toxic species involved in neurodegeneration whereas the tetrameric form represents a more stable and perhaps a neuroprotective *SNCA* species [116, 240]. Further, phosphorylation at two specific serine residues – S129, Lewy body specific, and S87, possibly neuroprotective – has suggested its role in possible Lewy body formation and interaction with membrane proteins [58, 241]. However, it is unclear whether native *SNCA* exists as a homogenous population of unstructured monomeric states or in equilibrium with different oligomeric intermediate states and what individual roles these multimers play in PD pathogenesis [242, 243]. Furthermore, little is known regarding *SNCA* states within different subcellular neuronal compartments. This is especially important considering the cellular transportation of specific form of *SNCA* can have salient role to play in PD pathogenesis. Recent conflicting data concerning *SNCA* properties underline the complexity of *SNCA* biology in neurodegeneration [242, 243]. It is also becoming apparent that *SNCA* characteristics are different depending on the cell 1 94 type and tissue [244]. It is highly conceivable that the

potential neurotoxicity of specific intermediates in neurodegeneration may depend on a combination of conformation and multimerization. The relationship between the different states of *SNCA* and how some of these intermediates may drive neurotoxicity represent exciting prospects. The premise for this study was to define these subcellular specific *SNCA* intermediates and their change in characteristics in neurodegeneration because this is crucial for our understanding of *SNCA* dynamics in PD.

6.1.2 Study design and key findings

In this study we have employed subcellular fractionation, high-performance liquid chromatography, and mass spectrometric analysis to identify the multimeric *SNCA* species in different compartments of the neuronal and non-neuronal cells. We establish that in cell lines as well as human brain tissue, *SNCA* exists as well-defined, subcellular-specific populations of intermediate states in equilibrium with monomeric *SNCA*. Indeed, the profiles of *SNCA* in HEK293 subcellular fractions differ substantially from both SH-SY5Y cells and brain tissue. Moreover, our data shows that the defined *SNCA* intermediates in the cytosol, membrane and nuclear soluble fractions of neurons exhibit dynamic profile changes and altered phosphorylation status in response to oxidative stress in neuronal cell lines and in human cerebellum of PD subjects. We found that nuclear ~68kDa and membrane-bound ~150kDa *SNCA* species were phosphorylated at S129, which suggests that these two species are probably aggregation drivers. On the contrary, the cytosolic 1 95 ~68kDa was found to be phosphorylated at S87 suggesting a possible neuroprotective role. These findings are consistent with a recently published report (334). *SNCA* exists physiologically as well-defined, stable, subcellular-specific intermediates in equilibrium with monomeric *SNCA* but that despite their inherent stability this equilibrium shifts in

response to increased oxidative stress and PD pathogenesis. We have also identified a PD specific ~36kDa *SNCA* species, which we postulate, can be a potential pathogenic *SNCA* species contributing to PD pathology. The presence of ~36kDa band in the PD brain, neuronal cells overexpressing WTS and A53TS *SNCA*, is probably suggesting it to be a pathologically relevant *SNCA* species which might modulate neurotoxicity. We also overexpressed *SNCA* WT and its mutations known to cause PD to profile the different *SNCA* multimers in cellular compartments with these pathogenic states under normal condition and oxidative stress (neurotoxic levels of H2O2 and L-Dopa). Our data suggests that *SNCA* does not exist solely as either a monomeric or tetrameric structure but as a complex combination of several structural and oligomeric intermediate states. The data also highlighted the translocation of different *SNCA* species to different cellular compartments under oxidative stress. Furthermore, our data allows for the identification of neurotoxic *SNCA* intermediates, which represent prime targets to reduce *SNCA* pathogenicity. It is plausible that *SNCA* aggregation pathway(s) and toxicity are modulated, at least in part, via some of these subcellular-specific intermediates and our findings provide a 1 96 platform for the purification and characterization of these intermediates *in vivo*. The targeted manipulation of these intermediates represents hopeful neuroprotective therapeutic targets for individuals suffering from PD and other synucleinopathies.

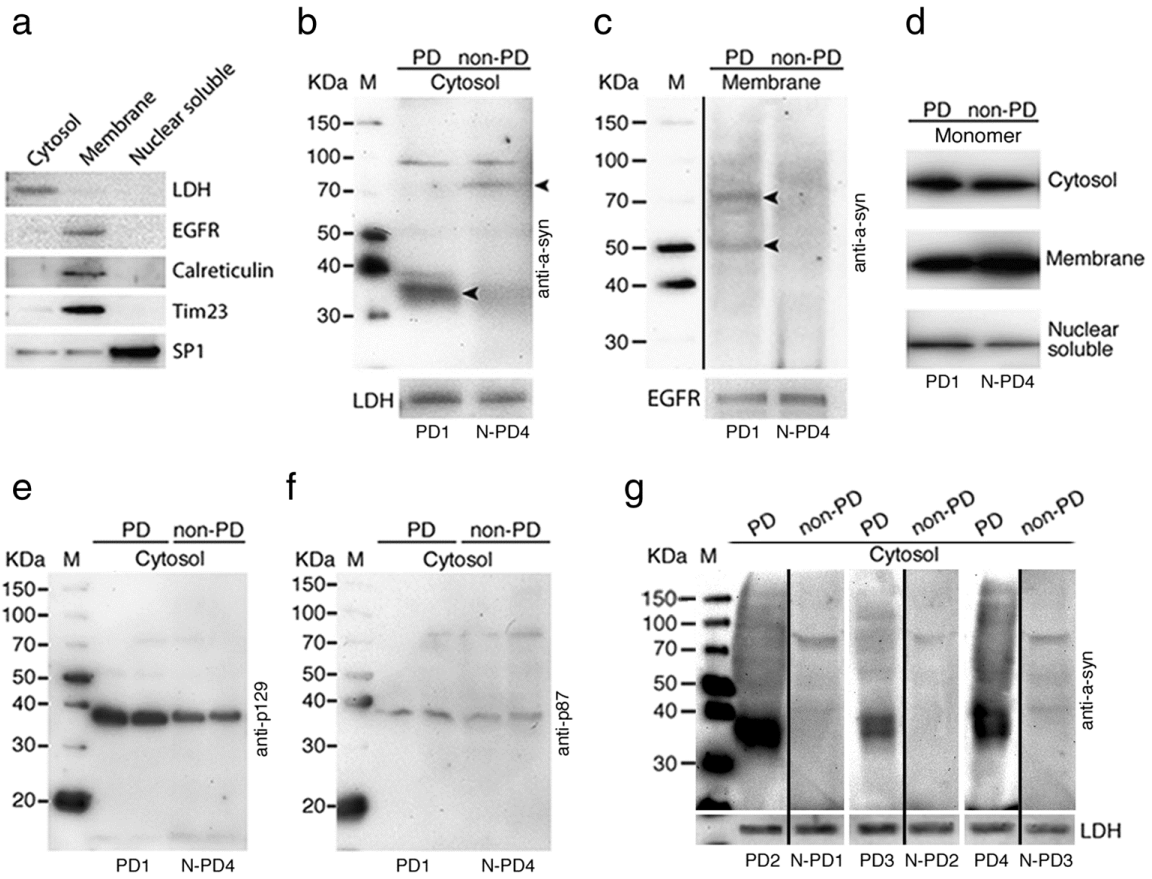

Figure 16. Subcellular-specific a-syn profile changes in human brain tissue. Total of n = 4 PD positive brains (PD1–PD4) were fractionated and n = 4 PD-negative brains (N-PD1–N-PD4) were fractionated. a) Quality control of fractionations of human cerebellum and frontal Cortex. b) Cytosolic a-syn profiles in cerebellum from non-PD and PD subjects. Arrowheads, ~36- and ~70- kDa a-syn species in cerebellum. c) Membrane a-syn profiles in cerebellum. Arrowheads, ~50- and ~70-kDa a-syn species in cerebellum. d) Monomeric a-syn in. e S129 phosphorylation of a-syn in cerebellum. f) S87 phosphorylation of a-syn in cerebellum. g) Representative Western blots of additional fractionated human frontal cortex brain samples demonstrating the enrichment of the cytosolic ~36-kDa a-syn species in PD samples as compared with non-PD samples.

6.1.3 My contribution

I worked with Dr. Abdullah to conduct subcellular fractionations of human brain tissue samples. I also performed SDS-PAGE and western blot analysis of fractions probing for a-syn and quality control markers. The assays showed PD brains were enriched with ~36 kDa a-syn and that fractions had little to no cross contamination.

6.2 Dissecting the mechanism behind pathogenesis of *SNCA* mutants

6.2.1 Introduction

One of the earliest known and most researched protein in PD is *SNCA*. Although the exact function of *SNCA* is yet unknown, its implications in PD pathogenesis are clear. We have reported that the intermediate *SNCA* species are dynamically regulated in a subcellular-specific manner depending on the exposure to oxidative stress [40]. In the above-mentioned report we have established a baseline for various *SNCA* species and their regulation in response to stress in neuroblastoma as well as non-neuronal cell lines. We also demonstrated the role of phosphorylation in regulation of these species. The key to deciphering the functional role of *SNCA* is not in the study of the *SNCA* monomer but the *SNCA* binding partners as found in the larger complexes found in our preliminary analysis. There are three main A30P, E46K, and A53T mutations along with recently found D2A, H50Q, and G51D mutations are known to be pathogenic. It is also known that the mutants have higher propensity to form aggregates. Most of the research has been focused on ability/inability of *SNCA* to form aggregates. D2A, H50Q, and G51D mutations are involved in copper binding in *SNCA*. The differences in PD onset or progression in patients with different mutations or duplication/triplication events of *SNCA* is yet unresolved. All

the experiments and data analysis for this project is yet incomplete and is expected to be ready for publication by summer 2016.

Further we sought to determine the binding partners associated with *SNCA* as well as the overall proteome change brought about by *SNCA* WT or mutant expression in neuroblastoma cells. This should provide a new insight into how *SNCA* behaves in neuronal cell and is able to exert neurotoxic effect as the disease progresses.

6.2.2 Study design and key findings

We hypothesized that the expression and regulation of different *SNCA* species in different subcellular compartments varies from mutation to mutation. To this end we expressed mutant *SNCA* proteins in SH-SY5Y cells and performed subcellular fractionation to track the changes in *SNCA* species. Our findings indicate a distinctive variation in *SNCA* multimer regulation amongst different mutation. We observed the ~36kDa *SNCA* species to be up-regulated due to WT, A30P, A53T *SNCA* but not due to H50Q, and G51D *SNCA* overexpression. We observed this regulation of ~36kDa *SNCA* in whole cell lysates and cytosolic fraction. The ~36kDa species, due to A53T *SNCA*, was up regulated in cytosol in response to H2O2Smediated oxidative stress. In our previous report we did not detect any *SNCA* species in the cytoskeletal fraction. Meanwhile we detected *SNCA* monomer in the cytoskeletal fractions of cells overexpressing WT *SNCA*. Moreover, when we overexpressed G51D *SNCA* in SH-SY5Y cells, there is marked up regulation of *SNCA* monomer due to H2O2 and L-DOPA induced stress.

For tracking proteome changes resulting from pathogenic *SNCA* conditions we utilized 2D-PAGE/MS to screen for the candidate proteins that can either be interacting with *SNCA* or are affected by the pathogenic overexpression or mutation *SNCA* in

neuroblastoma cells. We further plan to verify these results by western blot and track these protein changes in subcellular compartments to ascertain a possible association with specific *SNCA* multimer.

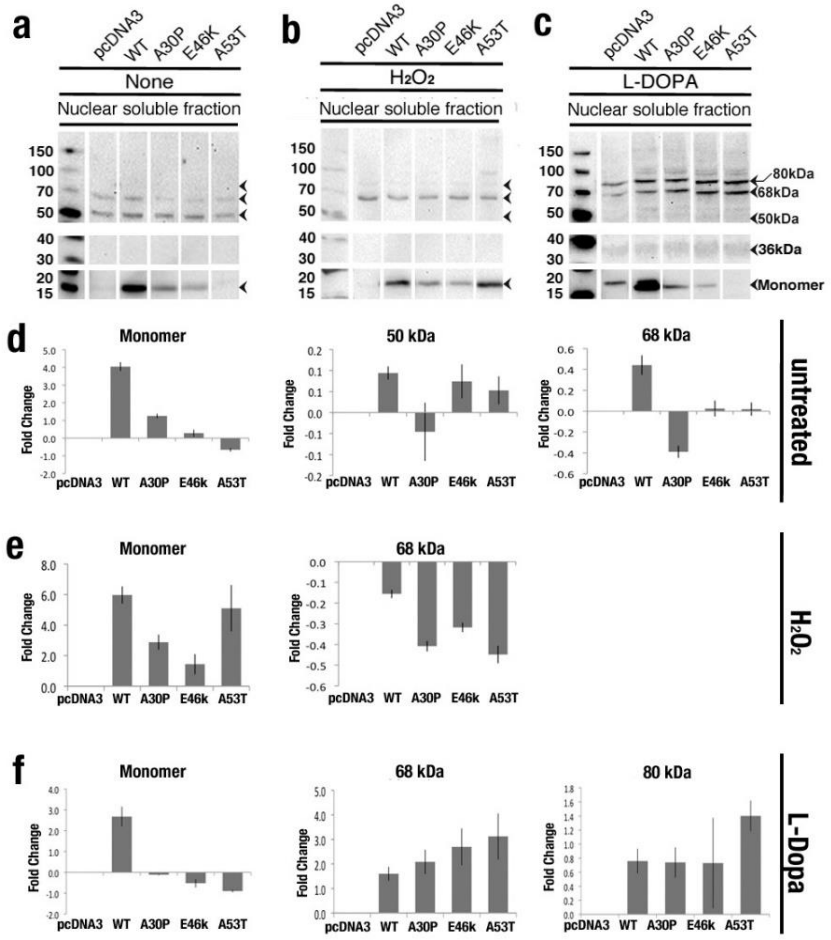

Figure 17. The multimeric a-syn species found in the nuclear soluble fraction of SH-SY5Y cells transfected with pathological variants of *SNCA* under treatments. a) The a-syn multimeric profile of pathological *SNCA* transfections in the nuclear soluble fraction under no treatment conditions, b) under H2O2 treatment, and c) under L-Dopa treatment. d) Analysis of a-syn multimeric species relative changes in abundance in the 16 nuclear soluble fractions under untreated conditions, e) under H2O2 oxidative stress conditions, and f) under L-Dopa oxidative stress conditions.

6.2.3 My contribution

I maintained SH-SY5Y cultures and performed transfection experiments with treatments. I performed subcellular fractionations of cultured cells, followed by SDS-PAGE and western blot analysis of the fractions. I also cloned His-EK tagged *SNCA* with clinical mutations (G51D and H50Q) into pcDNA3 and performed transfections for a-syn purification by high performance liquid chromatography (data not shown). The assays showed that a-syn multimerization is altered dependent on clinical mutations of *SNCA* and stress.

6.3 Neuroprotection by miR-335-5p and miR-3613-3p may involve regulation of ATXN3, BAG5, and ATG5

6.3.1 Introduction

MicroRNAs (miRs) are small non-coding RNAs which are 20-22 nucleotides in length and function in gene regulation and silencing [245]. miRs have also been extensively studied as potential biomarkers due to their extracellular stability and altered disease state expression [246]. A recent study highlighted the differences in miRNA levels from PD and non-diseased brains stating that microRNAs are differentially expressed in patients with PD allowing for classification of PD within a 5% error [247]. While this is taking a potential diagnostic approach there have been studies which show regulatory effects of microRNAs in PD. One specific study showed the regulatory effects of miR-34b/c on key Parkinson's proteins Parkin and DJ1 causing a loss in cell viability [248]. A considerable number of miRs have been reported for their regulatory roles in PD [249]We investigated miR-335-5p and miR-3613-3p which have been associated with an array of diseases from

cancer to gestational diabetes, however there are no studies to date that show the relationship between miR-335-5p and miR-3613-3p and PD.

In this study we show that miR-335-5p and miR-3613-3p levels are significantly elevated in patients that have PD compared to healthy individuals which further corroborated our previous findings [250]. This increase in miR expression was also prevalent in post-mortem frontal cortex samples for both PD and age-matched controls. We further report that miR-335-5p and miR-3613-3p overexpression may have a neuroprotective function as it increases cell viability in SH-SY5Y cells induced with oxidative stress. We also show that oxidative stress causes miR-335-5p and miR-3613-3p overexpression not seen under normal conditions. This increase leads to increased expression of ATG5 and BAG5 while decreasing expression of ATXN3.

6.3.2 Study design and key findings

We hypothesized that our previously reported increased miRs in PD patient serum would reflect changes in brain miR profiles. We isolated miRNA from frontal cortex samples and found by qRT-PCR that miR-335-5p and has-miR-3613-3p levels were significantly upgraded in PD brains. In SH-SY5Y cells transfected with miR-335 and miR-3613, we showed a rescue of cell viability under stress by hydrogen peroxide. Interestingly, we found an increase in endogenous expression of miRs 335 and 3613 in our stable cell lines over expressing *SNCA* mutants which further corroborates our claim that miRs 335 and 3613 expression is increased in neurotoxic conditions. Transfection of those *SNCA* mutant cell lines with miRs 335 and 3613 rescued cell viability under hydrogen peroxide stress. These results suggest miR-335 and miR-3613 serve a neuroprotective function and their overexpression is a cellular defense mechanism in PD serum, PD brain, and *SNCA* mutant

cell lines. We identified ATG5, BAG5, and Ataxin -3 as potential targets for miRs 335 and 3613 by *in silico* prediction analysis (miRTarBase, Partek Genomics Suite) and our previously reported LC-MS data [246]. We tested protein levels in miR transfected SH-SY5Y cells and found that miR-335-5p regulated all three targets, while miR-3613-3p regulated ATG5 and Ataxin-3. These data elucidate part of the likely expansive mechanisms of neuroprotectivity provided by these miRs.

6.3.3 My contribution

I maintained and cryopreserved stable *SNCA*-variant-expressing cell lines. I also worked with Alberim to perform miRNA transfections, including treatments, and neutral red uptake assays. The assays showed that miR-335-5p and miR-3613-3p expression is increased in *SNCA*-variant-expressing cells and the miRNA transfected cells were partially rescued under H_2O_2 stress.

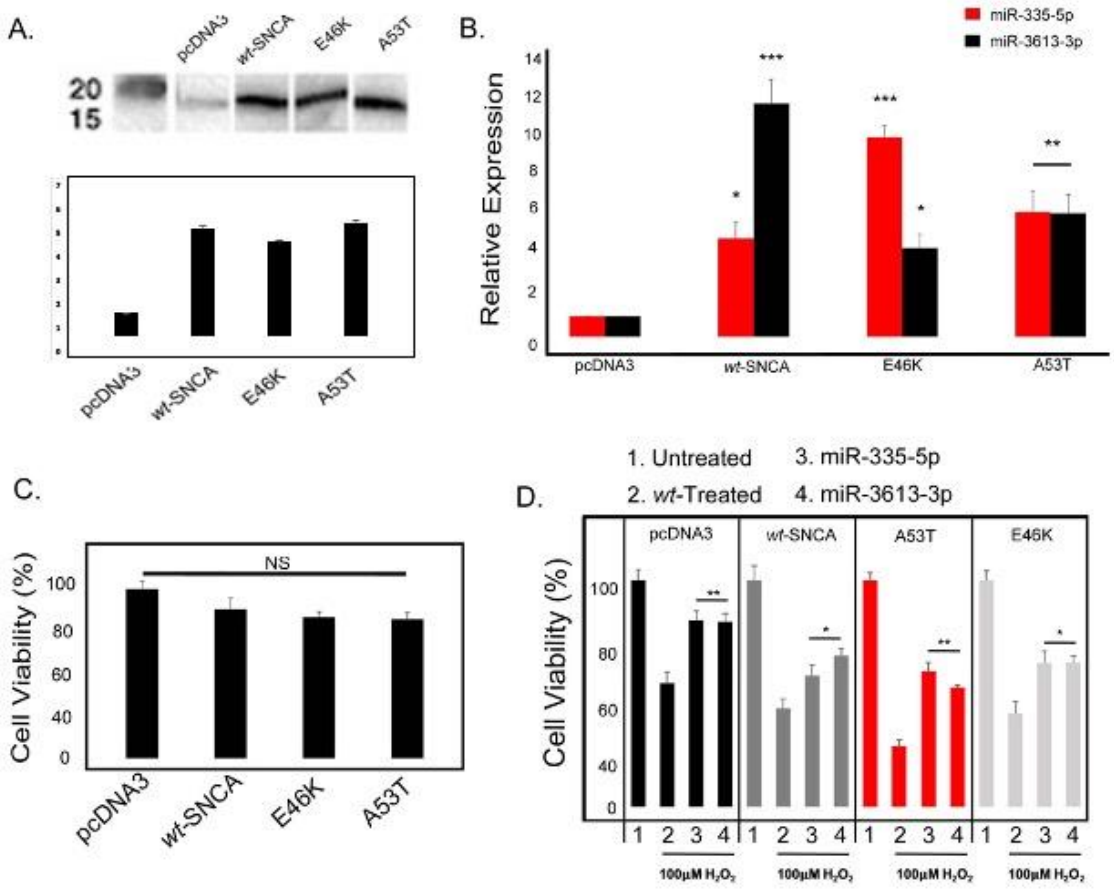

Figure 18. PARKmiRs show increased cell viability under neurotoxic conditions.

(A) Western blot analysis showing overexpression of monomeric a-syn Lane's 1-4: pcDNA3, WT *SNCA*, E46K, A53T. (B) Overexpression of endogenous miR-335-5p and miR-3613-3p in mutant cell lines using qRT-PCR. (C) pcDNA3, *WT SNCA*, E46K, A53T cells were treated with neutral red and cell viability was assayed (n=3, ns- no significance). (D) Indicated cells were treated with 100uM H_2O_2 for 6 hours followed by neutral red assay for cell viability Lane 1-4, Untreated, Treated, miR-335-5p treated, miR-3613-3p treated (n=3, *p< 0.05, **p<0.01, t test).

7 Publications and projects to date

1. **Benjamin Rosen**, Ketan S. Patil, Guido W. Alves, Simon G. Møller. Subcellular-specific Alpha-synuclein in Parkinson's Disease. *The Neuroscience of Parkinson's Disease* (2020).
2. Kurtishi A*, **Rosen B***, Patil KS, Alves GW, Møller SG (2019 May). Cellular Proteostasis in Neurodegeneration. *Molecular Neurobiology*. 56(5):3676-3689
3. Abdullah R, Patil KS, **Rosen B**, Pal R, Prabhudesai S, Lee S, Basak I, Hoedt E, Yang P, Panick K, Ho HP, Chang E, Tzoulis C, Larsen JP, Neubert TA, Alves G, Møller SG (2017 December). Subcellular Parkinson's Disease-Specific Alpha-synuclein Species Show Altered Behavior in Neurodegeneration. *Molecular Neurobiology*. 54(10): 7639-7655
4. Benjamin Rosen*, Alberim Kurtishi, Gonzalo Vazquez-Jimenez, Simon Geir Møller. The Intersection of Parkinson's Disease, Viral Infections and COVID-19. *Molecular Neurobiology*. (submitted Dec. 2020)
5. **Benjamin Rosen**, Alberim Kurtishi, Michael Padron, Ketan Patil, Francisco X. Vazquez, Simon Geir Møller. Alpha-synuclein Multimerization is Dependent on Structural Characteristics of Repeated KTKEGV Regions. *Journal of Biological Chemistry* (submit Q2 2021)
6. Alberim Kurtishi, Benjamin Rosen, Ketan S. Patil, Guido W. Alves, Simon Geir Møller microRNA regulation of ATXN3, BAG5, and ATG5 by miRs 335 and 3613. *Molecular Neurobiology.* (submit Q2 2021)

*denotes equal contribution

8 Appendix

8.1 pJET1.2

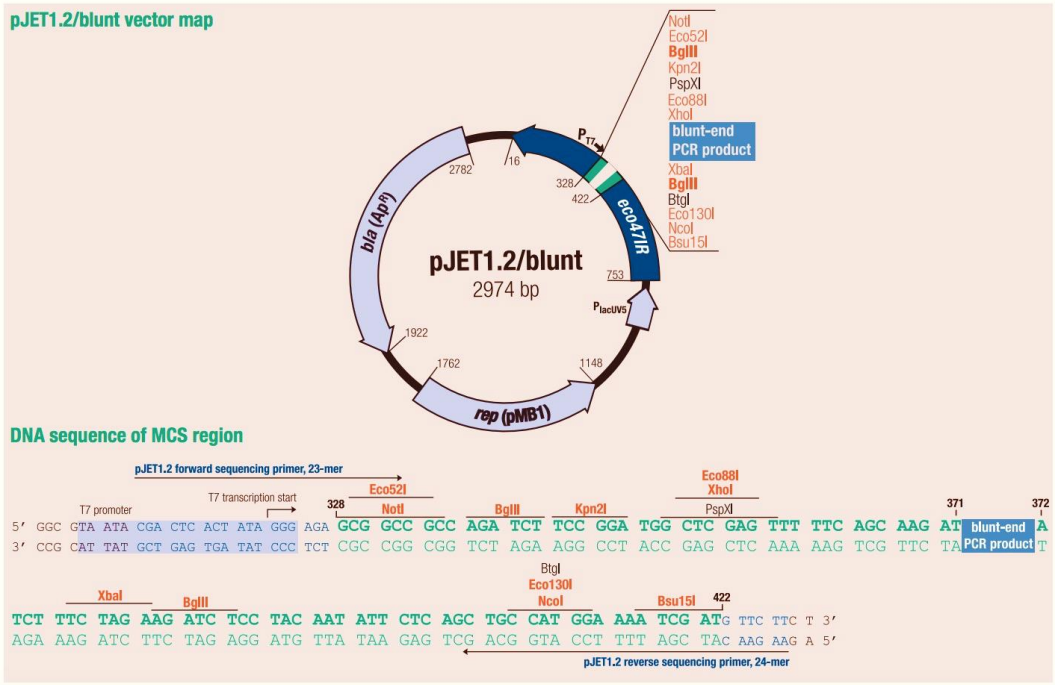

8.2 pcDNA3

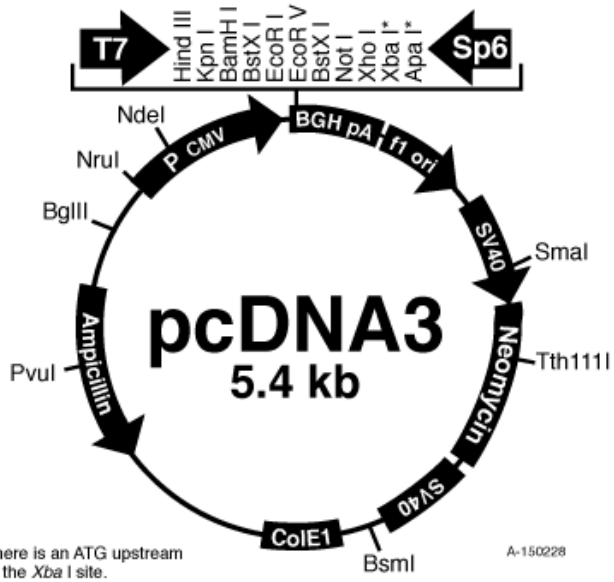

8.3 PageRuler Unstained Broad Range Protein Ladder

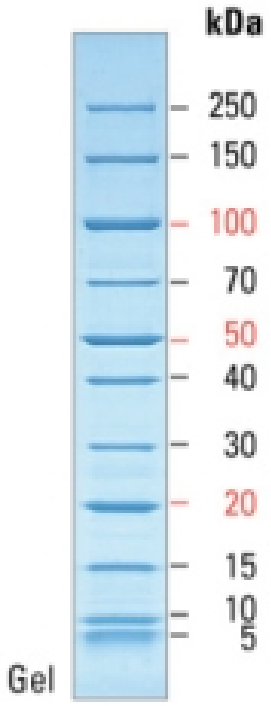

8.4 HiLO DNA Marker

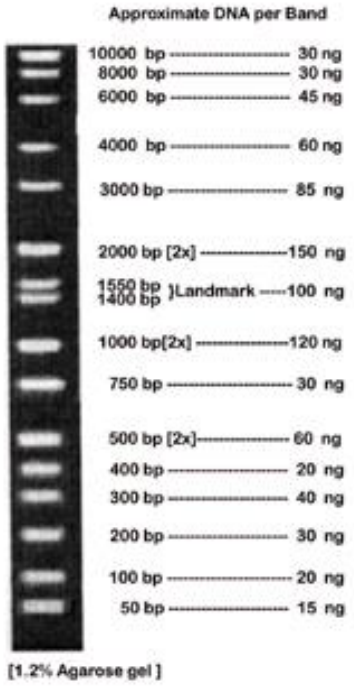

9 References

1. Polymeropoulos, M.H., et al., *Mutation in the alpha-synuclein gene identified in families with Parkinson's disease.* Science, 1997. **276**(5321): p. 2045-7.
2. Abdullah, R., et al., *Parkinson's disease and age: The obvious but largely unexplored link.* Exp Gerontol, 2015. **68**: p. 33-8.
3. Spillantini, M.G., et al., *Alpha-synuclein in Lewy bodies.* Nature, 1997. **388**(6645): p. 839-40.
4. Garcia Ruiz, P.J., *[Prehistory of Parkinson's disease].* Neurologia, 2004. **19**(10): p. 735-7.
5. Goetz, C.G., *The history of Parkinson's disease: early clinical descriptions and neurological therapies.* Cold Spring Harb Perspect Med, 2011. **1**(1): p. a008862.
6. Mhyre, T.R., et al., *Parkinson's disease.* Subcell Biochem, 2012. **65**: p. 389-455.
7. Kurtishi, A., et al., *Cellular Proteostasis in Neurodegeneration.* Molecular Neurobiology, 2019. **56**(5): p. 3676-3689.
8. Goedert, M., et al., *100 years of Lewy pathology.* Nature Reviews Neurology, 2013. **9**(1): p. 13-24.
9. Dorsey, E.R., et al., *Global, regional, and national burden of Parkinson's disease, 1990–2016: a systematic analysis for the Global Burden of Disease Study 2016.* The Lancet Neurology, 2018. **17**(11): p. 939-953.
10. de Lau, L.M.L. and M.M.B. Breteler, *Epidemiology of Parkinson's disease.* The Lancet Neurology, 2006. **5**(6): p. 525-535.
11. Dorsey, E.R. and B.R. Bloem, *The Parkinson pandemic—a call to action.* JAMA neurology, 2018. **75**(1): p. 9-10.
12. Jankovic, J., *Parkinson's disease: clinical features and diagnosis.* Journal of Neurology, Neurosurgery & Psychiatry, 2008. **79**(4): p. 368.
13. Schilder, J.C., et al., *The terminology of akinesia, bradykinesia and hypokinesia: Past, present and future.* Parkinsonism Relat Disord, 2017. **37**: p. 27-35.
14. Sveinbjornsdottir, S., *The clinical symptoms of Parkinson's disease.* Journal of Neurochemistry, 2016. **139**(S1): p. 318-324.
15. Marsili, L., G. Rizzo, and C. Colosimo, *Diagnostic Criteria for Parkinson's Disease: From James Parkinson to the Concept of Prodromal Disease.* Frontiers in neurology, 2018. **9**: p. 156-156.
16. Berardelli, A., et al., *Pathophysiology of bradykinesia in Parkinson's disease.* Brain, 2001. **124**(11): p. 2131-2146.
17. Koller, W.C., B. Vetere-Overfield, and R. Barter, *Tremors in early Parkinson's disease.* Clin Neuropharmacol, 1989. **12**(4): p. 293-7.
18. Nijhof, G., *Parkinson's Disease as a problem of shame in public appearance.* Sociology of Health & Illness, 1995. **17**(2): p. 193-205.
19. Ferreira-Sánchez, M.d.R., M. Moreno-Verdú, and R. Cano-de-la-Cuerda, *Quantitative Measurement of Rigidity in Parkinson's Disease: A Systematic Review.* Sensors, 2020. **20**(3): p. 880.
20. Kiesmann, M., et al., *Parkinsonian gait in elderly people: Significance of the threshold value of two and more falls per year.* Revue Neurologique, 2020.

21. Ponsen, M.M., et al., *Idiopathic hyposmia as a preclinical sign of Parkinson's disease.* Ann Neurol, 2004. **56**(2): p. 173-81.
22. Schapira, A.H.V., K.R. Chaudhuri, and P. Jenner, *Non-motor features of Parkinson disease.* Nat Rev Neurosci, 2017. **18**(7): p. 435-450.
23. LeWitt, P.A., *Levodopa therapy for Parkinson's disease: Pharmacokinetics and pharmacodynamics.* Mov Disord, 2015. **30**(1): p. 64-72.
24. Zhu, H., et al., *Carbidopa, a drug in use for management of Parkinson disease inhibits T cell activation and autoimmunity.* PLoS One, 2017. **12**(9): p. e0183484.
25. Rivest, J., C.L. Barclay, and O. Suchowersky, *COMT inhibitors in Parkinson's disease.* Can J Neurol Sci, 1999. **26 Suppl 2**: p. S34-8.
26. Fox, S.H. and A.E. Lang, *'Don't delay, start today': delaying levodopa does not delay motor complications.* Brain, 2014. **137**(10): p. 2628-2630.
27. Inamdar, N.N., et al., *Parkinson's disease: genetics and beyond.* Current neuropharmacology, 2007. **5**(2): p. 99-113.
28. Abdullah, R., et al., *Parkinson's disease and age: The obvious but largely unexplored link.* Exp Gerontol, 2015. **68**: p. 33-8.
29. Hipp, M.S., S.H. Park, and F.U. Hartl, *Proteostasis impairment in protein-misfolding and -aggregation diseases.* Trends Cell Biol, 2014. **24**(9): p. 506-14.
30. Hetz, C., *The unfolded protein response: controlling cell fate decisions under ER stress and beyond.* Nature Reviews Molecular Cell Biology, 2012. **13**: p. 89.
31. Komatsu, M., et al., *Constitutive autophagy: vital role in clearance of unfavorable proteins in neurons.* Cell Death And Differentiation, 2007. **14**: p. 887.
32. Tanaka, K. and N. Matsuda, *Proteostasis and neurodegeneration: the roles of proteasomal degradation and autophagy.* Biochim Biophys Acta, 2014. **1843**(1): p. 197-204.
33. Drazic, A., et al., *The world of protein acetylation.* Biochim Biophys Acta, 2016. **1864**(10): p. 1372-401.
34. Saudou, F., et al., *Huntingtin Acts in the Nucleus to Induce Apoptosis but Death Does Not Correlate with the Formation of Intranuclear Inclusions.* Cell. **95**(1): p. 55-66.
35. Cheng, I.H., et al., *Accelerating Amyloid-β Fibrillization Reduces Oligomer Levels and Functional Deficits in Alzheimer Disease Mouse Models.* Journal of Biological Chemistry, 2007. **282**(33): p. 23818-23828.
36. Winklhofer, K.F., J. Tatzelt, and C. Haass, *The two faces of protein misfolding: gain- and loss-of-function in neurodegenerative diseases.* The EMBO Journal, 2008. **27**(2): p. 336-349.
37. Araki, K., et al., *Parkinson's disease is a type of amyloidosis featuring accumulation of amyloid fibrils of α-synuclein.* Proceedings of the National Academy of Sciences, 2019. **116**(36): p. 17963-17969.
38. Helwig, M., et al., *Brain propagation of transduced alpha-synuclein involves non-fibrillar protein species and is enhanced in alpha-synuclein null mice.* Brain, 2016. **139**(Pt 3): p. 856-70.
39. Luk, K.C., et al., *Exogenous α-synuclein fibrils seed the formation of Lewy body-like intracellular inclusions in cultured cells.* Proceedings of the National Academy of Sciences, 2009. **106**(47): p. 20051-20056.
40. Abdullah, R., et al., *Subcellular Parkinson's Disease-Specific Alpha-Synuclein Species Show Altered Behavior in Neurodegeneration*. 2016.
41. Winner, B., et al., *In vivo demonstration that alpha-synuclein oligomers are toxic.* Proc Natl Acad Sci U S A, 2011. **108**(10): p. 4194-9.

42. Prots, I., et al., *alpha-Synuclein oligomers impair neuronal microtubule-kinesin interplay.* J Biol Chem, 2013. **288**(30): p. 21742-54.
43. Burré, J., M. Sharma, and T.C. Südhof, *Cell Biology and Pathophysiology of α-Synuclein.* Cold Spring Harbor perspectives in medicine, 2018. **8**(3): p. a024091.
44. Sharon, R., et al., *alpha-Synuclein occurs in lipid-rich high molecular weight complexes, binds fatty acids, and shows homology to the fatty acid-binding proteins.* Proc Natl Acad Sci U S A, 2001. **98**(16): p. 9110-5.
45. Westphal, C.H. and S.S. Chandra, *Monomeric synucleins generate membrane curvature.* J Biol Chem, 2013. **288**(3): p. 1829-40.
46. Ahn, B.H., et al., *alpha-Synuclein interacts with phospholipase D isozymes and inhibits pervanadate-induced phospholipase D activation in human embryonic kidney-293 cells.* J Biol Chem, 2002. **277**(14): p. 12334-42.
47. Ouberai, M.M., et al., *α-Synuclein senses lipid packing defects and induces lateral expansion of lipids leading to membrane remodeling.* J Biol Chem, 2013. **288**(29): p. 20883-20895.
48. Burré, J., et al., *Alpha-synuclein promotes SNARE-complex assembly in vivo and in vitro.* Science, 2010. **329**(5999): p. 1663-7.
49. Ostrerova, N., et al., *alpha-Synuclein shares physical and functional homology with 14-3-3 proteins.* J Neurosci, 1999. **19**(14): p. 5782-91.
50. Kim, T.D., et al., *Alpha-synuclein has structural and functional similarities to small heat shock proteins.* Biochem Biophys Res Commun, 2004. **324**(4): p. 1352-9.
51. Gosavi, N., et al., *Golgi fragmentation occurs in the cells with prefibrillar alpha-synuclein aggregates and precedes the formation of fibrillar inclusion.* J Biol Chem, 2002. **277**(50): p. 48984-92.
52. Thayanidhi, N., et al., *Alpha-synuclein delays endoplasmic reticulum (ER)-to-Golgi transport in mammalian cells by antagonizing ER/Golgi SNAREs.* Mol Biol Cell, 2010. **21**(11): p. 1850-63.
53. Perez, R.G., et al., *A role for alpha-synuclein in the regulation of dopamine biosynthesis.* J Neurosci, 2002. **22**(8): p. 3090-9.
54. Guo, J.T., et al., *Inhibition of vesicular monoamine transporter-2 activity in alpha-synuclein stably transfected SH-SY5Y cells.* Cell Mol Neurobiol, 2008. **28**(1): p. 35-47.
55. Emamzadeh, F.N., *Alpha-synuclein structure, functions, and interactions.* Journal of Research in Medical Sciences : The Official Journal of Isfahan University of Medical Sciences, 2016. **21**: p. 29.
56. Didonna, A. and F. Benetti, *Post-translational modifications in neurodegeneration.* AIMS Biophysics, 2015. **3**(1): p. 27-49.
57. Waxman, E.A. and B.I. Giasson, *Characterization of kinases involved in the phosphorylation of aggregated alpha-synuclein.* J Neurosci Res, 2011. **89**(2): p. 231-47.
58. Anderson, J.P., et al., *Phosphorylation of Ser-129 is the dominant pathological modification of alpha-synuclein in familial and sporadic Lewy body disease.* J Biol Chem, 2006. **281**(40): p. 29739-52.
59. Cavallarin, N., M. Vicario, and A. Negro, *The role of phosphorylation in synucleinopathies: focus on Parkinson's disease.* CNS Neurol Disord Drug Targets, 2010. **9**(4): p. 471-81.
60. Goncalves, S. and T.F. Outeiro, *Assessing the subcellular dynamics of alpha-synuclein using photoactivation microscopy.* Mol Neurobiol, 2013. **47**(3): p. 1081-92.
61. Harrison, I.F. and D.T. Dexter, *Epigenetic targeting of histone deacetylase: Therapeutic potential in Parkinson's disease?* Pharmacology & Therapeutics, 2013. **140**(1): p. 34-52.

62. Wilkinson, K.D., *Protein ubiquitination: a regulatory post-translational modification.* Anticancer Drug Des, 1987. **2**(2): p. 211-29.
63. Pickart, C.M., *Targeting of substrates to the 26S proteasome.* The FASEB Journal, 1997. **11**(13): p. 1055-1066.
64. Kane, L.A., et al., *PINK1 phosphorylates ubiquitin to activate Parkin E3 ubiquitin ligase activity.* J Cell Biol, 2014. **205**(2): p. 143-53.
65. Kazlauskaite, A., et al., *Binding to serine 65-phosphorylated ubiquitin primes Parkin for optimal PINK1-dependent phosphorylation and activation.* EMBO Rep, 2015. **16**(8): p. 939-54.
66. Ko, H.S., et al., *Phosphorylation by the c-Abl protein tyrosine kinase inhibits parkin's ubiquitination and protective function.* Proc Natl Acad Sci U S A, 2010. **107**(38): p. 16691-6.
67. Song, P., et al., *Parkin promotes proteasomal degradation of p62: implication of selective vulnerability of neuronal cells in the pathogenesis of Parkinson's disease.* Protein Cell, 2016. **7**(2): p. 114-29.
68. Vicente Miranda, H., et al., *Posttranslational modifications of blood-derived alpha-synuclein as biochemical markers for Parkinson's disease.* Sci Rep, 2017. **7**(1): p. 13713.
69. Krumova, P., et al., *Sumoylation inhibits alpha-synuclein aggregation and toxicity.* J Cell Biol, 2011. **194**(1): p. 49-60.
70. Colla, E., et al., *Accumulation of toxic α-synuclein oligomer within endoplasmic reticulum occurs in α-synucleinopathy in vivo.* The Journal of neuroscience : the official journal of the Society for Neuroscience, 2012. **32**(10): p. 3301-3305.
71. Credle, J.J., et al., *alpha-Synuclein-mediated inhibition of ATF6 processing into COPII vesicles disrupts UPR signaling in Parkinson's disease.* Neurobiol Dis, 2015. **76**: p. 112-25.
72. Omura, T., et al., *Endoplasmic reticulum stress and Parkinson's disease: the role of HRD1 in averting apoptosis in neurodegenerative disease.* Oxid Med Cell Longev, 2013. **2013**: p. 239854.
73. Ryu, E.J., et al., *Endoplasmic reticulum stress and the unfolded protein response in cellular models of Parkinson's disease.* J Neurosci, 2002. **22**(24): p. 10690-8.
74. Menzies, F.M., K. Moreau, and D.C. Rubinsztein, *Protein misfolding disorders and macroautophagy.* Curr Opin Cell Biol, 2011. **23**(2): p. 190-7.
75. Mizushima, N., et al., *Autophagy fights disease through cellular self-digestion.* Nature, 2008. **451**(7182): p. 1069-75.
76. Lum, J.J., R.J. DeBerardinis, and C.B. Thompson, *Autophagy in metazoans: cell survival in the land of plenty.* Nat Rev Mol Cell Biol, 2005. **6**(6): p. 439-48.
77. Wong, E. and A.M. Cuervo, *Autophagy gone awry in neurodegenerative diseases.* Nat Neurosci, 2010. **13**(7): p. 805-11.
78. Vidal, R.L., et al., *Targeting autophagy in neurodegenerative diseases.* Trends Pharmacol Sci, 2014. **35**(11): p. 583-91.
79. Marino, G., F. Madeo, and G. Kroemer, *Autophagy for tissue homeostasis and neuroprotection.* Curr Opin Cell Biol, 2011. **23**(2): p. 198-206.
80. Cuervo, A.M., et al., *Impaired degradation of mutant alpha-synuclein by chaperone-mediated autophagy.* Science, 2004. **305**(5688): p. 1292-5.
81. Krebiehl, G., et al., *Reduced basal autophagy and impaired mitochondrial dynamics due to loss of Parkinson's disease-associated protein DJ-1.* PLoS One, 2010. **5**(2): p. e9367.
82. Poole, A.C., et al., *The PINK1/Parkin pathway regulates mitochondrial morphology.* Proc Natl Acad Sci U S A, 2008. **105**(5): p. 1638-43.

83. Narendra, D., et al., *Parkin is recruited selectively to impaired mitochondria and promotes their autophagy.* J Cell Biol, 2008. **183**(5): p. 795-803.
84. Abdullah, R., et al., *Parkinson's disease and age: The obvious but largely unexplored link*. 2014.
85. Kawamoto, Y., et al., *Accumulation of HtrA2/Omi in neuronal and glial inclusions in brains with alpha-synucleinopathies.* J Neuropathol Exp Neurol, 2008. **67**(10): p. 984-93.
86. Moisoi, N., et al., *Mitochondrial dysfunction triggered by loss of HtrA2 results in the activation of a brain-specific transcriptional stress response.* Cell Death Differ, 2009. **16**(3): p. 449-64.
87. Thomas, K.J., et al., *DJ-1 acts in parallel to the PINK1/parkin pathway to control mitochondrial function and autophagy.* Hum Mol Genet, 2011. **20**(1): p. 40-50.
88. Johri, A. and M.F. Beal, *Mitochondrial Dysfunction in Neurodegenerative Diseases*, in *J Pharmacol Exp Ther*. 2012. p. 619-30.
89. Siddiqui, A., et al., *Selective binding of nuclear alpha-synuclein to the PGC1alpha promoter under conditions of oxidative stress may contribute to losses in mitochondrial function: implications for Parkinson's disease.* Free radical biology & medicine, 2012. **53**(4): p. 993-1003.
90. Martin, I., V.L. Dawson, and T.M. Dawson, *Recent advances in the genetics of Parkinson's disease.* Annu Rev Genomics Hum Genet, 2011. **12**: p. 301-25.
91. Simon, D.K., C.M. Tanner, and P. Brundin, *Parkinson Disease Epidemiology, Pathology, Genetics, and Pathophysiology.* Clinics in geriatric medicine, 2020. **36**(1): p. 1-12.
92. Chartier-Harlin, M.C., et al., *Alpha-synuclein locus duplication as a cause of familial Parkinson's disease.* Lancet, 2004. **364**(9440): p. 1167-9.
93. Gómez-Suaga, P., et al., *Novel insights into the neurobiology underlying LRRK2-linked Parkinson's disease.* Neuropharmacology, 2014. **85**: p. 45-56.
94. Haugarvoll, K. and Z.K. Wszolek, *Clinical features of LRRK2 parkinsonism.* Parkinsonism Relat Disord, 2009. **15 Suppl 3**: p. S205-8.
95. Cookson, M.R., *The role of leucine-rich repeat kinase 2 (LRRK2) in Parkinson's disease.* Nat Rev Neurosci, 2010. **11**(12): p. 791-7.
96. Orenstein, S.J., et al., *Interplay of LRRK2 with chaperone-mediated autophagy.* Nat Neurosci, 2013. **16**(4): p. 394-406.
97. Greggio, E. and M.R. Cookson, *Leucine-rich repeat kinase 2 mutations and Parkinson's disease: three questions.* ASN Neuro, 2009. **1**(1).
98. Valente, E.M., et al., *Hereditary early-onset Parkinson's disease caused by mutations in PINK1.* Science, 2004. **304**(5674): p. 1158-60.
99. Cook Shukla, L., et al., *Parkinson Disease Overview*, in *GeneReviews(®)*, M.P. Adam, et al., Editors. 1993, University of Washington, Seattle

100. Geisler, S., et al., *PINK1/Parkin-mediated mitophagy is dependent on VDAC1 and p62/SQSTM1.* Nat Cell Biol, 2010. **12**(2): p. 119-31.
101. Kondapalli, C., et al., *PINK1 is activated by mitochondrial membrane potential depolarization and stimulates Parkin E3 ligase activity by phosphorylating Serine 65.* Open Biol, 2012. **2**(5): p. 120080.
102. Vives-Bauza, C., et al., *PINK1-dependent recruitment of Parkin to mitochondria in mitophagy.* Proceedings of the National Academy of Sciences, 2010. **107**(1): p. 378.

103. Dagda, R.K. and C.T. Chu, *Mitochondrial quality control: insights on how Parkinson's disease related genes PINK1, parkin, and Omi/HtrA2 interact to maintain mitochondrial homeostasis.* J Bioenerg Biomembr, 2009. **41**(6): p. 473-9.
104. Wang, X., et al., *PINK1 and Parkin target Miro for phosphorylation and degradation to arrest mitochondrial motility.* Cell, 2011. **147**(4): p. 893-906.
105. Shimura, H., et al., *Familial Parkinson disease gene product, parkin, is a ubiquitin-protein ligase.* Nat Genet, 2000. **25**(3): p. 302-5.
106. Fiesel, F.C., et al., *Structural and Functional Impact of Parkinson Disease-Associated Mutations in the E3 Ubiquitin Ligase Parkin.* Hum Mutat, 2015. **36**(8): p. 774-86.
107. Butters, T.D., *Gaucher disease.* Curr Opin Chem Biol, 2007. **11**(4): p. 412-8.
108. Swan, M. and R. Saunders-Pullman, *The association between ß-glucocerebrosidase mutations and parkinsonism.* Curr Neurol Neurosci Rep, 2013. **13**(8): p. 368.
109. Du, T.T., et al., *GBA deficiency promotes SNCA/α-synuclein accumulation through autophagic inhibition by inactivated PPP2A.* Autophagy, 2015. **11**(10): p. 1803-20.
110. Riboldi, G.M. and A.B. Di Fonzo, *GBA, Gaucher Disease, and Parkinson's Disease: From Genetic to Clinic to New Therapeutic Approaches.* Cells, 2019. **8**(4).
111. Cox, T.M. and J.P. Schofield, *Gaucher's disease: clinical features and natural history.* Baillieres Clin Haematol, 1997. **10**(4): p. 657-89.
112. Neumann, J., et al., *Glucocerebrosidase mutations in clinical and pathologically proven Parkinson's disease.* Brain, 2009. **132**(7): p. 1783-1794.
113. Goker-Alpan, O., et al., *Parkinsonism among Gaucher disease carriers.* J Med Genet, 2004. **41**(12): p. 937-40.
114. Beavan, M.S. and A.H. Schapira, *Glucocerebrosidase mutations and the pathogenesis of Parkinson disease.* Ann Med, 2013. **45**(8): p. 511-21.
115. Dettmer, U., et al., *Parkinson-causing alpha-synuclein missense mutations shift native tetramers to monomers as a mechanism for disease initiation.* Nat Commun, 2015. **6**: p. 7314.
116. Dettmer, U., et al., *KTKEGV repeat motifs are key mediators of normal alpha-synuclein tetramerization: Their mutation causes excess monomers and neurotoxicity.* Proc Natl Acad Sci U S A, 2015. **112**(31): p. 9596-601.
117. Repetto, G., A. del Peso, and J.L. Zurita, *Neutral red uptake assay for the estimation of cell viability/cytotoxicity.* Nature Protocols, 2008. **3**(7): p. 1125-1131.
118. Jiang, P., et al., *Proaggregant nuclear factor(s) trigger rapid formation of α-synuclein aggregates in apoptotic neurons.* Acta neuropathologica, 2016. **132**(1): p. 77-91.
119. Kim, T.D., et al., *Structural changes in alpha-synuclein affect its chaperone-like activity in vitro.* Protein science : a publication of the Protein Society, 2000. **9**(12): p. 2489-2496.
120. Burré, J., M. Sharma, and T.C. Südhof, *α-Synuclein assembles into higher-order multimers upon membrane binding to promote SNARE complex formation.* Proc Natl Acad Sci U S A, 2014. **111**(40): p. E4274-83.
121. Goers, J., et al., *Nuclear localization of alpha-synuclein and its interaction with histones.* Biochemistry, 2003. **42**(28): p. 8465-71.
122. Kontopoulos, E., J.D. Parvin, and M.B. Feany, *Alpha-synuclein acts in the nucleus to inhibit histone acetylation and promote neurotoxicity.* Hum Mol Genet, 2006. **15**(20): p. 3012-23.
123. Zhang, J., X. Li, and J.-D. Li, *The Roles of Post-translational Modifications on α-Synuclein in the Pathogenesis of Parkinson's Diseases.* Frontiers in Neuroscience, 2019. **13**(381).
124. Allen, M.P. and D.J. Tildesley, *Computer simulation of liquids*. Book, ed. M.P. Allen and D.J. Tildesley. Vol. 18. 1989: Oxford University Press. 385.

125. Miao, Y., V.A. Feher, and J.A. McCammon, *Gaussian Accelerated Molecular Dynamics: Unconstrained Enhanced Sampling and Free Energy Calculation.* Journal of Chemical Theory and Computation, 2015. **11**(8): p. 3584-3595.
126. Miao, Y., et al., *Improved Reweighting of Accelerated Molecular Dynamics Simulations for Free Energy Calculation.* Journal of Chemical Theory and Computation, 2014. **10**(7): p. 2677-2689.
127. Hamelberg, D., J. Mongan, and J.A. McCammon, *Accelerated molecular dynamics: A promising and efficient simulation method for biomolecules.* The Journal of Chemical Physics, 2004. **120**(24): p. 11919-11929.
128. Hamelberg, D., C.A.F. de Oliveira, and J.A. McCammon, *Sampling of slow diffusive conformational transitions with accelerated molecular dynamics.* The Journal of Chemical Physics, 2007. **127**(15): p. 155102.
129. Shao, J., et al., *Clustering Molecular Dynamics Trajectories: 1. Characterizing the Performance of Different Clustering Algorithms.* Journal of Chemical Theory and Computation, 2007. **3**(6): p. 2312-2334.
130. Michell, A.W., et al., *The Effect of Truncated Human α-Synuclein (1–120) on Dopaminergic Cells in a Transgenic Mouse Model of Parkinson's Disease.* Cell Transplantation, 2007. **16**(5): p. 461-474.
131. Prasad, K., et al., *Critical Role of Truncated α-Synuclein and Aggregates in Parkinson's Disease and Incidental Lewy Body Disease.* Brain Pathology, 2012. **22**(6): p. 811-825.
132. Killinger, B.A., et al., *The vermiform appendix impacts the risk of developing Parkinson's disease.* Science Translational Medicine, 2018. **10**(465): p. eaar5280.
133. Kabsch, W. and C. Sander, *Dictionary of protein secondary structure: Pattern recognition of hydrogen-bonded and geometrical features.* Biopolymers, 1983. **22**(12): p. 2577-2637.
134. Elkouzi, A. September 14, 2020]; Available from: https://www.parkinson.org/understanding-parkinsons/what-is-parkinsons.
135. Braak, H., et al., *Stages in the development of Parkinson's disease-related pathology.* Cell Tissue Res, 2004. **318**(1): p. 121-34.
136. Braak, H., et al., *Staging of brain pathology related to sporadic Parkinson's disease.* Neurobiology of Aging, 2003. **24**(2): p. 197-211.
137. Garg, D. and R.K. Dhamija, *The Challenge of Managing Parkinson's Disease Patients during the COVID-19 Pandemic.* Annals of Indian Academy of Neurology, 2020. **23**(Suppl 1): p. S24-S27.
138. Garg, D. and R.K. Dhamija, *The Challenge of Managing Parkinson's Disease Patients during the COVID-19 Pandemic.* Ann Indian Acad Neurol, 2020. **23**(Suppl 1): p. S24-s27.
139. Chandra, S., et al., *Alpha-synuclein cooperates with CSPalpha in preventing neurodegeneration.* Cell, 2005. **123**(3): p. 383-96.
140. Fortin, D.L., et al., *Neural activity controls the synaptic accumulation of alpha-synuclein.* J Neurosci, 2005. **25**(47): p. 10913-21.
141. Abdullah, R., et al., *Parkinson's disease and age: The obvious but largely unexplored link.* Experimental Gerontology, 2015. **68**: p. 33-38.
142. Massey, A.R., et al., *Alpha-synuclein expression supports interferon stimulated gene expression in neurons.* bioRxiv, 2020: p. 2020.04.25.061762.
143. Bantle, C.M., et al., *Infection with mosquito-borne alphavirus induces selective loss of dopaminergic neurons, neuroinflammation and widespread protein aggregation.* npj Parkinson's Disease, 2019. **5**(1): p. 20.
144. Beatman, E.L., et al., *Alpha-Synuclein Expression Restricts RNA Viral Infections in the Brain.* J Virol, 2015. **90**(6): p. 2767-82.

145. Labrie, V. and P. Brundin, *Alpha-Synuclein to the Rescue: Immune Cell Recruitment by Alpha-Synuclein during Gastrointestinal Infection.* Journal of Innate Immunity, 2017. **9**(5): p. 437-440.
146. Stolzenberg, E., et al., *A Role for Neuronal Alpha-Synuclein in Gastrointestinal Immunity.* J Innate Immun, 2017. **9**(5): p. 456-463.
147. Massey, A.R. and J.D. Beckham, *Alpha-Synuclein, a Novel Viral Restriction Factor Hiding in Plain Sight.* DNA Cell Biol, 2016. **35**(11): p. 643-645.
148. Ait Wahmane, S., et al., *The Possible Protective Role of α-Synuclein Against Severe Acute Respiratory Syndrome Coronavirus 2 Infections in Patients With Parkinson's Disease.* Movement Disorders, 2020. **35**(8): p. 1293-1294.
149. Rizzi, G. and K.R. Tan, *Dopamine and Acetylcholine, a Circuit Point of View in Parkinson's Disease.* Frontiers in neural circuits, 2017. **11**: p. 110-110.
150. Horkowitz, A.P., et al., *Acetylcholine Regulates Pulmonary Pathology During Viral Infection and Recovery.* ImmunoTargets and therapy, 2020. **9**: p. 333-350.
151. Phillips, J.A., A. Horkowitz, and R. Feuer, *Acetylcholine and Cholinergic Lymphocytes in the Immune Response to Influenza.* The Journal of Immunology, 2019. **202**(1 Supplement): p. 66.20.
152. Contoli, M., et al., *Role of the acetylcholine in the virus-induced bronchoconstriction.* European Respiratory Journal, 2016. **48**(suppl 60): p. PA4103.
153. Oliver, K.R., P. Brennan, and J.K. Fazakerley, *Specific infection and destruction of dopaminergic neurons in the substantia nigra by Theiler's virus.* Journal of virology, 1997. **71**(8): p. 6179-6182.
154. Dias, V., E. Junn, and M.M. Mouradian, *The role of oxidative stress in Parkinson's disease.* J Parkinsons Dis, 2013. **3**(4): p. 461-91.
155. Hauser, D.N. and T.G. Hastings, *Mitochondrial dysfunction and oxidative stress in Parkinson's disease and monogenic parkinsonism.* Neurobiol Dis, 2013. **51**: p. 35-42.
156. Zhu, J. and C.T. Chu, *Mitochondrial dysfunction in Parkinson's disease.* J Alzheimers Dis, 2010. **20 Suppl 2**: p. S325-34.
157. Muriel, P., *Role of free radicals in liver diseases.* Hepatol Int, 2009. **3**(4): p. 526-36.
158. Paracha, U.Z., et al., *Oxidative stress and hepatitis C virus.* Virol J, 2013. **10**: p. 251.
159. Ledur, P.F., et al., *Zika virus infection leads to mitochondrial failure, oxidative stress and DNA damage in human iPSC-derived astrocytes.* Sci Rep, 2020. **10**(1): p. 1218.
160. Li, G., et al., *Characterization of cytopathic factors through genome-wide analysis of the Zika viral proteins in fission yeast.* Proc Natl Acad Sci U S A, 2017. **114**(3): p. E376-E385.
161. Medvedev, R., D. Ploen, and E. Hildt, *HCV and Oxidative Stress: Implications for HCV Life Cycle and HCV-Associated Pathogenesis.* Oxid Med Cell Longev, 2016. **2016**: p. 9012580.
162. Potokar, M., J. Jorgacevski, and R. Zorec, *Astrocytes in Flavivirus Infections.* Int J Mol Sci, 2019. **20**(3).
163. Racette, B.A., et al., *Immunosuppressants and risk of Parkinson disease.* Annals of Clinical and Translational Neurology, 2018. **5**(7): p. 870-875.
164. Müller, T., et al., *Short communication Interleukin-6 levels in cerebrospinal fluid inversely correlate to severity of Parkinson's disease.* Acta Neurologica Scandinavica, 1998. **98**(2): p. 142-144.
165. Koziorowski, D., et al., *Inflammatory cytokines and NT-proCNP in Parkinson's disease patients.* Cytokine, 2012. **60**(3): p. 762-6.
166. Ahn, D.G., et al., *Biochemical characterization of a recombinant SARS coronavirus nsp12 RNA-dependent RNA polymerase capable of copying viral RNA templates.* Arch Virol, 2012. **157**(11): p. 2095-104.

167. Mogi, M., et al., *Interleukin-1β, interleukin-6, epidermal growth factor and transforming growth factor-α are elevated in the brain from parkinsonian patients.* Neuroscience letters, 1994. **180**(2): p. 147-150.
168. Menza, M., et al., *The role of inflammatory cytokines in cognition and other non-motor symptoms of Parkinson's disease.* Psychosomatics, 2010. **51**(6): p. 474-9.
169. Lindqvist, D., et al., *Non-motor symptoms in patients with Parkinson's disease - correlations with inflammatory cytokines in serum.* PLoS One, 2012. **7**(10): p. e47387.
170. Ross, G.W., et al., *Association of olfactory dysfunction with risk for future Parkinson's disease.* Annals of Neurology, 2008. **63**(2): p. 167-173.
171. Lake, M.A., *What we know so far: COVID-19 current clinical knowledge and research.* Clin Med (Lond), 2020. **20**(2): p. 124-127.
172. Caggiu, E., et al., *Homologous HSV1 and alpha-synuclein peptides stimulate a T cell response in Parkinson's disease.* J Neuroimmunol, 2017. **310**: p. 26-31.
173. McGeer, P.L., et al., *Reactive microglia are positive for HLA-DR in the substantia nigra of Parkinson's and Alzheimer's disease brains.* Neurology, 1988. **38**(8): p. 1285-1285.
174. Brochard, V., et al., *Infiltration of CD4+ lymphocytes into the brain contributes to neurodegeneration in a mouse model of Parkinson disease.* J Clin Invest, 2009. **119**(1): p. 182-92.
175. Gerhard, A., et al., *In vivo imaging of microglial activation with [11C](R)-PK11195 PET in idiopathic Parkinson's disease.* Neurobiol Dis, 2006. **21**(2): p. 404-12.
176. Tansey, M.G., M.K. McCoy, and T.C. Frank-Cannon, *Neuroinflammatory mechanisms in Parkinson's disease: Potential environmental triggers, pathways, and targets for early therapeutic intervention.* Experimental Neurology, 2007. **208**(1): p. 1-25.
177. Klein, R.S., et al., *Neuroinflammation During RNA Viral Infections.* Annu Rev Immunol, 2019. **37**: p. 73-95.
178. Wyss-Coray, T. and L. Mucke, *Inflammation in Neurodegenerative Disease—A Double-Edged Sword.* Neuron, 2002. **35**(3): p. 419-432.
179. Paterson, R.W., et al., *The emerging spectrum of COVID-19 neurology: clinical, radiological and laboratory findings.* Brain, 2020.
180. Feldstein, L.R., et al., *Multisystem Inflammatory Syndrome in U.S. Children and Adolescents.* New England Journal of Medicine, 2020. **383**(4): p. 334-346.
181. Nagatsu, T., et al., *Cytokines in Parkinson's disease.* J Neural Transm Suppl, 2000(58): p. 143-51.
182. Achar, A. and C. Ghosh, *COVID-19-Associated Neurological Disorders: The Potential Route of CNS Invasion and Blood-Brain Relevance.* Cells, 2020. **9**(11).
183. Nile, S.H., et al., *COVID-19: Pathogenesis, cytokine storm and therapeutic potential of interferons.* Cytokine Growth Factor Rev, 2020. **53**: p. 66-70.
184. Montgomery, E.B., Jr., *Heavy metals and the etiology of Parkinson's disease and other movement disorders.* Toxicology, 1995. **97**(1-3): p. 3-9.
185. Drakesmith, H. and A. Prentice, *Viral infection and iron metabolism.* Nat Rev Microbiol, 2008. **6**(7): p. 541-52.
186. Aslam, N., et al., *Effects of chelating agents on heavy metals in Hepatitis C Virus (HCV) patients.* Math Biosci Eng, 2019. **16**(3): p. 1138-1149.
187. Hawkes, C.H., K. Del Tredici, and H. Braak, *Parkinson's disease: a dual-hit hypothesis.* Neuropathology and Applied Neurobiology, 2007. **33**(6): p. 599-614.
188. Hawkes, C., K. Del Tredici, and H. Braak, *Parkinson's Disease: The Dual Hit Theory Revisited.* Annals of the New York Academy of Sciences, 2009. **1170**: p. 615-22.

189. Ross, G.W., et al., *Association of olfactory dysfunction with incidental Lewy bodies.* Movement Disorders, 2006. **21**(12): p. 2062-2067.
190. Cersosimo, M.G., et al., *Gastrointestinal manifestations in Parkinson's disease: prevalence and occurrence before motor symptoms.* Journal of Neurology, 2013. **260**(5): p. 1332-1338.
191. Shannon, K.M., et al., *Alpha-synuclein in colonic submucosa in early untreated Parkinson's disease.* Movement Disorders, 2012. **27**(6): p. 709-715.
192. Saito, Y., et al., *Lewy body pathology involves the olfactory cells in Parkinson's disease and related disorders.* Mov Disord, 2016. **31**(1): p. 135-8.
193. Funabe, S., et al., *Neuropathologic analysis of Lewy-related α-synucleinopathy in olfactory mucosa.* Neuropathology, 2013. **33**(1): p. 47-58.
194. Kupsky, W.J., et al., *Parkinson's disease and megacolon: concentric hyaline inclusions (Lewy bodies) in enteric ganglion cells.* Neurology, 1987. **37**(7): p. 1253-5.
195. Wakabayashi, K., et al., *Parkinson's disease: the presence of Lewy bodies in Auerbach's and Meissner's plexuses.* Acta Neuropathol, 1988. **76**(3): p. 217-221.
196. Rothschild, D., et al., *Environment dominates over host genetics in shaping human gut microbiota.* Nature, 2018. **555**(7695): p. 210-215.
197. Piewngam, P., et al., *Pathogen elimination by probiotic Bacillus via signalling interference.* Nature, 2018. **562**(7728): p. 532-537.
198. Karst, S.M., *The influence of commensal bacteria on infection with enteric viruses.* Nat Rev Microbiol, 2016. **14**(4): p. 197-204.
199. Dhar, D. and A. Mohanty, *Gut microbiota and Covid-19- possible link and implications.* Virus Res, 2020. **285**: p. 198018.
200. Cersosimo, M.G. and E.E. Benarroch, *Pathological correlates of gastrointestinal dysfunction in Parkinson's disease.* Neurobiol Dis, 2012. **46**(3): p. 559-64.
201. Dutta, S.K., et al., *Parkinson's Disease: The Emerging Role of Gut Dysbiosis, Antibiotics, Probiotics, and Fecal Microbiota Transplantation.* J Neurogastroenterol Motil, 2019. **25**(3): p. 363-376.
202. Tedesco, D., et al., *Alterations in Intestinal Microbiota Lead to Production of Interleukin 17 by Intrahepatic gammadelta T-Cell Receptor-Positive Cells and Pathogenesis of Cholestatic Liver Disease.* Gastroenterology, 2018. **154**(8): p. 2178-2193.
203. Groves, H.T., et al., *Respiratory Disease following Viral Lung Infection Alters the Murine Gut Microbiota.* Front Immunol, 2018. **9**: p. 182.
204. Edouard, S., et al., *The nasopharyngeal microbiota in patients with viral respiratory tract infections is enriched in bacterial pathogens.* Eur J Clin Microbiol Infect Dis, 2018. **37**(9): p. 1725-1733.
205. Hensley-McBain, T., et al., *Effects of Fecal Microbial Transplantation on Microbiome and Immunity in Simian Immunodeficiency Virus-Infected Macaques.* J Virol, 2016. **90**(10): p. 4981-4989.
206. Park, M.K., et al., *Lactobacillus plantarum DK119 as a probiotic confers protection against influenza virus by modulating innate immunity.* PLoS One, 2013. **8**(10): p. e75368.
207. Wang, J., et al., *Gut Microbial Dysbiosis Is Associated with Altered Hepatic Functions and Serum Metabolites in Chronic Hepatitis B Patients.* Front Microbiol, 2017. **8**: p. 2222.
208. Sulzer, D., et al., *COVID-19 and possible links with Parkinson's disease and parkinsonism: from bench to bedside.* NPJ Parkinsons Dis, 2020. **6**: p. 18.

209. Menendez, C.M., J.K. Jinkins, and D.J. Carr, *Resident T Cells Are Unable To Control Herpes Simplex Virus-1 Activity in the Brain Ependymal Region during Latency.* J Immunol, 2016. **197**(4): p. 1262-75.
210. Wangensteen, K.J., et al., *Hepatitis C virus infection: a risk factor for Parkinson's disease.* J Viral Hepat, 2016. **23**(7): p. 535.
211. Costa Sa, A.C., H. Madsen, and J.R. Brown, *Shared Molecular Signatures Across Neurodegenerative Diseases and Herpes Virus Infections Highlights Potential Mechanisms for Maladaptive Innate Immune Responses.* Sci Rep, 2019. **9**(1): p. 8795.
212. Wu, Y., et al., *Prolonged presence of SARS-CoV-2 viral RNA in faecal samples.* Lancet Gastroenterol Hepatol, 2020. **5**(5): p. 434-435.
213. Yeoh, Y.K., et al., *Gut microbiota composition reflects disease severity and dysfunctional immune responses in patients with COVID-19.* Gut, 2021. **70**(4): p. 698.
214. Sampson, T.R., et al., *Gut Microbiota Regulate Motor Deficits and Neuroinflammation in a Model of Parkinson's Disease.* Cell, 2016. **167**(6): p. 1469-1480 e12.
215. Brai, E., T. Hummel, and L. Albéri. *Smell, an Underrated Early Biomarker for Brain Aging*. in *Frontiers in Neuroscience*. 2020.
216. Brozzetti, L., et al., *Neurodegeneration-Associated Proteins in Human Olfactory Neurons Collected by Nasal Brushing.* Front Neurosci, 2020. **14**: p. 145.
217. Alves, G., et al., *Epidemiology of Parkinson's disease.* Journal of Neurology, 2008. **255**(5): p. 18-32.
218. Ponsen, M.M., et al., *Olfactory testing combined with dopamine transporter imaging as a method to detect prodromal Parkinson's disease.* J Neurol Neurosurg Psychiatry, 2010. **81**(4): p. 396-9.
219. Godoy, M.D., et al., *Olfaction in neurologic and neurodegenerative diseases: a literature review.* Int Arch Otorhinolaryngol, 2015. **19**(2): p. 176-9.
220. Passarelli, P.C., et al., *Taste and smell as chemosensory dysfunctions in COVID-19 infection.* Am J Dent, 2020. **33**(3): p. 135-137.
221. David, P. and Y. Shoenfeld, *The Smell in COVID-19 Infection: Diagnostic Opportunities.* Isr Med Assoc J, 2020. **7**(22): p. 335-337.
222. Brann, D.H., et al., *Non-neuronal expression of SARS-CoV-2 entry genes in the olfactory system suggests mechanisms underlying COVID-19-associated anosmia.* Science Advances, 2020. **6**(31): p. eabc5801.
223. Liang, F., *Sustentacular Cell Enwrapment of Olfactory Receptor Neuronal Dendrites: An Update.* Genes, 2020. **11**(5): p. 493.
224. Marreiros, R., et al., *Disruption of cellular proteostasis by H1N1 influenza A virus causes α-synuclein aggregation.* Proc Natl Acad Sci U S A, 2020. **117**(12): p. 6741-6751.
225. Tremblay, M.-E., M.R. Cookson, and L. Civiero, *Glial phagocytic clearance in Parkinson's disease.* Molecular Neurodegeneration, 2019. **14**(1): p. 16.
226. Kurtishi, A., et al., *Cellular Proteostasis in Neurodegeneration.* Molecular Neurobiology, 2018. **56**.
227. Helmich, R.C. and B.R. Bloem, *The Impact of the COVID-19 Pandemic on Parkinson's Disease: Hidden Sorrows and Emerging Opportunities.* Journal of Parkinson's disease, 2020. **10**(2): p. 351-354.
228. Brown, E.G., et al., *The Effect of the COVID-19 Pandemic on People with Parkinson's Disease.* Journal of Parkinson's Disease, 2020. **10**: p. 1365-1377.
229. Salari, N., et al., *Prevalence of stress, anxiety, depression among the general population during the COVID-19 pandemic: a systematic review and meta-analysis.* Global Health, 2020. **16**(1): p. 57.

230. Dolhun, R. *Ask the MD: Coronavirus and Parkinson's*. 2020; Available from: https://www.michaeljfox.org/news/ask-md-coronavirus-and-parkinsons.
231. Vistven, A. September 14, 2020]; Available from: https://parkinson.no/behandling-og-rehabilitering/trening.
232. Savica, R., et al., *Time Trends in the Incidence of Parkinson Disease.* JAMA Neurology, 2016. **73**(8): p. 981-989.
233. Siddiqui, A., et al., *Selective binding of nuclear alpha-synuclein to the PGC1alpha promoter under conditions of oxidative stress may contribute to losses in mitochondrial function: implications for Parkinson's disease.* Free Radic Biol Med, 2012. **53**(4): p. 993-1003.
234. Schaser, A.J., et al., *Alpha-synuclein is a DNA binding protein that modulates DNA repair with implications for Lewy body disorders.* Scientific Reports, 2019. **9**(1): p. 10919.
235. Zheng, B., et al., *PGC-1α, a potential therapeutic target for early intervention in Parkinson's disease.* Sci Transl Med, 2010. **2**(52): p. 52ra73.
236. Kovalevich, J. and D. Langford, *Considerations for the use of SH-SY5Y neuroblastoma cells in neurobiology.* Methods Mol Biol, 2013. **1078**: p. 9-21.
237. Chen, Y., et al., *Engineering synucleinopathy-resistant human dopaminergic neurons by CRISPR-mediated deletion of the SNCA gene.* Eur J Neurosci, 2019. **49**(4): p. 510-524.
238. Spillantini, M.G., et al., *α-Synuclein in Lewy bodies.* Nature, 1997. **388**(6645): p. 839-840.
239. Tong, J., et al., *Brain alpha-synuclein accumulation in multiple system atrophy, Parkinson's disease and progressive supranuclear palsy: a comparative investigation.* Brain, 2010. **133**(Pt 1): p. 172-88.
240. Bartels, T., J.G. Choi, and D.J. Selkoe, *α-Synuclein occurs physiologically as a helically folded tetramer that resists aggregation.* Nature, 2011. **477**(7362): p. 107-10.
241. Paleologou, K.E., et al., *Phosphorylation at S87 is enhanced in synucleinopathies, inhibits alpha-synuclein oligomerization, and influences synuclein-membrane interactions.* J Neurosci, 2010. **30**(9): p. 3184-98.
242. Wales, P., et al., *Limelight on alpha-synuclein: pathological and mechanistic implications in neurodegeneration.* J Parkinsons Dis, 2013. **3**(4): p. 415-59.
243. Conway, K.A., J.D. Harper, and P.T. Lansbury, *Accelerated in vitro fibril formation by a mutant alpha-synuclein linked to early-onset Parkinson disease.* Nat Med, 1998. **4**(11): p. 1318-20.
244. Kuwahara, T., et al., *Phosphorylation of α-synuclein protein at Ser-129 reduces neuronal dysfunction by lowering its membrane binding property in Caenorhabditis elegans.* J Biol Chem, 2012. **287**(10): p. 7098-109.
245. McNeill, E. and D. Van Vactor, *MicroRNAs shape the neuronal landscape.* Neuron, 2012. **75**(3): p. 363-79.
246. Patil, K.S., et al., *Combinatory microRNA serum signatures as classifiers of Parkinson's disease.* Parkinsonism Relat Disord, 2019. **64**: p. 202-210.
247. Hoss, A.G., et al., *microRNA Profiles in Parkinson's Disease Prefrontal Cortex.* Front Aging Neurosci, 2016. **8**: p. 36.
248. Miñones-Moyano, E., et al., *MicroRNA profiling of Parkinson's disease brains identifies early downregulation of miR-34b/c which modulate mitochondrial function.* Hum Mol Genet, 2011. **20**(15): p. 3067-78.
249. Mouradian, M.M., *MicroRNAs in Parkinson's disease.* Neurobiol Dis, 2012. **46**(2): p. 279-84.
250. Patil, K.S., et al., *Combinatory microRNA serum signatures as classifiers of Parkinson's disease.* Parkinsonism Relat Disord, 2019. **64**: p. 202-210.

VITA

Name:	*Benjamin Ira Rosen*
Baccalaureate Degree:	*Bachelor of Science* *Ithaca College* *Ithaca, NY* *Major: Biochemistry*
Date Graduated:	*May 2012*
Other Degrees and Certificates:	*Master of Science* *St. John's University* *Queens, NY* *Major: Biology*
Date Graduated:	*December 2015*